CAPACITY ADJUSTMENT FACTORS FOR CONNECTED AND AUTOMATED VEHICLES IN THE *HIGHWAY CAPACITY MANUAL*

Phase 1 and 2 Final Report

POOLED FUND STUDY Led by

OREGON DOT

Oregon Department of Transportation

CAPACITY ADJUSTMENT FACTORS FOR CONNECTED AND AUTOMATED VEHICLES IN THE *HIGHWAY CAPACITY MANUAL*

Phase 1 and 2 Final Report

POOLED FUND STUDY Led by

OREGON DOT

by

Bastian Schroeder, PhD, PE, Abby Morgan, PhD, PE, Paul Ryus, PE, Burak Cesme, PhD, Apoorba Bibeka, Lee Rodegerdts, PE, and Jiaqi Ma, PhD

for

Oregon Department of Transportation
Research Section
555 13th Street NE, Suite 1
Salem OR 97301

and

Federal Highway Administration
1200 New Jersey Avenue SE
Washington, DC 20590

March 2022

Technical Report Documentation Page

1. Report No.	2. Government Accession No.	3. Recipient's Catalog No.
FHWA-OR-RD-22-11		

4. Title and Subtitle	5. Report Date
Capacity Adjustment Factors for Connected and Automated Vehicles in the *Highway Capacity Manual*: Phase 1 and 2 Final Report	March 2022
	6. Performing Organization Code

7. Author(s)	8. Performing Organization Report No.
Bastian Schroeder, PhD, PE - 0000-0001-8916-421X Abby Morgan, PhD, PE - 0000-0002-4278-438X Paul Ryus, PE - 0000-0002-9471-7701 Burak Cesme, PhD - 0000-0002-1265-981X Apoorba Bibeka - 0000-0001-6060-9676 Lee Rodegerdts, PE - 0000-0002-5580-4140 Jiaqi Ma, PhD - 0000-0002-8184-5157	

9. Performing Organization Name and Address	10. Work Unit No. (TRAIS)
Oregon Department of Transportation Research Section 555 13th Street NE, Suite 1 Salem, OR 97301	11. Contract or Grant No.

12. Sponsoring Agency Name and Address		13. Type of Report and Period Covered
Oregon Dept. of Transportation Research Section 555 13th Street NE, Suite 1 Salem, OR 97301	Federal Highway Admin. 1200 New Jersey Avenue SE Washington, DC 20590	Final Report
		14. Sponsoring Agency Code

15. Supplementary Notes

16. Abstract

This project's objective was to develop capacity adjustment factors (CAFs) for connected and automated vehicles (CAVs) at different levels of market penetration to allow the HCM to be used to analyze CAV applications on freeways and urban streets. The primary approach to this problem was through an "agent-based" (i.e., fully customizable vehicle and driver behavior) simulation modeling framework in which CAV and non-CAV behavior could be modeled differently. The products of this research are highway capacity adjustment lookup tables and figures for different transportation system elements (e.g., freeways, roundabouts, signalized intersections) at different levels of CAV market penetration, and example scenarios demonstrating the application of the CAFs to planning studies.

17. Key Words	18. Distribution Statement
Connected Vehicles, Automated Vehicles, CAV, Highway Capacity Manual, HCM, Planning, Capacity, Capacity Adjustment Factors	Copies available from NTIS, and online at www.oregon.gov/ODOT/TD/TP_RES/

19. Security Classification (of this report)	20. Security Classification (of this page)	21. No. of Pages	22. Price
Unclassified	Unclassified	160	

SI* (MODERN METRIC) CONVERSION FACTORS

APPROXIMATE CONVERSIONS TO SI UNITS

Symbol	You Know	Multiply By	To Find	Symbol
		LENGTH		
in	inches	25.4	millimeters	mm
ft	feet	0.305	meters	m
yd	yards	0.914	meters	m
mi	miles	1.61	kilometers	km
		AREA		
in^2	square inches	645.2	millimeters squared	mm^2
ft^2	square feet	0.093	meters squared	m^2
yd^2	square yards	0.836	meters squared	m^2
ac	acres	0.405	hectares	ha
mi^2	square miles	2.59	kilometers squared	km^2
		VOLUME		
fl oz	fluid ounces	29.57	milliliters	ml
gal	gallons	3.785	liters	L
ft^3	cubic feet	0.028	meters cubed	m^3
yd^3	cubic yards	0.765	meters cubed	m^3
~NOTE: Volumes greater than 1000 L shall be shown in m^3.				
		MASS		
oz	ounces	28.35	grams	g
lb	pounds	0.454	kilograms	kg
T	short tons (2000 lb)	0.907	megagrams	Mg
		TEMPERATURE (exact)		
°F	Fahrenheit	(F-32)/1.8	Celsius	°C

APPROXIMATE CONVERSIONS FROM SI UNITS

Symbol	You Know	Multiply By	To Find	Symbol
		LENGTH		
mm	millimeters	0.039	inches	in
m	meters	3.28	feet	ft
m	meters	1.09	yards	yd
km	kilometers	0.621	miles	mi
		AREA		
mm^2	millimeters squared	0.0016	square inches	in^2
m^2	meters squared	10.764	square feet	ft^2
m^2	meters squared	1.196	square yards	yd^2
ha	hectares	2.47	acres	ac
km^2	kilometers squared	0.386	square miles	mi^2
		VOLUME		
ml	milliliters	0.034	fluid ounces	fl oz
L	liters	0.264	gallons	gal
m^3	meters cubed	35.315	cubic feet	ft^3
m^3	meters cubed	1.308	cubic yards	yd^3
		MASS		
g	grams	0.035	ounces	oz
kg	kilograms	2.205	pounds	lb
Mg	megagrams	1.102	short tons (2000 lb)	T
		TEMPERATURE (exact)		
°C	Celsius	1.8C+32	Fahrenheit	°F

*SI is the symbol for the International System of Measurement

ACKNOWLEDGEMENTS

Ten states (AR, CT, FL, IN, MD, NC, OR, TX, UT, and WA) participated in this research through a Transportation Pooled Fund Program. Each state committed funds and assigned a member to the Technical Advisory Committee, which reviewed researchers' work and offered guidance. The Transportation Research Board's Committee on Highway Capacity and Quality of Service also guided and technically reviewed this research.

Technical Advisory Committee
Brian Dunn, Oregon DOT
Tony Knudson, Oregon DOT
Peter Calcaterra, Connecticut DOT
Grant Farnsworth, Utah DOT
Joe Hummer, North Carolina DOT
Jessie Jones, Arkansas DOT
Jim Mahugh, Washington State DOT
Bill Knowles, Texas DOT
Subrat Mahapatra, Maryland DOT State Highway Administration
Maria Overton, Florida DOT
Brad Steckler, Indiana DOT

DISCLAIMER

TABLE OF CONTENTS

LIST OF TABLES

LIST OF FIGURES

1.0 EXECUTIVE SUMMARY

1.1 PROJECT BACKGROUND AND PURPOSE

Connected and automated vehicle (CAV) capability is progressing quickly—particularly regarding technological performance and the potentially wide-ranging effects of CAVs on roadway safety, operations, and regulation. Often, existing CAV research is limited in scope, scale, approach, or underlying assumptions and insufficiently addresses questions about the large-scale impacts of CAV on highway capacity. These factors are critical to decision-makers who must decide whether to widen existing roadways (at great expense) to meet future demand or whether CAVs will be able to use existing roadway space more efficiently, thereby serving future demand without the need for widening.

The *Highway Capacity Manual* (HCM) (TRB, 2016) is the leading national document for planning-level analysis of the capacity and quality of service of freeways, highways, and urban streets. However, because its procedures are based on many years of human-driven vehicle studies, the HCM's relevance and usefulness is at risk as CAV technologies become more widespread. Such limitations drive the need to develop capacity adjustment factors (CAFs) for HCM analysis procedures to allow future roadway capacity to be estimated under varying proportions of CAVs in traffic.

To develop these CAFs, ten states (AR, CT, FL, IN, MD, NC, OR, TX, UT, and WA) participated in a Transportation Pooled Fund Program. Each state committed funds for this research project and assigned a member to the Technical Advisory Committee, who reviewed researchers' work and offered guidance.

The project approached this problem using an "agent-based" (i.e., fully customizable vehicle and driver behavior) simulation modeling framework in which CAV and non-CAV behavior could be modeled differently. The project tested varying levels of CAVs in the vehicle traffic stream, referred to as the *CAV market penetration rate* in this study. By varying CAV market penetration and traffic volumes, the research team observed how market penetration affected throughput (i.e., maximum pre-breakdown flow rate).

This project measured how CAVs will influence the capacity of the different transportation system elements defined by the HCM:

- **Basic freeway segments:** portions of the freeway not influenced by vehicles entering and exiting the freeway at on- and off-ramps
- **Freeway merge, diverge, and weaving segments:** portions of the freeway that experience traffic flow turbulence due to entering, exiting, and weaving vehicles
- **Signalized intersections:** intersections along urban streets controlled by traffic signals, considering the operation of both permissive and protected left turns

- **Stop-controlled intersections:** intersections along urban streets where the side-street approaches are controlled by STOP signs

- **Roundabouts:** circular intersections along urban streets where all entries are controlled by YIELD signs.

Phase 1 of this research produced capacity adjustment lookup tables and figures for freeways and urban street intersections at different levels of CAV market penetration. Phase 2 produced a series of scenarios illustrating the potential use of the CAFs in a variety of planning applications.

Unless stated otherwise, all references to HCM methodologies, pages, equations, and exhibits reflect the content in Version 6.0 of the HCM 6th Edition.

1.2 CONCEPTS

1.2.1 CAV Technology

CAVs integrate two separate types of technology: communications and automation. Both technologies must combine to achieve roadway capacity increases:

- **Connected vehicles** transmit or receive data about their status and their surroundings. A human still drives the connected vehicle; therefore, car-following and other behavior that influences freeway capacity is not expected to fundamentally change.

- **Automated vehicles** take over all or a portion of the driving task. Depending on the automation level, a human may still need to take over under certain conditions. In the absence of connectivity, automated driving systems may operate using time gaps between vehicles that are similar to or longer than gaps used by human drivers. Therefore, automated vehicles may decrease roadway capacity when used widely.

- **Connected and automated vehicles** communicate with each other and with roadside infrastructure. The connectivity element provides automated driving systems with more complete information about a vehicle's surroundings and enables cooperative vehicle maneuvers. Because their cooperative control allows CAVs to safely operate in platoons at shorter headways than are possible with either human-driven vehicles or automated vehicles without connectivity, CAVs may increase roadway capacity.

The CAVs modeled in this study correspond to Society of Automotive Engineers (SAE) Levels 4 and 5. They are capable of controlling the vehicle for part (e.g., only on freeways, or only within the defined operational design domain) or all of a trip, without requiring human intervention. At the time of writing, no vehicle meeting this definition is available in the commercial market.

1.2.2 Assumptions Affecting CAV Ability to Provide Higher Capacities

Given that CAV technology and regulation is still in development, assumptions necessarily have to be made when estimating CAVs' potential capacity benefit. A key assumption used in developing this project's CAFs was the minimum achievable intervehicle gap. Factors that could affect the eventual intervehicle gap include legal or regulatory requirements, liability concerns

from vehicle manufacturers, passenger comfort or discomfort concerns, the need for sufficient gaps to accommodate lane-changing and merging, and mechanical differences between vehicles that affect their operational characteristics, such as braking and acceleration.

The simulation modeling made assumptions related to human-driven vehicles and CAVs' behavior and vehicle performance. Described in more detail in the literature review chapter and in the methodology sections of each segment-type chapter, the assumptions covered:

- CAV capability
- Human-driven vehicle capability
- Platooning behavior
- Left-turn behavior
- Inter-platoon gaps
- Intra-platoon gaps
- Maximum platoon size
- System reliability
- Traffic stream composition (CAV market penetration rate)

1.3 MODELING APPROACH

The cooperative adaptive cruise control (CACC) car-following models used in this study to simulate CAV behavior were based on a well-accepted model developed by the California PATH program (Milanés & Shladover, 2014) that has been previously used (Liu et al., 2018a; Liu et al., 2018b). This model was adapted in VISSIM to allow various intra-platoon gap settings to be tested for sensitivity analysis. Additional CACC protocols were developed using the VISSIM application programming interface (API) to allow CACC vehicles to form or leave platoons and perform lane-changing under various conditions. Details about the modeling are provided in the body of this report and in Milanés & Shladover (2014). A base assumption for CAV analysis is that all necessary communication elements are in place and working with a high degree of reliability.

1.4 CAPACITY ADJUSTMENT FACTORS

1.4.1 Freeways

1.4.1.1 Basic Freeway and Freeway Diverge Segments

Table 1.1 provides CAFs for basic freeway and freeway diverge segments where CAVs are present in the traffic stream. These CAFs represent the increase in freeway capacity with the presence of a given proportion of CAVs in the traffic stream (e.g., a CAF of 1.10 indicates a 10% increase in capacity). To determine the CAF value to use, first calculate the segment's initial adjusted capacity in passenger cars per hour per lane (pc/h/ln) using HCM Equation 12-8, applying all other applicable CAFs (e.g., driver population, severe

weather). Next, determine the CAF for CAVs value from Table 1.1 based on the proportion of CAVs in the traffic stream and the initial adjusted capacity, interpolating as needed.

Table 1.1: CAFs for CAVs for Basic Freeway and Freeway Diverge Segments

Proportion of CAVs in Traffic Stream	Adjusted Segment Capacity		
	2,400 pc/h/ln	2,100 pc/h/ln	1,800 pc/h/ln
0	1.00	1.00	1.00
20	1.02	1.02	1.15
40	1.07	1.10	1.27
60	1.13	1.25	1.40
80	1.22	1.37	1.60
100	1.33	1.52	1.78

Notes:

- CAV = connected and automated vehicle, defined here as a vehicle with an operating cooperative adaptive cruise control system.
- Interpolate for other CAV proportions and adjusted segment capacities.
- Assumptions: Average intervehicle gap within CAV platoons = 0.71 s based on a distribution, CAV interplatoon gap = 2.0 s, maximum CAV platoon size = 10 pc, human-driven vehicles operate with average gaps calibrated to the given adjusted segment capacity.

1.4.1.2 Freeway Merge Segments

Table 1.2 gives CAFs for freeway merge segments where CAVs are present in the traffic stream, based on the proportion of CAVs in the traffic stream.

Table 1.2: CAFs for CAVs for Freeway Merge Segments

Proportion of CAVs in Traffic Stream	CAFCAV
0	1.00
20	1.02
40	1.07
60	1.16
80	1.33
100	1.45

Notes:

- CAV = connected and automated vehicle, defined here as a vehicle with an operating cooperative adaptive cruise control system.
- Interpolate for other CAV proportions and adjusted segment capacities.
- Assumptions: Average intervehicle gap within CAV platoons = 0.71 s based on a distribution, CAV interplatoon gap = 2.0 s, maximum CAV platoon size = 10 pc, human-driven vehicles operate with average gaps calibrated to 2,200 pc/h/ln.

1.4.1.3 Freeway Weaving Segments

Table 1.3 provides CAFs for freeway weaving segments where CAVs are present in the traffic stream. The CAF value is determined from the proportion of CAVs in the traffic stream and the volume ratio (i.e., the weaving volume divided by the total volume in the weaving segment).

Table 1.3: CAFs for CAVs for Freeway Weaving Segments

Proportion of CAVs in Traffic Stream	Volume Ratio		
	0.2	0.3	0.4
0	1.00	1.00	1.00
20	1.03	1.04	1.05
40	1.08	1.08	1.09
60	1.15	1.15	1.13
80	1.23	1.22	1.20
100	1.37	1.37	1.34

Notes:

- CAV = connected and automated vehicle, defined here as a vehicle with an operating cooperative adaptive cruise control system.
- Interpolate for other CAV proportions and volume ratios.
- The volume ratio is the weaving demand flow rate divided by the total demand flow rate in the segment.
- Assumptions: Average intervehicle gap within CAV platoons = 0.71 s based on a distribution, CAV interplatoon gap = 2.0 s, maximum CAV platoon size = 10 pc, human-driven vehicles operate with average gaps calibrated to 2,200 pc/h/ln.

1.4.2 Signalized Intersections

1.4.2.1 Through Movements

The capacity of a signalized intersection approach is essentially the base saturation flow rate (the rate at which vehicles enter the intersection after the first few vehicles have started up after the signal turns green) multiplied by the proportion of time the approach receives a green signal. Table 1.4 provides base saturation flow rates for through movements at signalized intersection approaches where CAVs are present in the traffic stream. The base saturation flow rate is applied in HCM Equation 19-8 along with a variety of adjustment factors to determine an adjusted saturation flow rate. Most of these adjustments also apply with CAVs; however, the adjustment for lane width should not be applied when CAVs are present.

Table 1.4: CAFs for CAVs for Through Movements at Signalized Intersections

Proportion of CAVs in Traffic Stream	Base Saturation Flow Rate (pc/h/ln)
0	1,900
20	2,000
40	2,150
60	2,250
80	2,550
100	2,900

Notes:

- CAV = connected and automated vehicle, defined here as a vehicle with an operating cooperative adaptive cruise control system.
- Interpolate for other CAV proportions.
- Assumes no interaction with non-motorized road users, no adverse weather impacts, and a facility without driveways or access points impacting saturation flow rates.

1.4.2.2 Protected Left Turns

Table 1.5 provides values of the saturation flow rate adjustment factor for protected left turns as a function of increasing proportion of CAVs in the traffic stream. This factor should be used as an additional adjustment in HCM Equation 19-8 to estimate the resulting saturation flow rate for protected left turns. Note that the factors in Table 1.5 are adjustments to the base saturation flow rate (with 0% CAVs). These factors should not be used in addition to the values in Table 1.4.

Table 1.5: Saturation Flow Rate Adjustments for CAVs for Protected Left Turns at Signalized Intersections

Proportion of CAVs in Traffic Stream	Saturation Flow Rate Adjustment for Protected Left Turns
0	1.00
20	1.01
40	1.07
60	1.11
80	1.21
100	1.56

Notes:

- CAV = connected and automated vehicle, defined here as a vehicle with an operating cooperative adaptive cruise control system.
- Assumptions: Average intervehicle gap within CAV platoons = 0.71 s, CAV interplatoon gap = 1.5 s, maximum CAV platoon size = 8 pc, human-driven vehicles operate with through movement saturation flow rates calibrated to 1,900, assumes no interaction with non-motorized road users, no adverse weather impacts, and a facility without driveways or access points impacting saturation flow rates.
- Interpolate for other CAV proportions.

1.4.2.3 Permitted Left Turns

Table 1.6 provides values of the CAV saturation flow rate adjustment factor for permitted left turns as a function of the total opposing through volume per lane. This factor should be used as an additional adjustment in HCM Equation 31-100 to estimate the resulting saturation flow rate for permitted left turns. The factors in Table 1.6 are adjustments to the base saturation flow rate (with 0% CAVs) and should not be used in addition to the values in Table 1.4 or Table 1.5.

Table 1.6: Saturation Flow Rate Adjustments for CAVs for Permitted Left Turns at Signalized Intersections

Proportion of CAVs in Traffic Stream	Saturation Flow Rate Adjustment for Permitted Left Turns by Opposing Through Volume Per Lane (pc/h/ln)			
	300	450	600	750
0	1.00	1.00	1.00	1.00
20	1.12	1.04	1.03	1.07
40	1.20	1.16	1.12	1.18
60	1.29	1.22	1.26	1.36
80	1.43	1.43	1.57	1.60
100	1.76	1.72	1.66	1.90

Notes:

- CAV = connected and automated vehicle, defined here as a vehicle with an operating cooperative adaptive cruise control system.
- Assumptions: Average intervehicle gap within CAV platoons = 0.71 s, CAV interplatoon gap = 1.5 s, maximum CAV platoon size = 8 pc, human-driven vehicles operate with through movement saturation flow rates calibrated to 1,900 pc/h, assumes no interaction with non-motorized road users, no adverse weather impacts, and a facility without driveways or access points impacting saturation flow rates.
- Interpolate for other CAV proportions.

1.4.3 Two-Way Stop-Controlled Intersections

The two-way stop-controlled intersection (TWSC) model results were inconclusive, as the simulation models could not be properly calibrated to HCM capacities. Furthermore, it is unclear what the behavior of CAVs at minor-street approaches of TWSC will be like in the future. For this work, it was assumed that all vehicles would still need to come to a full stop at the stop bar, which results in little to no capacity improvements due to CAVs or platooning (as platoons are broken up by the STOP sign). As a result, no capacity adjustment factors for CAV effects at TWSC intersections are currently proposed. The report does summarize the modeling activities for TWSC to serve as a foundation for future research efforts.

1.4.4 Roundabouts

Table 1.7 provides CAFs for CAVs at roundabouts. To determine the CAV-adjusted capacity, apply the CAFs f_A and f_B to the values for parameters A and B, respectively, used by the HCM's roundabout entry capacity model.

Table 1.7: CAFs for CAVs at Roundabouts

Proportion of CAVs in Traffic Stream	1-Lane Entry				2-Lane Entry					
	1 Circulating Lane		2 Circulating Lanes[a]		1 Circulating Lane, Both Lanes[a]		2 Circulating Lanes, Left Lane		2 Circulating Lanes, Right Lane	
	f_A	f_B	f_A	f_B	f_A	f_B	f_A	f_B	f_A	f_B
0	1.00	1.00	1.00	1.00	1.00	1.00	1.00	1.00	1.00	1.00
20	1.05	0.99	1.03	0.99	1.05	0.99	1.03	0.99	1.05	0.96
40	1.12	0.97	1.08	0.96	1.12	0.97	1.08	0.96	1.12	0.93
60	1.22	0.94	1.18	0.92	1.22	0.94	1.18	0.92	1.20	0.87
80	1.29	0.90	1.28	0.89	1.29	0.90	1.28	0.89	1.27	0.84
100	1.35	0.85	1.38	0.85	1.35	0.85	1.38	0.85	1.34	0.80

Notes: These cases were not specifically analyzed in the research and thus are suggested approximations.

- CAV = connected and automated vehicle, defined here as a vehicle with an operating cooperative adaptive cruise control system.
- Interpolate for other CAV proportions.
- Assumptions: Human-driven vehicles operate with average gaps calibrated to the entry lane capacity given by HCM Chapter 22.

1.5 HOW TO APPLY CAV CAPACITY ADJUSTMENT FACTORS

Any future conditions evaluation requires assumptions about future population growth, mode choice, travel demand, and travel patterns, among many other uncertain factors. Adding CAV-related assumptions—particularly when doing so using simulation that cannot yet be calibrated to actual operating conditions—only increases uncertainty in analysis inputs.

Because of this uncertainty, it is recommended that this report's CAV CAFs and service volume tables be used to evaluate "what-if" scenarios, rather than serve as the final word on what will happen once CAVs become widespread. In particular, the analyst should consider:

- **What if the minimum headway permitted by technology, regulation, or policy is longer than the modeling assumed? Or what if the average headway produced by different vehicles' user settings is longer than the modeling assumed?** In this case, the capacity increase would be less than predicted by the CAV CAFs.

- **How reliable will the necessary communications and automation technology be?** Because individual CAV-capable vehicles must be driven by a human in the event of equipment malfunction, the proportion of operating CAVs in the traffic stream will be less than the proportion of CAV-capable vehicles. (However, in the situation where only vehicles with functioning systems are allowed on the facility, demand will be lower.)

- **How quickly will CAV technology become available and adopted, and how will CAVs affect travel demand?** The assumptions made related to these questions will

determine the assumed volume and proportion of CAVs in the traffic stream, along with the assumed CAF.

1.6 CONCLUSIONS

This section summarizes the key findings for freeway segments (basic freeway, merge and diverge, and weave), signalized intersections, two-way stop-controlled intersections, and roundabouts.

1.6.1 Freeway Segments

The capacity benefit of CAVs increases with higher market penetration. However, when starting capacities are lower, the trend is more linear, with higher capacity benefits as the CAV market penetration rate increases. This result suggests that the capacity benefits differ across all facility design speeds and operating conditions.

The results indicated that different roadway merge capacities are achieved at different on-ramp demand levels. CACC coordination can potentially reduce the effect of merging disturbance at on-ramps when the market penetration rate is in excess of 60% CAVs. On weaving segments, the results showed that the capacity benefits of CACC decrease as the volume ratio increases. Weaving disturbances drastically reduce the effects of CACC coordination. Even when an advanced merging capability was provided in which vehicles cooperatively changed lanes in advance of a merge to provide gaps for merging vehicles, the effects of weaving intensity were still pronounced.

Although this project focused on CAVs, it also conducted experiments for freeways on the effects of adaptive cruise control (ACC)—technology currently available in many vehicles in the market—to show the importance of connectivity in enhancing capacity. ACC systems are built to prioritize comfort and safety, which generally results in more conservative driving behavior. For an ideal base capacity of 2,400 pc/h/ln (i.e., a freeway built to modern geometric standards with level terrain, no trucks, daylight conditions, familiar drivers, and good weather), freeway capacity decreases as the percentage of ACC-equipped vehicles increases, because ACC systems drive more conservatively than human-driven vehicles in traffic. On the other hand, for a lower base capacity of 1,800 pc/h/ln (i.e., a freeway with some combination of narrow lanes, narrow shoulders, high truck volumes, upgrades, unfamiliar drivers, and/or severe weather), capacity increases as the proportion of ACC-equipped vehicles increases. This result occurs because even though ACC systems are designed to drive conservatively, the resulting headways are still lower than those of human-driven vehicles under the same non-ideal conditions, which leads to capacity improvements. This finding suggests that ACC systems can perform better than human-driven vehicles under non-ideal conditions, likely due to the behavior of ACC systems that stabilizes the traffic flow.

1.6.2 Signalized Intersections

For signalized intersections, the saturation headway decreases considerably with increasing CAV market penetration rate. Higher benefits were observed for the protected left-turn movement, compared to the through movement. CAV effects on effective green time (essentially, the length

of time when vehicles enter the intersection at the saturation flow rate) were marginal. As a result, only the effects on the saturation flow rate (saturation headway) were included for the CAF development.

For the permitted left-turn scenario, the critical headway (i.e., the minimum time between vehicle arrivals in the opposing traffic stream that allows one vehicle to turn left) did not change with increasing CAV market penetration rate compared to human-driven vehicle traffic. However, by enhancing CAVs with platooning capabilities (CACC), the follow-up headway (i.e., the minimum additional time required for each subsequent vehicle to be able to turn left after the first vehicle in a queue turns left) decreases as the CAV market penetration rate increases. Also, due to the reduced discharge headway of CAVs, queues on the opposing approach dissipated more quickly, thereby providing more unblocked green time for permitted left-turn movements, and subsequently increasing the permitted left-turn capacity.

1.6.3 Roundabouts

This research tested CAV effects on capacity at a single-lane roundabout and a double-lane roundabout. The entry capacities increase as the CAV market penetration rate increase. The capacity increase is less substantial at low market penetration rates (20% and 40%) but very significant at higher rates (60%, 80%, and 100%). When the CAV market penetration rate increases, the follow-up headway and the critical headway decrease in both single-lane and double-lane roundabouts. The follow-up headway decreases significantly with increasing CAV market penetration rate, while the critical headway decreases only slightly.

1.7 FUTURE RESEARCH NEEDS

Capacity is a function of many factor and assumptions. This study addressed some of the most critical factors for interrupted flow facilities (freeways and managed lanes), uninterrupted flow facilities (signalized intersections, two-way stop-controlled intersections, and roundabouts), and other factors that impact capacity. Additional research is needed to explore the impacts of:

- More complex freeway scenarios, such as managed lanes, higher weaving ratios, and two-lane on-ramps
- Signalized intersections with shared lanes and more complex configurations
- Two-way stop-controlled intersections, including considerations of allowing CAVs to operate under yield control
- Higher resolution of conflicting and exiting flows at roundabouts, along with other roundabout models, such as single-lane entry against two conflicting lanes or a double-lane entry against one conflicting lane
- The effect of trucks (both automated and human-driven) on a traffic stream incorporating CAVs

- The combined effect of other CAV applications that could be implemented in the near future

- The combined effect of CAV market penetration rate and communication with the traffic signal controller, such as trajectory and signal optimization, both of which are likely to accompany CAV introduction

- The combined effect of other CAV functions at roundabouts, or automated operation in the absence of connectivity (i.e., ACC-only operation)

- How the behavior of truck and other heavy vehicle CAV platoons could impact capacity on different roadway and intersection types

2.0 INTRODUCTION

2.1 PROJECT BACKGROUND AND PURPOSE

The capability of *connected and automated vehicles* (CAVs) is progressing quickly with particular focus on technological performance and the potentially wide-ranging effects of CAVs on roadway safety, operations, and regulation. Existing CAV research is often limited in terms of scope, scale, approach, or underlying assumptions, and has not sufficiently addressed questions about the large-scale impacts of CAV on highway capacity, which are required by decision-makers to inform policies. Although consumers are not yet able to purchase CAVs capable of fully controlling the vehicle for an entire trip without the possible need for human intervention, such CAVs are expected to enter the consumer market within the time horizon of long-range transportation plans. Decision-makers already need to make decisions about whether to widen existing roadways, at great expense, to meet future demand or whether CAVs will be able to use existing roadway space more efficiently, serving future demand without the need for widening.

The *Highway Capacity Manual* (HCM) (TRB, 2016) is the leading national document for planning level analysis of the capacity and quality of service of freeways, highways, and urban streets. However, its procedures are based on many years of studies of human-driven vehicles. The HCM is at risk of becoming outdated or limited in its relevance and usefulness as CAV technologies become more widespread. The HCM's limitations drive a need to develop *capacity adjustment factors* (CAFs) for HCM analysis procedures to allow future roadway capacity to be estimated under varying levels of CAV market penetration.

To develop these CAFs, an FHWA pooled-fund project was created with ten states participating (AR, CT, FL, IN, MD, NC, OR, TX, UT, and WA). Each state committed funds for this research project and assigned a member to be a part of a Technical Advisory Committee to review the work done by the researchers and offer guidance.

This report presents the Phase 1 research used to develop HCM CAFs and service volumes for various elements of freeway and urban street facilities (e.g., freeway weaving segments, signalized intersections) when CAVs are present in the traffic stream. This report also provides the research findings in the form of tables and figures presenting the CAFs and resulting capacities for different levels of CAVs in the traffic stream (referred to in this report as CAV market penetration rates). The research also developed new HCM text and exhibits for incorporation into updated versions of Chapters 26 (Freeway and Highway Segments: Supplemental), 31 (Signalized Intersections: Supplemental), 32 (Stop-Controlled Intersections: Supplemental), and 33 (Roundabouts: Supplemental), which will be available online on HCM Volume 4 (hcmvolume4.org).

The report's appendix presents a series of scenarios developed during Phase 2 of the research. These scenarios demonstrate the potential application of the CAV CAFs to a variety of planning applications.

Unless stated otherwise, all references to HCM methodologies, pages, equations, and exhibits reflect the content in Version 6.0 of the HCM 6th Edition.

2.2 RESEARCH APPROACH

At the time of writing, CAVs capable of fully controlling the vehicle for an entire trip without the possible need for human intervention, either under specified operated conditions or under any operating condition were not yet in production for consumer use. Although HCM methodologies historically have been based on empirical observations of actual vehicles using actual roadway facilities, simulation calibrated to field-observed conditions, or both, these approaches are currently infeasible given the absence of fully automated and connected vehicles in the traffic stream. Consequently, the research was conducted by calibrating simulation models to HCM capacity for a traffic stream consisting of 100% human-driven vehicles, followed by modeling different percentages of CAVs in the traffic stream using CAV logic developed for the FHWA (Milanés & Shladover, 2014). An "agent-based" (i.e., fully customizable vehicle and driver behavior) simulation framework was applied in which CAV and non-CAV behavior could be modeled differently. Varying levels of traffic volumes were tested to determine throughput (i.e., maximum pre-breakdown flow rate) under various conditions.

Modeling began with the relatively simple operating environment of a basic freeway segment away from the influence of entering and exiting traffic and incrementally progressed to more-complex operating environments as follows:

- Freeway merge, diverge, and weaving segments with traffic entering and/or exiting the freeway;
- Protected left turns (i.e., when a green arrow is displayed) and through movements at signalized intersections, both of which can be made without conflicts with other traffic;
- Permitted left turns at signalized intersections, where left-turning traffic must yield to opposing traffic;
- Entry movements into roundabouts, which must yield to traffic in the circulatory roadway; and
- Movements at two-way stop-controlled intersections that must yield to one or more conflicting traffic streams (i.e., major street left and all minor street movements).

Capacity for a given combination of roadway system element and CAV proportion in the traffic stream was determined from the maximum 15-minute moving-average hourly flow rate observed in the simulation over a series of model runs, consistent with the HCM method for estimating capacity. The CAF for a given scenario was then determined as the capacity determined for that scenario divided by the HCM's base capacity for that system element. A CAF of 1.20, for example, would indicate that the system element's capacity is 20% higher than its HCM base capacity at the given CAV percentage in the traffic stream (referred to in this report as *CAV market penetration rate*).

2.3 GUIDANCE ON APPLYING CAV CAFs

Any evaluation of future conditions requires assumptions about future population growth, mode choice, travel demand, and travel patterns, among other factors—none of which are known with great certainty. Another uncertainty is how CAVs will operate in real-world applications in the hands of consumers because these vehicles are not yet in production. Adding assumptions related to CAVs, particularly when based on simulation that cannot yet be calibrated to actual operating conditions, only increases the uncertainty in the analysis inputs. Because of this uncertainty, it is recommended that the CAV CAFs and service volume tables presented in this report be applied to the evaluation of "*what if*" scenarios, rather than being taken as the final word on what *will* happen once CAVs become widespread.

When applying the CAV CAFs and service volume tables, the analyst should consider:

- **What if the minimum headway permitted by technology, regulation, or policy is longer than the modeling assumed? Or what if the average headway produced by different vehicles' user settings is longer than the modeling assumed?** In this case, the capacity increase would be less than predicted by the CAV CAFs or service volume tables.

- **How reliable will the necessary communications and automation technology be?** To the extent that individual CAV-capable vehicles must be driven by a human at any given time due to equipment malfunction or operational conditions, the proportion of operating CAVs in the traffic stream will be less than the proportion of CAV-capable vehicles. (Alternatively, the demand will be lower, in the situation where only vehicles with functioning systems are allowed on the facility.)

- **How quickly will CAV technology become available and adopted, and how will CAVs affect travel demand?** The assumptions made related to these questions will determine the assumed volume and proportion of CAVs in the traffic stream, along with the assumed CAF.

Regarding the last point, this report's literature review section notes that a wide range of predictions have been made as to how rapidly CAV technology will become available and adopted. It is unlikely that the technology will be adopted at the same rate throughout the United States. For example, fleet owners may adopt the technology at a faster rate than individuals, and some states may create incentives for CAV ownership (e.g., converting high-occupancy vehicle lanes into CAV-only lanes) while others do not. Additionally, CAV adoption rates may differ between rural and urban environments or uninterrupted flow and interrupted flow segments. Therefore, this report relies on the analyst to determine one or more likely market penetration rates suitable for the particular analysis horizon year and study area being analyzed, rather than specifying a default market penetration rate applicable to a given year.

2.4 DEFINITIONS

This section defines key terminology used throughout this report related to CAV technology and the *Highway Capacity Manual*. HCM Chapter 9, Glossary and Symbols, provides a comprehensive set of definitions of HCM terminology.

2.4.1 CAV Technology

- **Adaptive cruise control (ACC)—**A driver assistance system that automatically adjusts a vehicle's speed to maintain a set following distance from the vehicle in front (USDOT 2018), relying on data from on-board sensors (e.g., cameras, radar, lidar). ACC systems produce time gaps to preceding vehicles similar to, or longer than, those used by human drivers.

- **Cooperative adaptive cruise control (CACC)—**An ACC system that also integrates information communicated from preceding vehicles, roadside infrastructure, or both to allow faster reactions to changes in conditions and safe operation at shorter headways than possible with either human-driven vehicles or ACC systems relying solely on on-board sensors.

- **Automated vehicle (AV)—**A vehicle equipped with an automated driving system (ADS) capable of performing some or all driving functions without requiring intervention by a human in the vehicle. Fully automated vehicles perform all driving functions without any intervention from a human in the vehicle. Automated vehicles do not have to be connected and can use on-board sensors to detect their surroundings. Highly automated vehicles might not have a steering wheel or brake pedal in the passenger cabin.

- **Connected vehicle (CV)—**A vehicle capable of communicating vehicle status (e.g., location, speed, direction, brake status) to other vehicles and to transportation management centers (TMCs). CVs also receive information on infrastructure (e.g., queues ahead, weather, recommended speed) from roadside units and also receive status information (e.g., emerging braking application) from other vehicles. CVs display information about infrastructure and nearby CV status for use by the driver; the driver is in charge of taking appropriate action in response to the information or warnings and remains "in-the-loop" for the driving function.

- **Connected and automated vehicle (CAV)—**A vehicle that combines self-driving and connectivity features, allowing safe operation in platoons at shorter headways than possible by either human-driven vehicles or automated vehicles using adaptive cruise control only. CAVs are capable of driving without human intervention for specific parts of a trip (e.g., only on freeways) or all of a trip. For HCM purposes, a CAV is a vehicle with an operating CACC system.

- **Market penetration rate—**The percentage of the traffic stream composed of CAVs. For HCM purposes, it is the percentage of the vehicle fleet on a specific roadway with an operating CACC system, which may be larger or smaller than the overall fleet composition.

2.4.2 HCM Terminology

- **Capacity**—The maximum sustainable hourly flow rate at which persons or vehicles reasonably can be expected to traverse a point or a uniform section of a lane or roadway during a given time period under prevailing roadway, environmental, traffic, and control conditions.

- **Capacity adjustment factor (CAF)**—An adjustment to base capacity to reflect the effects of severe weather, incidents, and work zones, the presence of CAVs, or other factors.

2.5 REPORT ORGANIZATION

The remainder of the report is organized as follows:

- The literature review presents CAV concepts, a high-level summary of HCM methods for estimating capacity, a discussion of potential ways in which CAVs might affect roadway capacity, an overview of potential timelines for CAV adoption, a review of analysis tools capable of modeling CAV operations, and a summary of how the literature review findings were applied to the remainder of the study.

- Individual sections on freeway segments, signalized intersections, two-way stop-controlled intersections, and roundabouts present the methodologies used to develop the base model, to incorporate CAVs into the model, and to estimate capacity, followed by findings on the effects of CAVs on the system element's capacity at different CAV market penetration levels.

- Conclusions that summarize the study findings, describe potential applications for the work, and describe future research needs.

- A list of references containing all the work cited in the report.

- An appendix demonstrating the application of the CAFs developed by Phase 2 of this project to a variety of planning scenarios for freeway and urban street facilities.

3.0 LITERATURE REVIEW

3.1 CAV CONCEPTS

3.1.1 Connectivity

Connected vehicles (CVs) use any number of communication technologies to communicate to others. CVs can connect with other vehicles (vehicle-to-vehicle, or V2V), infrastructure (vehicle-to-infrastructure, or V2I), cloud (vehicle-to-cloud, or V2C), pedestrian (vehicle-to-pedestrian, V2P), or all of these (vehicle-to-anything, or V2X). Communication technologies include dedicated short-range communications (DSRC), cellular (5G), and Wi-Fi. The CV applications being pilot tested at present focus mainly on safety and route choice. Many of the safety-based CV technologies are similar to driver assistance technologies, which rely on in-vehicle sensors to detect the roadway environment and other vehicles. A CV will transmit, receive, and continually monitor signals that will provide it with a 360-degree view of other nearby vehicles.

Adding connected communication between vehicles, the roadside infrastructure, and other road users enables advanced detection, redundancy, and improved confidence not only to warn drivers, but also to take action. CVs have advantages over on-board vehicle sensors for several reasons. First, connected technologies have a greater detection range than on-board camera, radar, or lidar detection equipment. This feature is important because it allows a connected system to detect and issue alerts sooner, which may give a driver more time to react. Second, unlike on-board vehicle sensor systems, connected technology does not require line-of-sight communication. This means alerts can be issued for hazardous situations without having to "see" the situation occur. Examples of possible advanced warnings include notifications of crash risks such as a disabled vehicle or ice on the roadway, which is present around a curve or beyond a crest in the hill ahead (USDOT, 2020a). A third advantage of CV technology is that it is less expensive to install and maintain than some in-vehicle camera, radar, or lidar equipment.

Although vehicle connectivity has the potential to improve highway safety, it is most effective from a capacity perspective when paired with automation. Because the driver is still in the loop in a CV, many factors that influence capacity (particularly following distance) remain the same.

3.1.2 Automation

Automated vehicle (AV) technology enables a vehicle to perceive its surroundings, make decisions, and operate the vehicle with little to no human operation. An *automated driving system* (ADS) allows a driver to give up control of the vehicle under certain conditions. The specific traffic, roadway, and environmental conditions that an ADS is designed to operate defines the *operational design domain* (ODD) for that ADS. Depending on the level of automation, a driver may still be required to be alert and ready to act at any moment. The Society of Automotive Engineers (SAE) identifies six levels of automation, as shown in Figure 3.1:

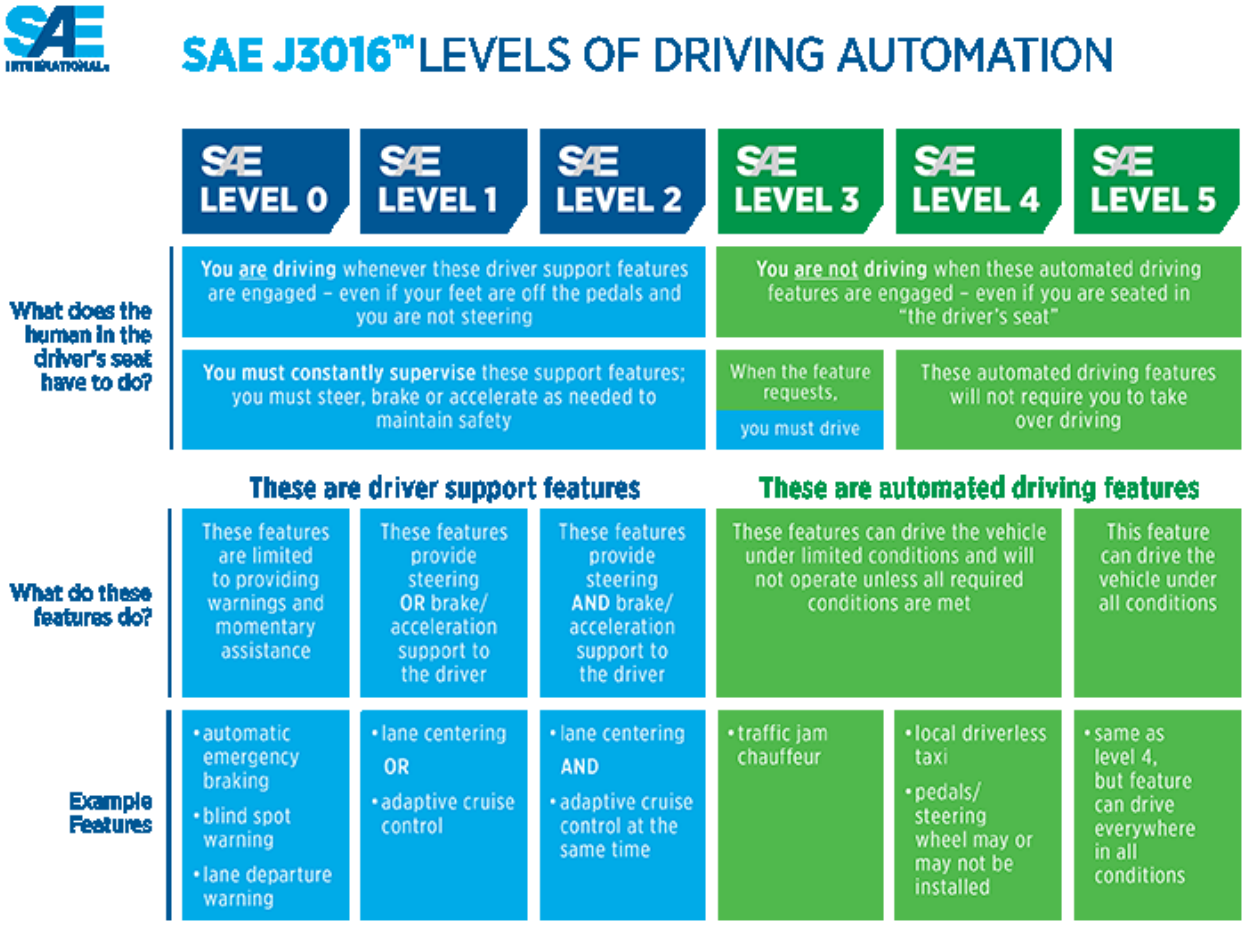

Figure 3.1: SAE automation levels (Source: SAE International, 2018).

- Level 0: No Automation. The human driver is responsible for controlling all aspects of the dynamic driving tasks even with enhanced warning and intervention systems.
    - Example: Conventional cruise control, automatic emergency braking, blind spot warning, lane departure warning
- Level 1: Driver Assistance: Automation assists the human driver with either steering or braking/accelerating (lateral or longitudinal).
    - Examples: Adaptive cruise control (longitudinal control) or lane-keeping assist (lateral control)
- Level 2: Partial Automation. Automation assists the human driver with both steering and braking/accelerating (lateral and longitudinal).
    - Examples: Tesla's AutoPilot system offers a combination of adaptive cruise control and lane-keeping assist.

- Level 3: Conditional Automation. The automated driving system can take full responsibility for driving tasks on certain parts of a trip within specific operational design domains. The human driver is expected to re-engage when the vehicle can no longer carry out driving duties. The driver shifts safety critical functions to the vehicle under certain traffic and environmental conditions.

    - Example: The vehicle can drive during stop-and-go traffic jam conditions, but the human driver must re-engage at the end of the traffic jam or if needed to change lanes to exit the facility.

- Level 4: High Automation. The vehicle can take full responsibility for driving tasks within specified operational design domains and will not require the driver to re-engage within those domains.

    - Example: The vehicle can manage operations on freeways and on- and off-ramps. There are no examples of SAE level 4 technology in production available to consumers today.

- Level 5: Full Automation. The vehicle can drive an entire trip on any road in any weather condition.

    - Example: There are no examples of SAE Level 5 technology in production available to consumers today.

It is expected that automated vehicles will offer benefits that improve safety, accessibility, and convenience. Examples of potential benefits derived from automated vehicles are (USDOT, 2020a):

- Reduction in the number of crashes caused by drivers or some conditions (e.g., weather and roadway conditions).

- Reduction in aggressive driving.

- Reduced travel time and improved travel time reliability.

- Expanded reach of transportation modes to disabled and older users, as well as providing "first-mile, last-mile" connectivity service for all users.

- Increased efficiency and effectiveness of existing transportation systems.

The greatest benefits of automated vehicles will be seen in high levels of automation, SAE Levels 4–5. However, even the higher levels of automation will be limited to their specified operational design domains. To realize the full potential performance and benefits of automated vehicles, the automated vehicles must incorporate connected vehicle technology.

3.1.3 Connected and Automated Vehicles

Combining connected vehicle technology with automated vehicle technology will provide the vehicle and driver with a greater awareness of the surroundings. At present, automated vehicles rely on on-board sensors to collect information about the vehicle's surroundings, while connected vehicles rely on information received wirelessly from other vehicles or from infrastructure. The fusion of communication technology and automated driving systems offers the potential for more advanced detection, as well as a redundancy in detection, which can enable an automated driving system to operate more efficiently and safely than with only one system (Krechmer et al., 2016).

The USDOT Intelligent Transportation System Joint Program Office identifies four categories of benefits from vehicles that are both connected and automated (*connected and automated vehicles*, CAVs) (Krechmer et al., 2016):

- **Safety.** Users will share information such as speed, location, and direction of travel, allowing drivers and vehicles to take preemptive actions to avoid or mitigate crashes.
- **Mobility.** Users will be able to make decisions in real time and operators will be able to manage road network performance in real time.
- **Environment.** Vehicles will be able to communicate with infrastructure to enhance fuel efficiency by avoiding unnecessary stops or excessive idling.
- **Data.** Cost-effective data sources and collection methods will be introduced, which will improve asset management, network operations, just-in-time maintenance, and incident response, among other functions.

3.2 HCM METHODS FOR ESTIMATING CAPACITY

This section summarizes how the HCM6 (TRB, 2016) defines capacity for different roadway system elements and the factors influencing the HCM's estimates of capacity. It also describes how CAVs may influence each of these factors, thereby potentially increasing or decreasing capacity from current levels.

This section is organized as:

- Uninterrupted Flow:
- Freeways and Multilane Highways (Basic Segments, Merge and Diverge, Weave, Managed Lanes)
- Two-Lane Highways
- Interrupted Flow:
- Signalized Intersections

- Unsignalized Intersections

3.2.1 Uninterrupted Flow

There are two categories of uninterrupted flow facilities in the HCM: Freeways and multilane highways, and two-lane highways. This section outlines the existing literature on both categories.

3.2.1.1 Freeways and Multilane Highways

The literature review summarizes the HCM Capacity definitions and factors and the potential impacts of CAVs on factors influencing HCM capacity.

HCM Capacity Definitions and Factors

This section summarizes the literature on the four segment types of freeways and multilane highways: basic segments, merge and diverge segments, weaving segments, and managed lanes.

Basic segments. The *capacity* of a freeway or multilane highway segment "is commonly understood to be a maximum flow rate associated with the occurrence of some type of breakdown, which results in lower speeds and higher densities" (HCM, p. 12-6). Capacity occurs at a vehicle density of approximately 45 passenger cars per mile per lane (pc/mi/ln), at which point "vehicles are spaced too closely to dampen the impact of any perturbation in flow, such as a lane change or a vehicle entering the roadway, without causing a disruption in flow that propagates upstream (HCM, p. 12-8).

The HCM's values of freeway and multilane highway capacity for basic segments with various free-flow speeds were established from empirical observations conducted by two NCHRP projects: Schoen et al. (1995) for freeways, and Reilly et al. (1990) for multilane highways. The base capacity values represent ideal conditions that include:

- 100% passenger cars in the traffic stream
- Level grades
- Motorists familiar with the facility
- Standard lane widths and shoulder clearances
- No incidents, crashes, or work zones
- Good weather
- Good visibility
- No pavement deterioration to the point where it affects operations

With the exceptions of pavement condition and the roadway illumination component of visibility, the HCM's basic segment capacity methods are capable of reducing capacity to account for non-ideal conditions (i.e., truck presence, narrow lanes, and work zone presence).

Base capacities represent the "maximum sustainable hourly flow rate at which persons or vehicles reasonably can be expected to traverse a point or a uniform section of a lane or roadway during a given time period under prevailing roadway, environmental, traffic, and control conditions" (HCM, p. 9-4). *Flow rate* is defined as the traffic volume experienced during the peak 15 minutes, expressed on an hourly basis (i.e., four times the peak-15-minute volume). Capacity "represents national norms" (i.e., could be different at a given location) and can vary from day to day at a given location. Finally, the HCM expresses capacity as an average flow rate across all lanes; this flow is not evenly distributed across all lanes, "thus one or two lanes could have stable base flows in excess of" the HCM's stated capacity value (HCM, p. 12-8).

Merge and diverge segments. At freeway on- and off-ramps (i.e., "merges" and "diverges"), the HCM's capacity immediately downstream of a merge or upstream of a diverge is the same as that of a basic segment. The HCM also defines maximum flow rates for the combination of the rightmost two lanes and (if present) on-ramp; exceeding these maximum flow rates does not necessarily mean that freeway operations will break down, but it does mean that operations will be worse than predicted by the HCM method (HCM, p. 14-23). The HCM acknowledges that "several sources in the literature suggest that [merge and diverge] capacities can be less than those of a basic segment," but notes that no national model has been developed to estimate merge and diverge capacity as a function of mainline and ramp volumes or other factors, and suggests making local observations of capacity when possible (HCM, p. 14-5). The HCM estimate of capacity can be calibrated to the local value by applying a capacity adjustment factor (CAF). The capacity of a ramp-metered merge is estimated to be 3% higher than a non–ramp-metered merge (HCM, p. 37-11). The capacity of ramp roadways for different free-flow speeds given in the HCM is based on empirical observations (Roess and Ulerio, 1993, Leisch, 1974).

Weaving segments. The capacity of a weaving segment is lower than that of a basic segment due to the additional turbulence that weaving maneuvers create in the traffic stream. The HCM defines the density at breakdown of a weaving segment to be 43 pc/mi/ln. In addition, a weaving segment is expected to break down when the weaving demand flow rate exceeds 2,400 pc/h (with 2 weaving lanes) or 3,500 pc/h (with 3 weaving lanes), recognizing "there is a practical limit to how many vehicles can cross each other's path without causing serious operational failures" (HCM, p. 13-21). The HCM's capacity-estimation method, based on reaching a density of 43 pc/mi/ln, considers the ratio of weaving demand to total demand within the weaving segment, the weaving area length, and the number of weaving lanes (HCM, p. 13-22).

Managed lanes. The base capacities of different types of freeway managed lanes were defined by an NCHRP research project (Wang et al., 2012). The HCM notes that managed lanes are typically operated with the intent that they should not break down and

therefore the number of available observations of capacity is limited. As a result, the HCM's base capacity values reflect maximum observed 15-minute flows without breakdowns, and may underestimate actual capacity (HCM, p. 12-12). Base capacities for basic managed lane segments vary by free-flow speed, the number of managed lanes provided (1 or 2), and the type of separation between the managed lanes and the general-purpose lanes.

Weaving across the general-purpose lanes between general-purpose ramps and the managed lane(s) reduces the general-purpose lane capacity. The amount of this reduction is a function of the number of lanes that must be weaved across, the length available to make the cross-weave, and the demand flow making the cross-weave.

Ramps directly serving the managed lanes (and any weaving associated with those ramps) are analyzed in the same manner as general-purpose ramps and weaving areas.

Potential Impacts of CAVs on Factors Influencing HCM Capacity

Headway. By far the greatest potential impact of CAVs on capacity is on the *headway between successive vehicles at capacity*. A density of 45 pc/mi/ln corresponds to an average vehicle spacing of 117 ft. For an urban freeway with a free-flow speed of 65 mph, the HCM's capacity of 2,350 pc/h corresponds to average vehicle headways (i.e., front of one car to the front of the following car) of 1.53 seconds. To the extent that CAV technology allows shorter headways than at present, capacity could be increased. However, there are several potential constraints on achieving headway reductions:

- **Safety and liability concerns.** The current vehicle spacing at capacity is less than the distance required for an anti-lock braking system to make an emergency stop from freeway speeds. Although in some kinds of deceleration events, the vehicle(s) ahead will also be slowing at roughly the same rate, in other kinds of events (e.g., load falling off a vehicle, truck tire shredding, deer running into the roadway), there will not be enough time for a vehicle to avoid a collision and thereby potentially lose control and start a chain-reaction crash.

- **Need for gaps for lane-changing, merging, and weaving.** At present, vehicles tend to be sorted across freeway lanes primarily by speed (with slower vehicles keeping to the right) and secondarily by destination (e.g., merging right as their desired exit approaches). In a 100% CAV environment, one possible outcome is that vehicles will travel at more uniform speeds, and that destination-based sorting will determine lane choice (e.g., cars making longer-distance trips keeping left), to minimize the need for lane changes and speed adjustments to provide gaps. With a smaller percentage of CAVs in the traffic stream, one possible outcome is that managed lanes will be provided for CAVs, which will also require lane changing to access. In any event, gaps will be needed to allow lane changing and merging while maintaining safe separation distances between vehicles, which will constrain the freeway's potential capacity.

- **More uniform vehicle speeds.** It is expected that CAVs will comply with speed limits and there will be less variation in vehicle speeds caused by differences in driver abilities and comfort levels. If vehicles in all lanes are traveling at nearly the same speed under near-capacity conditions, making lane changes could take more time than at present, unless (1) the CAV desiring to change lanes slows down to situate itself where there is an opening to change lanes, or (2) the CAV in the next lane slows down to create a gap once the first vehicle indicates it wants to change lanes. In either case, traffic flow is disrupted as one or the other vehicle (and the vehicles behind them) slow down to maintain safe separation distances.

- **Vehicle occupant comfort.** To avoid the need for frequent accelerations and decelerations to accommodate lane changing and merging in the traffic stream, automated driving systems might be designed to provide an extra headway buffer to allow the CAV to travel at a constant (or nearly constant) speed regardless of what is happening around the vehicle in the traffic stream under normal conditions. This extra buffer would again constrain the freeway's potential capacity.

Other factors. Other CAV-related factors that could affect capacity include the following:

- **Heavy vehicles.** Trucks will continue to be longer than passenger cars and will continue to have poorer acceleration and braking characteristics, which means they will consume more of a roadway's capacity than will passenger cars. Stopping sight distances (related to minimum safe vehicle headways) presented in the AASHTO Green Book currently acknowledge that the longer braking distances required by trucks are offset by truck drivers' higher seating position and better experience, allowing them to recognize and react to hazards more quickly (AASHTO, 2011, p. 3-6). In the future, this sight distance advantage for trucks may be eliminated, as CAVs may be able to "see ahead" at least as far as truck drivers and will be able to react even more quickly. However, the need to provide adequate braking distances for trucks will not change. Therefore, heavy vehicles—even automated heavy vehicles—may consume more roadway capacity in the future, relative to automated passenger cars.

- **Grades.** The HCM considers the effect of grades only on heavy vehicle operations, as passenger cars are able to maintain speeds on all but the most severe mountain freeway grades. Trucks will continue to perform more poorly on grades than passenger cars and automation would not be expected to change that situation.

- **Lane widths and clearances.** Lane-following technology would presumably be able to maintain a vehicle's position within a narrower (e.g., 10-foot) lane just as well as in a standard lane in good weather conditions, and automated control systems would not tend to shy away from, or slow down in the presence of, a barrier near the edge of the lane. Therefore, a capacity reduction for lane width and clearance might no longer be necessary when the entire traffic stream is

operating under automated driving systems. However, the ability of an automated driving system to follow a lane might depend on the clarity of the lane markings. For example, Las Vegas' original bus rapid transit buses were equipped with an automated docking system that followed painted stripes into a station to achieve very small gaps between the vehicle and the platform. However, the stripes quickly wore off in the harsh desert environment and the system was not able to function as planned.

- **Motorist familiarity.** An automated system would presumably be able to navigate a facility as well as familiar drivers and therefore no capacity reduction for unfamiliar drivers would be necessary.

- **Cross-weaves.** A potential CAV operations scenario would designate one or more freeway lanes as CAV-only. In this case, a managed lane would be provided to serve CAVs and the capacity of the adjacent general-purpose lanes might be reduced due to the introduction of cross-weaving maneuvers.

- **Single-lane managed lanes.** The HCM defines lower capacities for single-lane managed lanes, as vehicles cannot pass each other. In an all-CAV environment, vehicle speeds would be more uniform and the need for passing would be greatly reduced or eliminated, resulting in a higher capacity for a single-lane facility than currently defined.

- **Ramp metering.** Depending on the level of automation and market penetration, ramp metering (1) might need to become "smarter," releasing vehicles only when adequate gaps exist in the roadway, given the possibility of considerably shorter gaps in the traffic stream with automation, (2) might disappear, with individual vehicle control systems automatically providing longer headways when using an on-ramp, or (3) might become virtual, as part of an overall network traffic control system that communicates instructions to individual vehicles (either in real time or as a pre-assigned "flight plan" for the trip that also specifies routing). In any case, it is likely that some form of ramp control would become standard and therefore would not have a separate impact on capacity.

- **Access density.** Access density affects the capacity of multilane highways by lowering their free-flow speed. Because an automated system could react more quickly than a human driver to a car entering or exiting the highway and would be more capable of looking ahead to identify potential hazards, there would be less need for a car to slow down simply because of the presence of access points. At high levels of market penetration, vehicle movements would be more predictable (and unsafe movements would be reduced), thus minimizing the need to travel more slowly. Nevertheless, vehicles entering and exiting a multilane highway will disrupt the traffic stream at higher volume levels on the highway, resulting in reduced throughput.

3.2.1.2 Two-Lane Highways

HCM Capacity Definitions and Factors

The HCM defines the capacity of a two-lane highway as 1,700 pc/h in one direction, with a limit of 3,200 pc/h per hour in both directions, due to interactions between the two directions (HCM, p. 15-5). The HCM notes that flow rates of up to "3,400 pc/h can be observed for short segments fed by high demands from multiple or multilane facilities. This may occur at tunnels or bridges, for example, but such flow rates cannot be expected over extended segments" (HCM, p. 15-6). The types of factors that are used to adjust capacity in the HCM's freeway and multilane highway methods (e.g., heavy vehicles, grades, access density) do not affect capacity in the two-lane method; rather, they adjust free-flow speed, which is used in predicting various measures of two-lane highway operations, as well as the conversion of vehicles to passenger car equivalents.

Research for an update of the HCM two-lane highway method (Washburn et al., 2018) keeps the current HCM capacity values, but also notes that the capacity of passing sections may be lower than the capacity of the rest of the two-lane highway, due to merging turbulence at the end of the passing lane. The capacity of passing lanes is a function of the heavy vehicle percentage and the highway's vertical alignment.

Potential Impacts of CAVs on Factors Influencing HCM Capacity

As with other types of roadways, CAVs offer the potential for increased capacity due to shorter headways between vehicles. The same potential safety, liability, and vehicle occupant comfort constraints mentioned for freeways are also considerations for how much of a capacity increase can be realized for two-lane highways. The same considerations for heavy vehicles on freeways would also apply to two-lane highways.

CAVs may also affect two-lane highway operations by providing more uniform speeds and by adhering to speed limits. When all vehicles travel at the speed limit (or the safe speed for a given stretch of two-lane highway), the need to pass is eliminated. "Familiarity" with the road characteristics would allow an automated system to drive a horizontal curve at the highest safe speed, whereas an unfamiliar driver might drive it more cautiously. Only in the cases of heavy vehicles on upgrades, farm equipment, and other lower-performance vehicles unable to maintain the speed limit (including bicycles using the travel lane), would there be a need for vehicles to pass. As a result, there would be less interaction between the two directions of travel (allowing for higher two-directional capacities) and less need for passing lanes on level sections of road (eliminating the capacity-reducing effect of merging turbulence).

3.2.2 Interrupted Flow

3.2.2.1 Signalized Intersections

HCM Capacity Definitions and Factors

The capacity of a signalized intersection is defined as "the maximum number of vehicles that can reasonably be expected to pass through the intersection under prevailing traffic, roadway, and signalization conditions during a 15-min period" (HCM, p. 19-12). Capacity is the product of the saturation flow rate (the average flow rate for the lane group), the number of lanes, and the effective green–to–cycle length ratio (the proportion of the time that traffic can enter the intersection).

Potential Impacts of CAVs on Factors Influencing HCM Capacity

Saturation flow rate. The saturation flow rate reflects the average headway between vehicles in exclusive through lanes. The HCM's default value of 1,900 veh/h/ln for larger urban areas is equivalent to an average headway of 1.9 seconds. To the extent that CAV technology permits shorter headways, the saturation flow rate could be increased. Factors that could work against the ability to provide shorter headways include:

- **Safety and liability concerns.** Compared to freeway conditions, much more activity and potential hazards are present on an urban street. In particular, the presence of vulnerable road users must be considered, as they may move in unpredictable ways and any collision will be more likely to result in serious or fatal injuries, compared to vehicle–vehicle collisions.

- **Need for gaps for lane-changing.** On multiple-lane streets, the right lane is often used by turning vehicles, buses stopping to serve passengers, cars making parking maneuvers, etc. As a result, vehicles will desirably avoid the right lane to avoid delays and acceleration/deceleration discomfort to vehicle occupants. Similarly, cars will need to merge left to make left turns. Gaps will be required in traffic to allow vehicles to make these maneuvers when needed.

- **Vehicle occupant comfort.** Similar to other situations, vehicle manufacturers may decide to provide longer headways than the minimum needed for safety in order to minimize the number of times a vehicle must accelerate or decelerate in reaction to the vehicle in front, sparing the vehicle occupants from uncomfortable jerk sensations.

- **Gap acceptance behavior for permitted turns.** CAVs might be less aggressive than human drivers when choosing gaps in conflicting vehicular, bicycle, and pedestrian traffic when making permitted left turns, or when crossing bicycle lanes and crosswalks when making right turns, which could reduce the capacity of those turning movements.

Signal timing. CAVs may influence the effective green time in the following ways:

- Start-up lost time would be reduced, as computer control could react nearly instantaneously to the start of green. It would not be entirely eliminated, however, because the first few vehicles would still enter the intersection with longer headways, as they accelerate up to running speed.

- Clearance lost time would probably remain the same, as visual signal indications would still need to be provided for the non-CAV component of the traffic stream (i.e., older cars, bicyclists, pedestrians), as well as for CAVs at traffic signals lacking direct communication to vehicles about how much green time remains.

3.2.2.2 Unsignalized Intersections

HCM Capacity Definitions and Factors

Capacity at unsignalized intersections reflects how many vehicles making a given controlled movement, or on a given controlled approach, can reasonably be expected to pass through the intersection in a given 15-minute period. For two-way stop-controlled intersections and roundabouts, capacity is a function of "the distribution of gaps in the major-street traffic stream, driver judgment in selecting gaps through which to execute the desired maneuvers, and the follow-up headways required by each driver in a queue" (HCM, p. 20-3). At all-way stop-controlled intersections, capacity is a function of the saturation headway on an approach, considering both the need to stop and then accelerate through the intersection, and to yield the right-of-way to conflicting vehicles that arrived first.

Potential Impacts of CAVs on Factors Influencing HCM Capacity

CAVs may influence unsignalized intersection capacity in the following ways:

- **Gap acceptance behavior.** CAVs might be less aggressive than human drivers in selecting gaps. Even though the computer in theory could select a smaller gap that would just avoid a collision, it would probably not be programmed to do so because of safety and liability concerns (what happens in the event of an electronic or mechanical failure while making the maneuver?). Therefore, CAVs might only select gaps where conflicting vehicles could safely stop in an emergency and would not exhibit the tendency of human drivers to select shorter gaps as their waiting time increases. In addition, with less than 100% market penetration, CAVs might be more cautious than human drivers when choosing to take a gap when a conflicting vehicle is signaling it will turn (and will therefore not conflict). Both of these factors would tend to reduce capacity from current HCM levels.

- **Follow-up time.** Follow-up time reflects the time for the second driver in a queue to move to the front of a queue, identify potential conflicts, and enter the intersection if no conflicts are observed. A CAV may be able to do this more quickly than a human driver, which would reduce the follow-up time and increase capacity. If CAVs were exempt from the requirement to come to a full stop at

stop-controlled intersections, follow-up time (and critical gap) would be further reduced.

- **Behavior at all-way stops.** The HCM notes that "although giving priority to the driver on the right is a recognized rule in some areas, it is not a good descriptor of actual intersection operations. Drivers develop a consensus of right-of-way that alternates between the drivers on the intersection approaches, a consensus that depends primarily on the intersection geometry and the arrival patterns at the stop line" (HCM, p. 21-2). In a mixed environment of CAVs and non-CAVs, it might be more difficult for CAVs to develop this informal consensus with human drivers (as they will have difficulty interpreting other drivers' intentions and gestures and vice versa), and therefore may react more cautiously, which would tend to decrease capacity. In a 100% CAV environment, algorithms would definitively determine the order in which vehicles proceed, and capacity would increase.

3.3 POTENTIAL CAPACITY EFFECTS OF CAVs

With the rapid advancement of CAVs and the projected rapid growth in market penetration rate (MPR), there has been a strong research interest for the last few years to understand the potential capacity effects of CAVs under various MPRs and roadway facility types. This has resulted in many research papers that have attempted to model CAV impacts. However, CAV deployments are still limited, and their capacity effects are still unknown. Due to the uncertainty involved, most studies depend heavily on underlying assumptions and factors to estimate the potential capacity impacts of CAVs, which results in mixed findings. In the literature, positive as well as negative impacts of CAVs have been reported. This section provides a summary of literature that examines the relationship between CAVs and their capacity effects.

Table 3.1 lists the key research papers found in the literature that studied the capacity effects of CAVs. The table also lists the methodology applied along with key assumptions, major findings, and main limitations. The papers are ordered based on the methodology applied. First, research that relied on microsimulation is listed, followed by papers that used analytical models, and finally driving simulators.

The following summarizes the literature review for the potential capacity effects of CAVs:

- Most of the research in the literature focuses on basic freeway segments (e.g., a single-lane freeway scenario) without any merge, diverge, or weave segments. The effect of CAVs on more real-world geometric conditions is required. In addition, the research on the effects of CAVs at signalized intersections and especially arterials are limited, requiring further research.

- The documented capacity benefits of CAVs vary widely in the literature based on the underlying assumptions. More realistic headway and lane changing assumptions are necessary based on the CAV technology capabilities along with policy guidance and Original Equipment Manufacturer (OEM) safety margins that can incorporate risk and insurance calculations.

- Microsimulation and analytical models are the two most common methods used to explore the potential capacity effects of CAVs. For research that relied on microsimulation, one of the main limitations found is that some researchers utilized built-in driver models to model CAVs; these built-in models are intended to simulate human driver behavior.

- Almost all researchers reported that capacity effects of CAVs are small under low MPRs (e.g., 10–15 percent), and higher MPRs are generally required for the capacity benefits to be realized. Furthermore, some studies found that an increase in MPR provides a greater capacity benefit when the MPR is low (e.g., 10–25 percent), while the capacity benefit remains almost the same under high MPRs (e.g., 75–90 percent).

- For freeway segments, maintaining extremely short headways may not provide sufficient gaps for lane changes, reducing the capacity benefit for weaving segments and undermining the potential capacity benefits of CAVs.

Table 3.1: Literature Summary of Potential Capacity Effects of CAVs

Paper	Methodology	Key Assumptions	Limitations	Key Findings
Hartmann et al. (2017)	Microscopic simulation	• AVs have the capability of following their predecessor with a constant headway • Headway assumptions: Conventional vehicle = 1.1 sec; Partially AV = 1.8 sec; Highly AV = 1.8 sec; CAV = 0.9 sec • For the operation of CAVs, desired gap time of 0.9 sec if following another CAV and 1.8 sec if following a non-CAV vehicle	• VISSIM's built-in driver model is used to model CAVs, which is intended to simulate human driver behavior	• Capacity deteriorates due to a gradual increase in MPR of AVs due to the conservative headway assumptions compared to conventional vehicles • CAV benefits are not significant in low MPRs. The capacity benefit can be realized when automated technology is combined with connected technologies when extremely short headways are allowed. • The automation of vehicles has the potential to increase the capacity by 45% in basic road segments. • Keeping the extremely short headways does not provide sufficient gaps for lane changes, reducing the benefit for the weaving segments
Kesting et al. (2010)	Microscopic simulation	• A new car-following model is used to simulate ACC vehicles. The model is based on the Intelligent Driver Model developed by Treiber et al., 2000. • 0% – 100% MPR was tested on a multilane highway • 0.5 – 1.0 sec headway distribution was assumed • Only CVs were considered	• Right turn traffic was not considered.	• For the maximum free flow, an approximately linear increase was found between capacity and ACC fraction (capacity increase by about 0.3% per 1% ACC fraction). • The dynamic capacity shows a non-linear relationship with an increase of about 0.24% per 1% ACC fraction for small equipment rates.
Calvert et al. (2017)	Microscopic simulation	• Three types of vehicles are defined: Regular manual vehicles; low-level automated	• The applied Lane-change Model with Relaxation and Synchronization	• There is a small decrease in capacity for a share of 10–80% of ACC vehicles compared to 2% of ACC (which is what was used for the reference capacity). Only for a share of above 90% of

Paper	Methodology	Key Assumptions	Limitations	Key Findings
		adaptive cruise control (ACC) vehicles; and manual trucks • Minimum CV lane change headway is assumed as 0.8 sec • CV time headway assumed distribution between 0.2 sec and 2.0 sec (extreme values) where most headways are in the 0.8 sec to 1.6 sec range • MPR of 2% to 100% was explored.	(LMRS)-IDM+ model combination offers an improvement in model development but still lacks full implementation of real driver behavior due to a lack of empirical ground truths and theoretical constructs.	ACC vehicles, an improvement was observed in traffic flow and capacity. • The influence of a higher and lower onramp flow gave an unsurprising reduction and increase in capacity and travel times, respectively, as the bottleneck became more severe. The only real outcome of interest for the onramp flow percentage is that, for a low onramp flow, there is no significant deterioration of traffic flow, as seen from higher onramp flows. • Experiments showed that a relatively low share (less than 30% low-level automated vehicles) has a limited effect, compared to higher arbitrary penetration levels.
Aria et al. (2016)	Microscopic simulation	• 0% – 100% MPR, in increments of 10%, was tested • The analysis focused on freeways • Time headway of 0.3 sec is assumed using the Wiedemann 99 car following model	• VISSIM's built-in driver model is used to model CAVs, which is intended to simulate human driver behavior	• Average density of the investigated freeway segment in the AV scenario remarkably improved by 8.1% during the p.m. peak. • Average travel speed increased both on the mainline freeway (8.5%) and the weaving segment (7.9%) in the AV scenario • Not surprisingly, the results of the microscopic simulation in this study revealed that the positive effects of AV are especially highlighted when the network was congested (e.g. during the a.m. or p.m. peak).
Ntousakis et al. (2015)	Microscopic simulation	• 0% – 100% MPR, in increments of 25%, was tested • The analysis focused on freeways	• The simulation was only applied to a single lane scenario	• The capacity increases with ACC penetration rate as long as the time-gap setting is less than 1.10 – 1.20 sec. In cases where this value is higher, the capacity decreases with the penetration rate.

Paper	Methodology	Key Assumptions	Limitations	Key Findings
		• The reaction time (to acceleration, deceleration, etc.) of 0.1 sec and 0.7 sec is used for ACC vehicles and manual vehicles, respectively. • Different time headways were used (ranging from 0.8 sec to 2.0 sec) • Typical values of acceleration are 2–3 m/s^2 and deceleration are 3–5m/s^2		• A high ACC penetration rate combined with a long-desired time-gap setting could lead to a very low capacity. It is observed that density increases with the penetration rate as long as the time-gap setting is less than 1.10 sec. This is expected due to the fact that inter-vehicle spacing is smaller compared to manual vehicles.
Lazar et al. (2018)	Microscopic simulation	• A platoon of 16 vehicles was assumed (a leader and 15 followers) • 0% – 100% MPR, in increments of 10%, was tested • For the connected vehicles of the platoon, 0.7 sec headway was considered. For manually driven vehicles, 1.8 sec headway was assumed • The first 10 vehicles are organized in a platoon and other 6 vehicles are not part of the platoon (1.8 sec headway)	• Did not consider the possibility of lane changing by human drivers in the traffic stream	• Vehicle platooning with coordinated start generates shorter following gaps ensuring the arterial intersection improvement by increasing the urban arterial capacity. • The capacity of the urban arterials could increase considering that the vehicles are able to maintain a safe small distance between them while they pass through the intersection.
Le Vine et al. (2015)	Microscopic simulation	• The analysis focused on arterials. • Modeled AVs based on the acceleration and deceleration limits using rail transit systems.	• Hypothetical data were used • No heavy vehicles were assumed • Automated-vehicle platooning (i.e.	• Average delay (weighted average across all vehicles in the simulation) increased by 5% (Light rail transit (LRT) automation scenario) and 36% (high speed rail (HSR) automation scenario)

Paper	Methodology	Key Assumptions	Limitations	Key Findings
			reduced inter-vehicle headways in comparison to human drivers) or other behavior enabled by autonomous cars' reduced reaction times (relative to human drivers) were not modeled	• Capacity is correspondingly reduced by 4% (LRT) and 18% (HSR), respectively for 25% penetration. It was found that the trade-off between capacity and passenger-comfort is greater if autonomous car occupants program their vehicles to keep within the constraints of HSR (in comparison to LRT). • Further research is needed to understand whether changes to road-use regulations would be required to prevent autonomous-car occupants from programming their cars to operate relatively smooth acceleration/deceleration profiles.
Letter and Elefteriadou (2017)	Microscopic simulation	• 100% CAV MPR • The analysis focused on freeways • A saturation headway of 1 sec is assumed. A range of minimum time headway values ranging from 0.5 sec to 3.0 sec were tested	• Lane changing not considered • Hypothetical freeway merge was used • Vehicle entry headways are exponentially distributed. • Only passenger cars assumed	• The throughput of the merging process is greatly impacted by the selected minimum time gap. If the minimum time gap is set too high, the capacity of the roadway will be lower than that of a conventional traffic stream. • Improvement ranged from 3% to 7% for the lowest flow conditions. The magnitude of the improvement increased with higher demand for two of the safe time gap settings (1 sec and 1.5 sec) by as much as 61%.
Shladover et al. (2012)	Microscopic simulation	• Four vehicles types were modeled: (1) manual, (2) ACC, (3) "Here-I-Am" (i.e., manual but equipped with a DSRC radio providing its location and speed, and (4) CACC	• Only looked at single lane, straight, freeway segment • Lane-changing and possible curves were not considered	• If all vehicles in a lane were equipped with CACC capability and the drivers chose the same distribution of CACC time gaps as they chose in our field test, the lane capacity would increase to 3,970 vehicles per hour (vph) from 2,018 vph

Paper	Methodology	Key Assumptions	Limitations	Key Findings
		• 0% – 100% MPR, in increments of 10%, was tested • The analysis focused on freeways • Adopted a simple first-order dynamic response for ACC car following {ACC: 31.1% at 2.2 sec; 18.5% at 1.6 sec; 50.4% at 1.1 sec} {CACC: 12% at 1.1 sec; 7% at 0.9 sec; 24% at 0.7 sec; 57% at 0.6 sec} {Manual driving is from 1.48 to 1.8 sec}		• At a 20% MPR, the Here-I-Am (HIA) addition increases capacity by 7%, at 30% MPR it increases by more than 10% and in the 50% to 60% MPR range the increase is in the range of 15% compared to the cases without Vehicle Awareness Device (VADs).
Ghiasi et al. (2017)	Analytical capacity model	• 0% - 100% MPR, in increments of 10%, was tested • The headway values between two heavy vehicles (HVs) range from 0.7 to 2.4 s, those for a CAV following an HV from 0.5 to 2.6 s, those for an HV following a CAV from 0.6 to 2.6 s, and those between two CAVs from 0.3 through 2 sec.	• Lane changing maneuver impact on highway capacity in mixed traffic was not considered.	• Analytical analyses reveal that contrary to the ubiquitous assumption that higher CAV penetration rates and platooning intensities always yield greater mixed traffic capacity, these two factors may not always help improve highway capacity.
Ma et al. (2017)	Analytical model	• Four levels for congestion analyzed {saturation rate f s = 0.6, 0.9, 1.2, and 1.5}; four levels for segment length L {1000, 1500, 2000, 2500 m}, and four levels for signal cycle	• Used synthetics numerical data for examples • Considered an isolated intersection scenario.	• Numerical sub-gradient (NG) algorithm significantly improves the objective value from the initial solutions, with an average of 14.16% improvement • Total system performance can improve by 37% on average through CAV control, with travel time improved by 23%

Paper	Methodology	Key Assumptions	Limitations	Key Findings
		lengths C {20, 40, 60 and 80 sec} • Did not consider possibility of reduced headways for CAVs. 100% CAV MPR.	• Did not assume a mixed traffic scenario. Single lane scenario considered.	• Performance improvement increases significantly as the cycle length goes down • When the saturation rate is low, there is potentially less stop-and-go traffic; when the saturation rate is high, there is less room for CAVs to manipulate their trajectories; either case results in smaller improvements.
Ma et al. (2021)	Microscopic simulation	• The research was specific to the operation on CAVs on managed lanes • Time gap settings was adopted from field test by Nowakowski et al. {31.1 percent of vehicle following times at 2.2 sec, 18.5 percent at 1.6 sec; and 50.4 percent at 1.1 sec} • Maximum platoon length of 10 vehicles and 1.5 sec time gap between CACC strings • Assumed in the managed lane that 100 percent of vehicles are connected vehicles (or at least equipped with vehicle awareness devices, or VADs)	• Safety benefits of the combined use of the strategies was understated • Assumed 100% communication success rate • Real-world geometric and traffic conditions were not considered.	• A significant increase in capacity with the increase in CACC vehicle market penetration • At the MPRs of 30, 50, 70, and 100 percent, capacity increases by 15, 28, 41, and 56 percent, respectively. • With lower penetration rates, the benefit of cooperative merge becomes relatively small. • Higher CAV market penetration rates result in larger system benefits, around 15% and 65% improvements on average in throughput and delay, respectively, when the penetration rate is above 70%. • The incorporation of speed harmonization generates additional benefits due to more and larger gaps being made available and thus more opportunities for ramp vehicles to merge into the mainline managed lane.
Jiang et al. (2017)	Microscopic simulation	• 0% – 100% CAV MPR tested • Microscopic car-following model called Intelligent Driver Model (IDM) is adopted to predict acceleration profile of conventional vehicles.	• Lane-changing and overtaking maneuvers are not allowed • No turning or weaving maneuvers considered	• Benefits are significant as long as there is CAV and they grow with CAV's MPR until they level off at about 40% MPR. • The proposed system could save fuel by up to 58%, reduce emissions by up to 33% and improve throughput by up to 11%.

Paper	Methodology	Key Assumptions	Limitations	Key Findings
		• Used hypothetical intersection and Poisson distribution to model the vehicle arrival pattern.	• Desired speed of conventional vehicles equals the speed limit. These vehicles travel at the speed limit unless impeded by the preceding vehicle.	• The proposed system can effectively improve throughput when the intersection is saturated (v/c = 1.0) or oversaturated (v/c = 1.2). Under these two levels of saturation, more throughput benefits were achieved with higher MPR of CAV. The benefit under oversaturated condition is higher than under saturated condition at the same MPR level. Significant benefits are observed for all levels of MPR.
Liu et al. (2018b)	Analytical model	• Assumes shifted negative exponential distribution of arrival time • 0% - 100% MPR, in 20% increments, were tested • Time gap settings was adopted from field test by Nowakowski et al., (57% of the modeled drivers chose a time gap of 0.6 sec, 24% of them 0.7 sec, 7% of them 0.9 sec and 12% of them 1.1 sec) • Assumed that the parameter values are the same over different CACC market penetration cases.	• Lane changing behaviors for the CACC drivers are limited. • The study suggested future update of CACC Vehicle Managed Lane (ML) and Vehicle Awareness Devices (VAD) algorithm proposed to implement data from future field tests.	• Bottleneck capacity increases as the on-ramp traffic volume grows. • VAD can bring about greater improvement in the bottleneck capacity than the ML strategy. • Traffic flow becomes less congested with more CACC vehicles in the traffic stream • The rapid decrease of vehicle travel times is not apparent until the CACC market penetration is 20% and higher. The total vehicle travel times is almost the same between 0% and 20% CACC cases • The space mean speed has the same trend as the total vehicle travel times. At 100% market penetration, the freeway capacity is roughly 90% higher than at 0% market penetration • ML and VAD were helpful at low and medium market penetrations as they increase the probability of forming CACC strings, and they can lead to a capacity improvement ranging from 8% to 23%.

Paper	Methodology	Key Assumptions	Limitations	Key Findings
Shi and Prevedouros (2016)	Analytical model	• 0.1%, 1%, 5%, 10%-60%, 90%, 100% MPR were tested • Basic freeway and freeway weaving segments were considered • 0.5 sec for CV and 1.0 sec for AV headways were assumed	• More advanced settings, such as adaptive headways	• Driverless cars (DLCs) will provide low or no improvement in LOS in low density conditions. DLC shares below 2% are unlikely to produce detectable improvements in the quality of traffic flow. More improvement on LOS can be achieved by shortening the DLC car following headway • DLC benefits in freeway operations may take decades to materialize. V2V and V2I communications between vehicles and infrastructure may provide more efficient traffic flow, particularly at the weaving flows of freeway merges and diverges. Thus, there are two ways of improving traffic flow by adopting DLC: Either by improving their technological capability with short headways or by increasing the traffic compositions of DLC in traffic, as long as DLC are tuned with headways that are shorter than the average driver's • When DLCs reach 100% share, capacity triples.

Paper	Methodology	Key Assumptions	Limitations	Key Findings
Gouy et al. (2014)	Driving simulator	• 0.3 – 1.4 sec headways. • Focused on freeways • The first factor had two levels: in one condition (THW03) the time headway adopted in platoons was 0.3 sec; in the other (THW14) the time headway was 1.4 sec. • Trucks were selected to form platoons instead of cars as they are more prominent than cars. Trucks were therefore meant to increase prominence in the visual channel with platoons, increasing the probability of nearby drivers to pay attention to this channel and in turn to be influenced by platoons. Hence, the number of vehicles in a platoon (10 trucks in THW03 and 4 trucks in THW14) and the distance between the vehicles were manipulated.	• Further work needed to investigate whether behavioral adaptation of non-platoon drivers to short THWs in platoons is the result of a combination of social and perceptual mechanisms or primarily one mechanism • Car drivers are perhaps more likely to reproduce behavior from other drivers similar to themselves.	• The analysis of the mean THW showed that there was a significant difference between the two platoon conditions. Therefore, results verified the hypothesis that the presence of platoons of trucks maintaining short THWs in traffic have an influence on drivers' tactic as measured by mean THW. • Drivers tend to reduce their THW toward a lead vehicle when driving in the vicinity of a platoon keeping short THWs. A decrease in THW increases the probability of a collision. • The results showed the impact of short THWs on unequipped vehicle drivers in a very specific driving situation.

3.4 POTENTIAL TIMELINES FOR CAVs

Two terms for the transition from human driver to automated driving systems are being used in the auto industry. First, there is the *evolutionary* path to automated vehicles, where today's cars get self-driving features incrementally—for example, Tesla's AutoPilot feature. Second, there is the *revolutionary* path, where fully self-driving cars, such as the ones Waymo is working on, start as test vehicles and become more mainstream as they can drive in more places (Bhuiyan, 2016).

3.4.1 Understanding Fleet Turnover

The average age of light duty motor vehicles on the road in the US is currently 11.6 years (as of 2016), and as of 2015, it takes 14.8 years for vehicle fleet turnover (Schwartz, 2018). The 2017 National Household Travel Survey (NHTS) reported that households held on to their cars, trucks, and vans longer (USEIA, 2018). As shown in Figure 3.2, the average light duty vehicle age in the U.S. was 8.4 years in 1995, 10.3 years in 2009, and 11.6 years in 2016 (BTS, 2019).

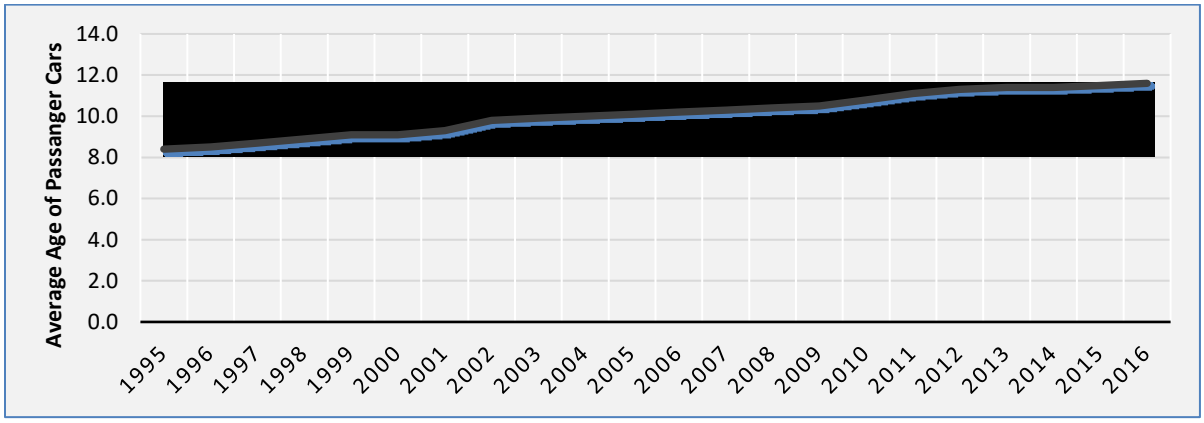

Figure 3.2: Average age of passenger cars in the U.S. (Source: Derived from Bureau of Transportation Statistics, 2019).

New vehicles are becoming more durable, which in turn prolongs fleet turnover. As new vehicle technologies emerge it may require three to five decades for those new technologies to penetrate 90% of new vehicles fleets (Litman, 2019).

Looking at examples of previous vehicle technology deployments to reach 90% of new vehicle fleets:

- Automatic transmissions took about 50 years
- Hybrid vehicles took over 25 years
- Navigation systems took over 30 years

Even if automated vehicle technologies penetrate the new vehicle market during the 2020s, most vehicles in the U.S. fleet will not be capable of operating at high levels of automation until the 2040s or 50s (Litman, 2019).

3.4.2 Connected Vehicle/Technology Turnover

Some car manufacturers already incorporate direct communications to their vehicles via the cellular network (e.g., Toyota, General Motors' OnStar). Other manufacturers have announced the installation of dedicated short-range communications (DSRC) units in some models after 2020 (e.g., Cadillac, Ford) (Alleven, 2018; Ambuelsamid, 2018).

The technical challenges for the future of connected vehicles are related mostly to regulatory uncertainty, slow turnover of vehicles in the marketplace, and infrastructure costs. There is also uncertainty about the future of the communications band currently allocated for DSRC communications. FCC allocation of the bandwidth for DSRC is temporary. The value of connectivity increases as more vehicles are equipped with that capability. Until federal incentives or regulations are developed to spur CV installations, the US fleet will not reach 100% CV penetration for a long time.

3.4.3 Automated Vehicle/Technology Turnover

The following timeline reflects different opinions about potential fleet turnover. Implementing automated features has proven more challenging than forecasted, which has delayed some projections.

- 2017–2019 (Bhuiyan, 2016)
    - Driver-assistance features get more sophisticated and sync up with GPS and navigation. The automated driving system can take control for some driving tasks and return control to human driver to conclude remaining driving tasks.
    - Commercial trucks will likely be the first production vehicles to hit the road with more advanced levels of automation, such as platooning (pending regulations).
- 2020
    - Cars equipped with semi-automated features will be able to navigate through traffic lights and intersections and stop-and-go traffic — which means a reduction in the limits and boundaries of the operational design domain for automated vehicles.
    - Most vehicles manufactured feature level 3 automation.
    - Highly automated cars — which can drive themselves, but still require a human to sit up front in case of emergency — hit the roads.
    - Tesla says it should have a self-driving a car road-ready by then.
    - Lyft and Uber expect to use highly automated cars in specific parts of highly mapped cities or more limited locations like college campuses.
- 2020–2023

    - Semi-automated features should work in more conditions, like in rain and at night. But automakers working on tech are unlikely to spend time bringing it to city streets. They will be more focused on enhancing long commutes.

    - Fully automated technology enters the market.

    - For certain, affluent buyers, automated cars may become more appealing than cars that switch between manual and automated modes.

    - The Ubers of the world may start using cars without any drivers at all. Those cars will rack up a ton of miles quickly, since they are always going to be in motion — they will only have to stop for fueling, pick-up, and drop-off. Which means the cars' shelf life will be much shorter.

- 2025–2030

    - Semi-automated features will continue to get better, but they will be less interesting, as the auto business moves to fully automated cars.

    - Now that most cars are fully automated, sales will decline: More consumers will rely on ride-sharing or may share a car with multiple owners.

    - Level 4–5 automated vehicles are available at a moderate premium price (Litman, 2019).

    - Car manufacturers will need to find new ways to generate recurring revenue from vehicles for things like data or access to different kinds of content.

- 2030

    - Automakers will stop manufacturing cars that do not have at least some highly automated features. This will happen more quickly if there is, as expected, a steep drop off in personal car ownership rates as more people depend on ride-hail services (Keeney, 2017).

    - Outside dense urban areas, automated taxis/rideshare vehicles and transit are relatively inconvenient and unlikely to replace private vehicles in suburban and rural areas (Litman, 2019).

    - Level 4–5 automated vehicles are available at a minimal premium price (Litman, 2019).

    - Less than 10% of fleet vehicles are level 4–5 automated (Forsgren et al., 2018).

    - Manual driving, meanwhile, will start becoming restricted to geo-fenced areas like a race or test track. Driving your own car will become a hobby or a luxury.

- 2045–2050

- It takes approximately 15 years for an auto fleet to turn over. Therefore, if automakers start producing nothing but fully automated cars in 2030, the streets and highways will still have a mix of manual, semi-automated, and manual cars until 2045 or later. The prevalence of used car marketplaces like today's Beepi and Shift exacerbate this turnover rate.

- Level 4–5 automated vehicles are standard on most new vehicles and make up 80–100% of vehicle sales, assuming level 4–5 vehicles become commercially available in the 2020s (Litman, 2019).

- 50% of new car sales feature automated vehicle technology, 35% of total fleet vehicles (Forsgren et al., 2018).

- Traffic signs and infrastructure may become sparse — replaced with smaller, cheaper equipment that only needs to communicate with cars.

3.4.4 Summary

- Some experts believe it will be decades and not years before a vehicle can drive itself at any speed on any road in any weather (Litman, 2019)

- AV penetration widespread enough to have a profound impact on the transportation system is likely to be far off (Forsgren et al., 2018)

- In order to see market saturation of highly automated vehicles, the technology needs perfecting. Once technology is perfected it is predicted that it will take another 13 years for 50% of cars and 27 years for 90% of cars to operate at highly automated levels (Straight, 2018).

CVs that communicate with other vehicles and with roadway infrastructure can use the real-time data they receive to anticipate what is ahead, make better route choices, and synchronize speeds to safely travel at shorter headways. All of these benefits should result in better use of roadway infrastructure, fewer breakdowns in vehicle flow, and reduced congestion (Forsgren et al., 2018). However, the revolutionary benefits gained through CAVs can only be realized with a high market penetration of vehicles with level 4 or 5 automation. When a significant share of vehicle travel is automated, lane capacity could increase by 5%–7% by 2030 to 2035 (Forsgren et al., 2018). Other market characteristics such as toll facilities, managed lanes, traffic infrastructure, and connected vehicle technology will also influence the operational design domain of automated driving systems and influence the extent to which CAVs disrupt the market.

There are several predictions and ranges as to when, how, and by how much CAVs infiltrate the market (Figure 3.3 and Figure 3.4). "People are overestimating how quickly level-5 autonomy will come and overestimating how widespread level-4 autonomy will become in the near future" (Brooks, 2017). While the evolution of CAV technologies continues to improve, there will still be a range of automated vehicles, and human driven vehicles sharing the roads for some time to come. In addition to the range of vehicles sharing the road, there will also be a range of automated vehicle levels on the road.

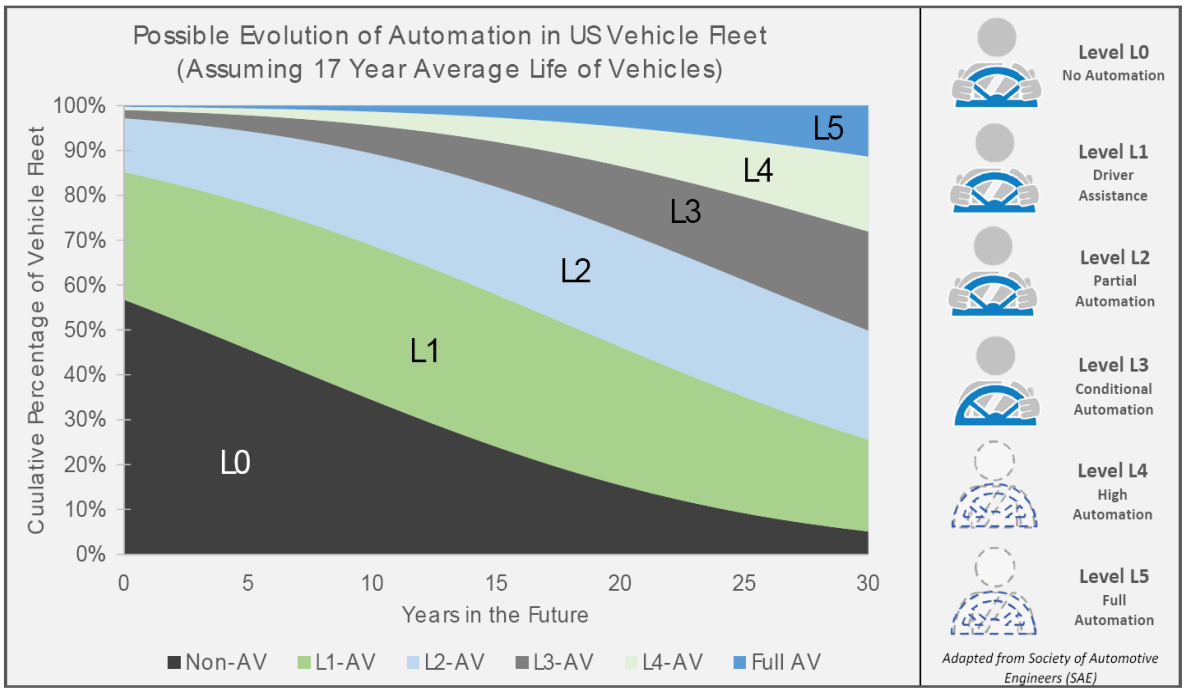

Figure 3.3: Possible evolution of automation in U.S. vehicle fleet (Source: Adapted from SAE (2018) and Litman (2019)).

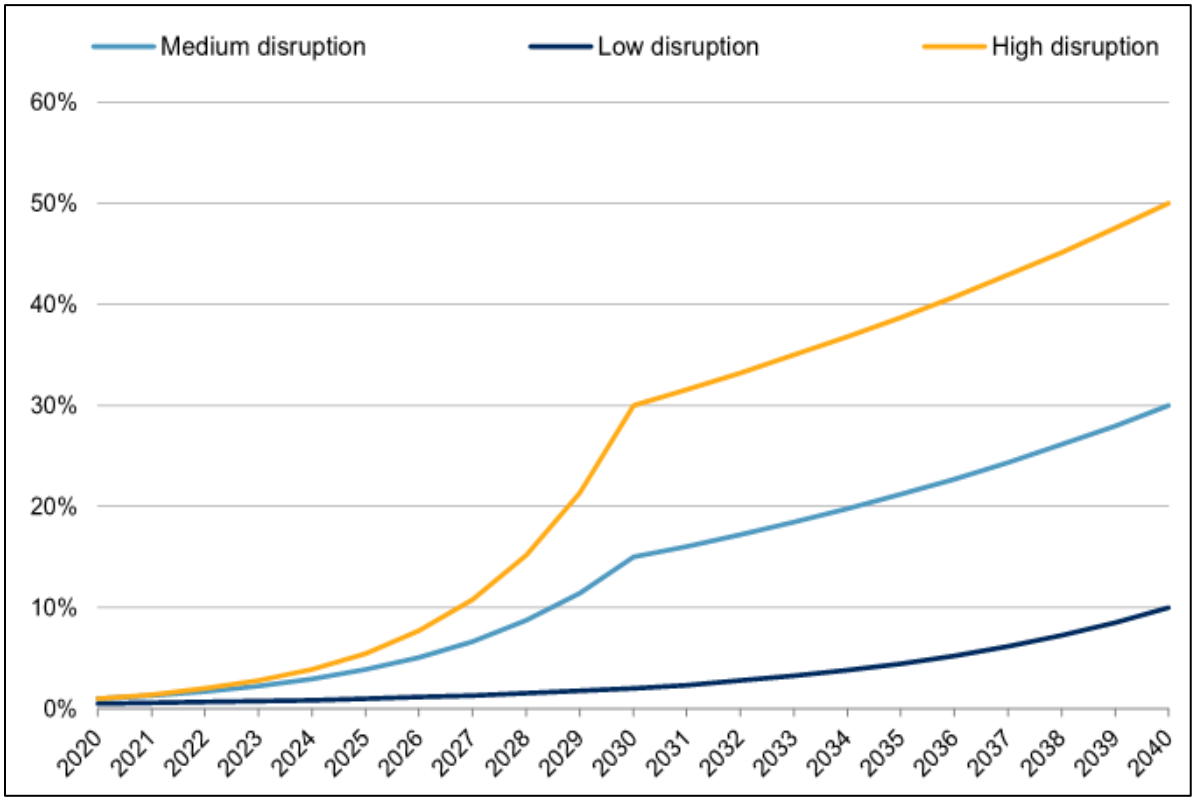

Figure 3.4: Automated vehicle adoption rate forecast (Source: Adapted from Forsgren et al., 2018).

3.5 MODELING AND SIMULATION TOOLS

3.5.1 Introduction

Transportation modeling has two main aspects: *modelling for planning*, which involves area/region-wide level of modeling, and *simulation models*, which are used to analyze subnetworks or specific roadway networks. Analysis/Modelling/Simulation (AMS) tools have been developed in the past to study various aspects of transportation systems operations and safety. While some provide platforms for investigating possible long-term facility improvements, others are used for investigating short-term improvements. AMS tools allow different scenarios of transportation infrastructure and operational adjustments to be tested, to help determine optimal choices.

Emerging CAV applications require adequate platforms for assessing their possible impacts on present roadway and traffic conditions. CAV applications such as cooperative adaptive cruise control (CACC), adaptive cruise control (ACC), and blind spot monitoring (BSM), forward collision warning (FCW), and Eco-CACC rely on on-board vehicle sensors or connectivity to function. Existing conventional traffic simulation tools are limited in their capability to model these applications because these tools were not originally designed to handle such intelligent systems.

Conducting a naturalistic study on CAVs can time-consuming, costly, and sometimes dangerous. Traffic simulation tools, when complemented with communication modeling, are the best alternative for assessing potential impacts of CAVs. They are cost-effective and time-efficient, and do not pose any safety threats. These tools can be used to evaluate potential macroscopic-, microscopic-, and mesoscopic-level CAV benefits. Macroscopic tools are used to quantify average values characterizing a roadway facility's conditions, while microscopic tools bring the analysis down to the vehicle level. Mesoscopic tools retain the flexibility of traveler representation with the convenience, robustness, and ease of calibration of closed-form analytical equations. Figure 3.5 depicts some of the common traffic simulation tools and the analysis level(s) in which each of the tools can be effective. Some tools, such as VISSIM, SUMO, CORSIM, and SimTraffic, focus on micro-level analysis of roadways. DynaMIT, DynaSMART, DynusT, Emme, Dynameq, VISUM, and CUBE Voyager can be utilized in both macro- and meso-level analysis. PARAMICS and CUBE Avenue are used for micro- and meso- level analysis, while AIMSUM and TransModeler cover all three levels of analysis.

This study focuses on microscopic simulation because the research goal is to analyze CAV effects on roadway facility capacity. Therefore, there is a need to model detailed CAV movements, such car-following, acceleration, and lane-change behavior, to understand the collective traffic performance on each modeled highway facility.

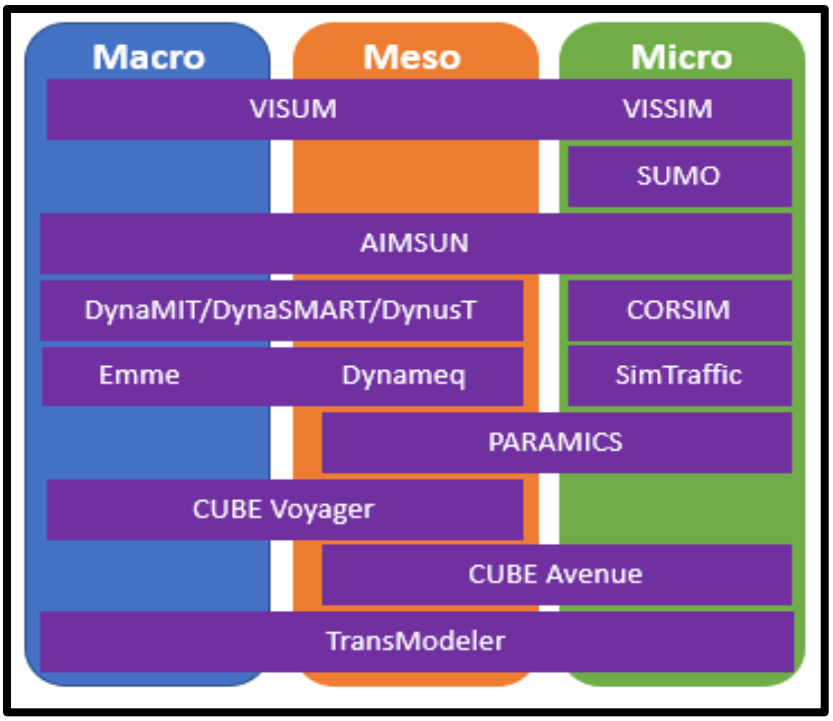

Figure 3.5: Traffic simulation analysis levels and relevant tools (Source: Reproduced from Mahmassani et al., 2018).

3.5.2 Microsimulation Tools

Modelling CAV applications requires a detailed vehicle-level approach. This need arises from not only the machine behavior originating from the embedded vehicle control algorithms and vehicle dynamics, but also the need to model the effects of connectivity between vehicles and infrastructure. Researchers have applied numerous traffic microsimulation tools in evaluating the potential benefits of CAVs, with some of the prominent tools being VISSIM, AIMSUN, and SUMO. These tools were not initially designed for CAV analysis purposes; therefore, they require some level of programming or integration with other network applications.

3.5.2.1 VISSIM

VISSIM is a microscopic traffic simulation tool used in the analysis and optimization of traffic flows. Applicable to both urban streets and highway facilities, it integrates both public and private transportation. The performance of existing transportation infrastructure can be investigated through high-level visualizations supported by realistic traffic flow models. VISSIM has been applied in corridor studies (Karakikes et al., 2017) to identify bottlenecks and potential improvements. It is also used in the study of traffic control (Stevanovic et al., 2008) such as contra-flow systems, variable speed limits, ramp metering, and route guidance. It gives high-level, detailed traffic variables such as different vehicle types (Siddharth & Ramadurai, 2013), pedestrians, and bicycles. It is one of the most popular traffic simulation tools which provide performance evaluation platform for various roadway sections such as basic freeway segments (Zhandong et al.,

2016), merge and diverge segments, weaving segments, roundabouts (Shaaban & Kim, 2015), intersections (Nyame-Baafi et al., 2018), and more (Abou-Senna & Radwan, 2013).

3.5.2.2 SUMO

Simulation of Urban Mobility (SUMO) "is an open-source, high-portable, and fast-in-run-time simulator which enables users to develop and integrate new algorithm" (Krajzewicz et al., 2012). It has been applied to investigating network performance, traffic assignment, vehicle routing, traffic impact, traffic emission, parking activities and more (Behrisch et al., 2011). Pedestrians, bicycles and their interactions with vehicles can also be simulated. It is purely microscopic: each vehicle is modeled explicitly and moves individually through the network (Song et al., 2014). It includes space-continuous and time-discrete vehicle movement (Krajzewicz et al., 2002), different vehicle types, multi-lane streets with lane changing, different right-of-way rules, and traffic lights (Vent, 2015). SUMO can be used for route choice and rerouting, traffic surveillance, vehicular communication, and traffic forecast (Behrisch et al., 2011). It has also been used for CAV modeling (Porfyri et al., 2018; Tideman & van Noort, 2013).

3.5.2.3 AIMSUN

AIMSUN provides macroscopic-, mesoscopic-, and microscopic-level simulation capabilities. It is applied in both offline and online transportation modeling. It is one of the most popular traffic simulation software packages and covers every aspect of transportation facilities such as freeways, roundabouts, intersections, weaving segments, corridors, and networks. Different control algorithms can be implemented in the modelled network by using AIMSUN's application programming interface (API).

3.5.3 CAV Modeling Capability of Simulation Tools

There are two general ways of modelling CAVs in simulation tools. One approach is to simply change the parameters in the tool's internal driver behavior model (such as the Wiedemann models in VISSIM). The other approach is to develop a custom driver-behavior model based on CAV concepts and apply it using the simulation tool's interfaces (e.g., VISSIM Driver Model API and COM Interface). In this section, VISSIM is used as an example to illustrate these different approaches. Platforms using other tools are introduced later in this section.

3.5.3.1 Internal Behavior Model Approach

In the first approach, the Wiedemann car-following parameters such as headway, safety distance, and look-ahead distance are adjusted to match the CAV machine behavior, the data for which are usually collected through small-scale field experiments. This method has been used effectively in past studies (e.g., Le Vine et al., 2015; Aria et al., 2016; Makridis et al., 2018). Few tools have provided CAV-specific behavior parameters at this point, in part because there are no field data of CAV operations that can be used for model calibration. One of the exceptions is the recently released VISSIM Version 11. PTV Group provides a detailed recommendation of parameter specifications for modeling CAVs in VISSIM Version 11. The VISSIM team conducted the research through a

European Union–funded project, CoEXist (European Commission, 2020), which collected data from a small-scale field experiments with two CAVs and a vehicle dynamics simulator, PreScan (Tass International, 2020). The Wiedemann parameters for different driving logics are provided in Table 3.2 and Table 3.3. A detailed description of each parameter can be found in any of the PTV VISSIM manuals.

Table 3.2: Wiedemann Following Parameter Variation for Different Driving Logics (Source: PTV Group, 2018)

			Driving Logic			
		Parameter	**Rail Safe**	**Cautious**	**Normal**	**All Knowing**
Following Behavior Model	**Wiedemann 99**	CC0	default	default	default	smaller
		CC1	default/higher	default/higher	default	smaller
		CC2	default/smaller	default/smaller	smaller	smaller
		CC3	default higher	default/higher	default	default
		CC4	smaller	default/smaller	default/smaller	smaller
		CC5	smaller	default/smaller	default/smaller	smaller
		CC6	default/smaller	default/smaller	default	smaller
		CC7	default/smaller	default/smaller	default/smaller	smaller
		CC8	smaller	smaller	default	default
		CC9	smaller	smaller	default	default
	W '74	ax	default	defaultault	default	smaller
		bxadd	default/higher	default/higher	default	smaller
		bxmult	default/higher	default/higher	default	smaller

Table 3.3: Wiedemann Following Parameter Values for Different Driving Logics (Source: PTV Group, 2018)

			Driving Logic				
		Parameter	**Rail Safe**	**Cautious**	**Normal**	**All Knowing**	**Default**
Following Behavior Model	**Wiedemann 99**	CC0	1.5	1.5	1.5	1	1.5
		CC1	1.5	1.5	0.9	0.6	0.9
		CC2	0	0	0	0	4
		CC3	−10	−10	−8	−6	−8
		CC4	−0.1	−0.1	−0.1	−0.1	−0.35
		CC5	0.1	0.1	0.1	0.1	0.35
		CC6	0	0	0f	0	11.44
		CC7	0.1	0.1	0.1	0.1	0.25
		CC8	2	3	3.5	4	3.5
		CC9	1.2	1.2	1.5	2	1.5
	W '74	ax	2	2	2	1.5	2
		bxadd	2	2	2	1.5	2
		bxmult	3	3	3	2	3

The driving logic relies on the vehicle's following behavior, lane change behavior, lateral behavior, signal control, and conflict resolution. In Table 3.2 and Table 3.3, the "rail safe" driving logic reflects vehicles that maintain large gaps, have a predefined route, do not make lane changes, and maintain large lateral separations. "Cautious" driving logic refers to vehicles that maintain large gaps and maintain cautious behavior, but not to the degree as "rail safe". "Normal" behavior is similar that of human drivers, but with higher safety performance. "All knowing" behavior, incorporating CAV features, maintains smaller, but safe gaps and introduces cooperative behavior.

Table 3.4 and Table 3.5 provide the necessary lane changing parameter variation and values, respectively. Table 3.6 and Table 3.7 present the necessary/free lane changing parameter variation and values, respectively. Table 3.8 and Table 3.9 are the vehicle reaction to signal control conditions. The "variation" tables give the PTV suggestion as to whether values should be lower than, higher than, or kept at the default. The "values" tables provide the actual values suggested by PTV for each of the parameters.

Table 3.4: Necessary Lane-change Parameter Variation for Different Driving Logics (Source: PTV Group, 2018)

	Control Logic					
	Cautious*		Normal		All Knowing	
Parameters	**Own**	**Trailing**	**Own**	**Trailing**	**Own**	**Trailing**
Maximum deceleration	smaller/ default	smaller/ default	default	smaller/ default	default	default/ higher
−1 m/s per distance	smaller/ default	smaller/ default	default	default	default	smaller/ default
Accepted deceleration	smaller/ default	smaller/ default	default	default	default	default/ higher

Note: *EABD (enforce absolute braking distance) must be on.

Table 3.5: Necessary Lane-change Parameter Values for Different Driving Logics (Source: PTV Group, 2018)

	Control Logic							
	Cautious*		Normal		All Knowing		Default	
Parameters	**Own**	**Trailing**	**Own**	**Trailing**	**Own**	**Trailing**	**Own**	**Trailing**
Maximum deceleration	−3.5	−2.5	−4	−3	−4	−4	−4	−3
−1 m/s per distance	80	80	100	100	100	100	100	100
Accepted deceleration	−1	−1	−1	−1	−1	−1.5	−1	−1

Notes: *EABD (enforce absolute braking distance) must be on.

Table 3.6: Necessary and Free Lane-change Parameter Variation for Different Driving Logics (Source: PTV Group, 2018)

	Control Logic		
Behavioral functionality	**Cautious**	**Normal**	**All Knowing**
Advanced merging*	on**/off	on**	on
Cooperative lane change*	on**/off	on**	on
Safety distance reduction factor	higher+EABD	smaller/default	smaller/default
Minimum headway (front/rear)	higher	default	default
Maximum deceleration for cooperative braking	smaller**	smaller**/default	default

Notes: *Depends on technical equipment and implemented connectivity and cooperative functions. **If the AV cannot detect that the other vehicle wants to change lanes, the value should be off/zero.

Table 3.7: Necessary and Free Lane-change Parameter Values for Different Driving Logics (Source: PTV Group, 2018)

	Control Logic			
Behavioral functionality	**Cautious**	**Normal**	**All Knowing**	**Default**
Advanced merging*	on**/off	on**	on	on
Cooperative lane change*	on**/off	on**	on	off
Safety distance reduction factor	1	0.6	0.5	0.6
Minimum headway (front/rear)	1	0.5	0.5	0.5
Maximum deceleration for cooperative braking	−2.5	−3	−6	−3

Notes: *Depends on technical equipment and implemented connectivity and cooperative functions. **If the AV cannot detect that the other vehicle wants to change lanes, the value should be off/zero.

Table 3.8: Signal Control Parameter Variation for Different Driving Logics (Source: PTV Group, 2018)

	Control Logic			
Attribute	**Rail Safe**	**Cautious**	**Normal**	**All Knowing**
Behavior at amber signal	continuous check	continuous check	one decision	on
Behavior at red/amber signal	stop	stop	stop/go	stop/go
Reaction time distribution	—	—	—	—
Safety distance reduction factor	higher+ EABD	higher+ EABD	default	smaller/ default
Start upstream of stop line	smaller/ default	smaller/ default	default	default/ higher
End downstream of stop line	smaller/ default	smaller/ default	default	default/ higher

Note: EABD = enforce absolute braking distance.

Table 3.9: Signal Control Parameter Values for Different Driving Logics (Source: PTV Group, 2018)

	Control Logic			
Attribute	**Rail Safe**	**Cautious**	**Normal**	**All Knowing**
Behavior at amber signal	continuous check	continuous check	one decision	on
Behavior at red/amber signal	stop	stop	stop	stop/go
Reaction time distribution	—	—	—	—
Safety distance reduction factor	1	1	1	1
Start upstream of stop line	100	100	100	100
End downstream of stop line	100	100	100	100

We believe there is a jump between "Normal" and "All knowing," similar to a jump from vehicles with advanced driver assistance systems (ADAS) to fully capable CAVs. Simply using VISSIM 11's new parameters cannot model different types of automation behavior, particularly different levels of automation and various market penetration rates of connectivity. The "Rail safe", "Cautious", and "Normal" logic do not consider connectivity between vehicles and focus only on how cautious or conservative the automated behavior is. Nevertheless, the new parameters provided by VISSIM present a good starting point of CAV modeling behavior. However, additional considerations, particularly for connectivity, will need to be programmed into the vehicle behavior logic.

3.5.3.2 Driver Model API Approach

In the second approach, CAV driving behavior is modeled using either the VISSIM Component Object Model (COM) or Dynamic Link Library (DLL) (DriverModel or DrivingSimulator) interfaces. All VISSIM data can be accessed using the COM interface; therefore, driving behavior and vehicle movements can be altered. COM is usable for V2V or V2I communication, for example to model platooning or time-slot-based intersection control. The DriverModel DLL can replace VISSIM's internal car-following behavior model with a customized algorithm. Customized algorithms for lane changing and reaction to traffic signals can be implemented as well. The DrivingSimulator DLL can be used to couple self-developed control algorithms (full behavior) with VISSIM and, optionally, to integrate nano-simulations for sensors and vehicle dynamics (e.g., PreScan, CarMaker), as was done in the CoEXist project.

Researchers have used a variety of approaches to developing, modeling, and validating CAV applications. While some have used analytical or numerical methods, many have also used microsimulation methods. Traffic simulation tools mentioned in previous sections have been used as stand-alone options and have also been integrated with other interfaces. Some applications developed using simulation tools include modeling CACC and ACC behavior. Table 3.10 presents studies which have used microsimulation tools as stand-alone or integrated alternatives to modeling the CAV environment. The network simulators are used to model vehicle connectivity within the traffic simulation platforms.

Table 3.10: CAV Modeling Use Cases

Author(s)	Traffic Simulator	Network Simulator	Application	Interface	Language
Ma et al. (2017), Ma et al. (2021)	VISSIM	Yes, NS-3	ACC, CACC, Coop. merge, etc.	DriverModel, COM	C++
Zhao & Sun (2013)	VISSIM	No	CACC, ACC	DriverModel	C++
Ntousakis et al. (2015)	AIMSUN	No	ACC	MicroSDK	C++
Aria et al. (2016)	VISSIM	No	ACC	Internal	None
Park et al. (2017)	VISSIM	No	VSC	COM	C++
Shladover et al. (2012)	AIMSUN	No	ACC/ACC	MicroSDK, API	C++
Le Vine et al. (2015)	VISSIM	No	CACC	Internal	None
Makridis et al. (2018)	AIMSUN	No	CACC	Internal	None
Letter & Elefteriadou (2017)	CORSIM	No	CACC	Internal	None
Perraki et al. (2018)	AIMSUN	No	VACS	MicroSDK	C++
Jiang et al. (2017)	VISSIM	No	Eco-CACC	COM	C++
Zheng et al. (2016)	VISSIM	NS-3.20	CACC	COM	C#
Bujanovic et al. (2018)	VISSIM	No	CACC/ACC	COM	C++
Zhao et al. (2018)	VISSIM	No	CACC	API	C++
Sharon et al. (2017)	AIM	No	N/A	N/A	C
Hartmann et al. (2017)	VISSIM	No	CACC	COM	C++
Li et al. (2014)	CORSIM	No	CACC/ACC	API	MATLAB
Lu et al. (2017)	AIMSUN	No	CACC/ACC	API	C++
Ala et al. (2016)	INTEGRATION	No	CACC/ACC	API	C++
Miloslavov et al. (2012b)	VISSIM	NCTUns	N/A	N/A	None
Miloslavov et al. (2012a)	VISSIM	NCTUns	N/A	N/A	None
Tomar et al. (2018)	SUMO	OMNeT++	N/A	Traci/VEINS	None

Note: ACC: adaptive cruise control; CACC: cooperative adaptive cruise control; Coop merge: cooperative merging.

3.5.4 CAV Simulation Platform Descriptions

This section introduces three other CAV simulation platforms: FHWA CAV Modeling Platform, which uses VISSIM, and platforms from the California PATH program and Virginia Tech, both of which employ other tools.

3.5.4.1 FHWA CAV Modeling Platform

The FHWA Turner-Fairbank Highway Research Center has developed a series of VISSIM Driver Model APIs (and COM codes) for modeling different CAV applications, including CACC, signalized intersection approach and departure, cooperative merge, and speed harmonization. The integrated CAV evaluation platform has been developed and maintained by the University of Cincinnati. This platform was originally developed for an FHWA guidebook on CAV simulation (USDOT, 2020a). Through a user-friendly input interface for setting simulation parameters, the purpose of the platform and guidebook is to enable agency staff to conduct CAV application evaluations using VISSIM without involving the heavy burden of computer programming. Also, as part of multiple completed or ongoing studies at the FHWA Saxton Transportation Operations Lab, the platform has been gradually enhanced, as demonstrated in Figure 3.6, to address the following needs:

- Modeling of automated vehicle behavior: model calibrated using available field experiment data; cooperative automation that considers collaborative behavior between vehicles, such as vehicle platooning, cooperative merge, and eco-approach and departure at signalized intersections.

- Modeling of wireless communication for CV applications to consider potential communication performance (package delay, drops): communication model calibration using the data collected at the FHWA Saxton Lab and Michigan Safety Pilot, and consideration of communication performance under various conditions (e.g., urban, suburban and rural areas).

Among all the functions, the integration of communication with the regular simulators requires running multiple simulation tools, a traffic simulator (VISSIM), and a communication simulator (e.g., NS-3) in parallel such that realistic communication behavior can be taken into consideration.

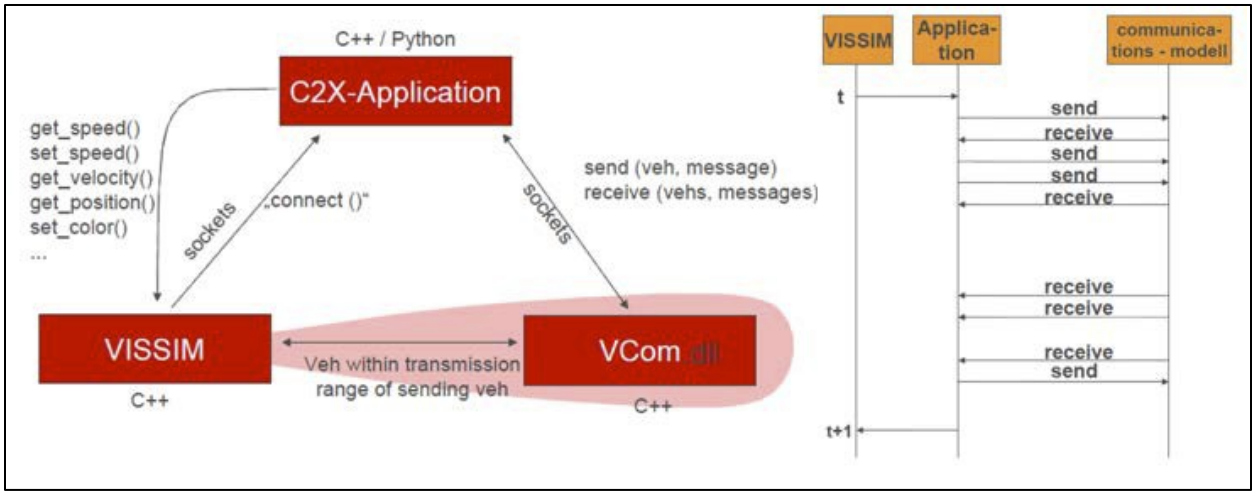

Figure 3.6: Architecture of integrated VISSIM-communication simulation

3.5.4.2 California PATH's CACC Traffic Simulation Tool

The California PATH developed a microsimulation tool using AIMSUM's Application Programming Interface (API) and Micro-SDK. The tool includes a vehicle-dispatching model, a human-driver behavior model, and an ACC/CACC model for CAVs. To simulate CACC strings for platooning, the vehicle-dispatching model determines how the vehicles enter the network and the vehicle-type distribution in the traffic stream.

To model human-driver behavior, the tool incorporates the NGSIM oversaturated flow model proposed by Yeo et al. (2008). The CACC driving behavior follows the models developed by Milanés & Shladover (2014). Using this model, CACC-equipped vehicles can form platoons that enable them to keep shorter headways. In addition, the model allows drivers of CACC-equipped vehicles to exit the platoon and drive on their own.

This tool does not explicitly model information exchange between CACC-equipped vehicles through wireless communication. As a result, it cannot be used to investigate the impacts of information loss or sensor failure on CAV driving behavior.

3.5.4.3 Virginia Tech's Eco-CACC Integration

The INTEGRATION simulation tool is a microscopic traffic assignment and simulation tool that allows detailed vehicle movement and lane changing analysis on a network. It is an agent-based simulation software that tracks the movement of individual vehicle every 0.1 second (Rakha & Ahn, 2004; Rakha et al., 2012). It is also flexible in recreating spatial and temporal variations in traffic characteristics. Along with performance measures such as stops and delays, INTEGRATION also measures fuel emission by individual vehicles. It can also estimate the expected number of vehicle crashes for use in network safety evaluations. The software provides traffic assignment/routing options such as distance-based routing, time-dependent external routing, and time-dependent dynamic traffic assignment. While there are many publications based on this tool, it is

only used by Rakha's team at Virginia Tech and the tool is not widely available to or used by the research community.

Rakha & Ahn (2004) developed an Eco-INTEGRATION modeling framework that estimates mobile emissions. The VT-Micro model was combined with the INTEGRATION microscopic simulation tool. This combined use of traffic modeling with energy and emission modeling can be utilized to investigate the environmental impact of intelligent transportation systems (ITS) and non-ITS applications (Rakha et al., 2012). Applying this combined approach to CACC traffic conditions, Almutairi et al. (2017) developed an Eco-CACC model for multiple signal systems. The objective of the Eco-CACC is to reduce fuel consumption of CACC-equipped vehicles by using the signal phase and timing (SPaT) information to control the vehicle trajectory over multiple intersections. Through V2I communication, speed limits are sent to CACC vehicle to prevent them from stopping completely at intersections, thereby reducing fuel consumption. This model was tested for different demand scenarios, market penetration, and network configurations.

4.0 FREEWAY SEGMENTS

4.1 INTRODUCTION

This section describes the development of capacity adjustment factors (CAFs) for CAVs for various freeway system elements at different levels of traffic demand and market penetration, to allow the HCM to be adapted to analyzing CAV applications. The goal of this effort was not only to quantify the effect of CAVs on basic freeway, freeway merge, and freeway weaving segments, but to also develop tables of CAFs and corresponding a statistical capacity prediction model that can be easily used to assess the impact of different future CAV implementation policies. The statistical models developed here are expected to be easily adaptable to changes in various parameters as CAV presence increases on the transportation system.

4.2 METHODOLOGY

4.2.1 Base Model Development

Three freeway segments were considered in this study as shown in Figure 4.1: a basic freeway segment (BFS), a freeway merge segment (FMS), and a freeway weaving segment (FWS). For the BFS, two hypothetical 3- and 2-lane networks were modeled in VISSIM. The FMS was a 2-lane mainline network with an on-ramp introduced one mile downstream of the start of the network. The acceleration length provided was 500 ft. Finally, the FWS was a 4-lane weaving segment, consisting of a 3-lane mainline and a single acceleration/deceleration lane, with the on- and off-ramps spaced 1000 ft apart.

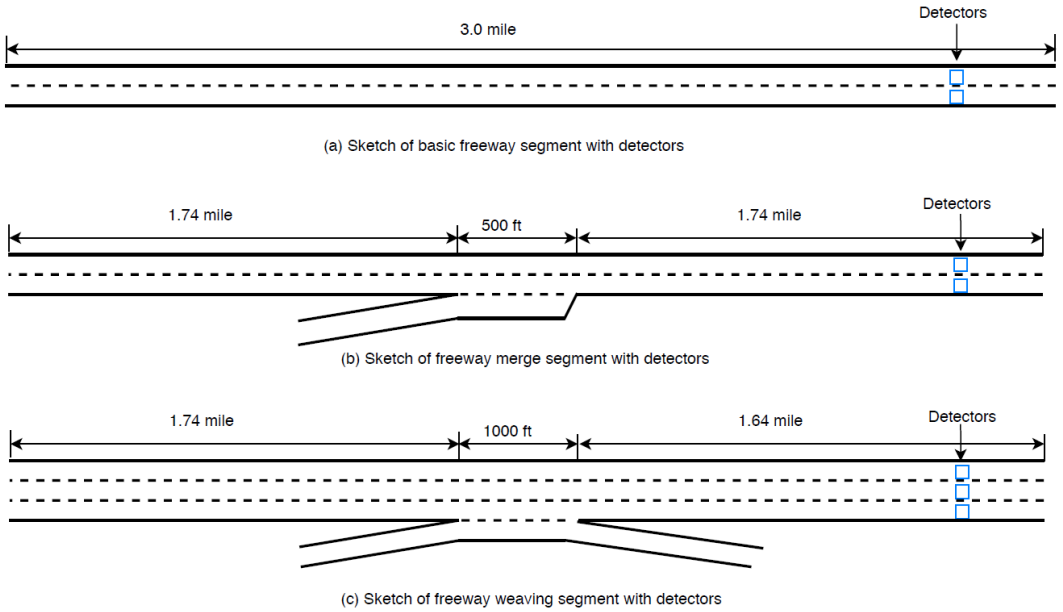

Figure 4.1: Freeway segments considered

To investigate the effects of CAVs on segments with different base capacities, the BFS was tested with base capacities of 2,400, 2,100, and 1,800 passenger cars per hour per lane (pc/h/ln). This test was conducted because a segment's base capacity can be lower than the ideal capacity of 2,400 pc/h/ln due to lower design speeds and the effects of severe weather conditions, among other factors. A selection of base capacities were only tested for the BFS; the analyses for the FMS and FWS used starting capacities of 2,400 pc/h/ln for all scenarios. This approach was taken was to limit the study scope to more common roadway configurations and to be able to analyze more facility types. In addition, a base capacity of 2,400 pc/h/ln is consistent with the HCM's ideal capacity value for a facility with a 70-mph design speed and therefore this study's results can be applied directly to existing HCM procedures. Note that although the driver behavior used for the BFS, FMS, and FWS targeted 2,400 pc/h/ln as the base capacity, the actual starting capacities for FMS and FWS were lower due to ramp and weaving disturbances.

Obtaining the desired capacity for a traffic stream consisting entirely of human-driven vehicles (HDVs) requires systematic calibration in the microsimulation model. The base model was calibrated using VISSIM's built-in driver behavior model developed by Wiedemann (1999). In this study, the Wiedemann '99 parameters, which are more suitable for freeway networks, were adjusted during calibration (Wiedemann, 1999). VISSIM provides ten calibration parameters, CC0 to CC9, which control the switching behavior of drivers. The time headway maintained by HDVs in this study was calibrated to 1.1 sec to match the base calibration. The major parameters used in calibration were CC0, CC1, and CC2, representing the standstill distance, the headway time, and the following variation respectively. The targeted starting capacities were achieved by slightly adjusting CC2. More detail on these parameters can be found in the VISSIM user's manual (PTV Group, 2018).

4.2.2 CAV Modeling

The CACC logic implemented in this study was based on a well-accepted study by Milanés & Shladover (2014) which has been previously used (Liu et al., 2018a and 2018b). Interested readers should refer to those studies for model details. We have included some basic introduction for completeness. We assumed a maximum platoon length of 10 vehicles to eliminate disturbances which could hinder the performance of the car-following algorithm at on- and off-ramps (if any) due to the necessary lane changes. If the platoon is too long, merging would be difficult and communication between the platoon leader and vehicles toward the back of the platoon would be unreliable. On the other hand, platoon lengths that are too short reduce the ability of CACC to improve capacity, because fewer vehicles will be traveling at short headways within a platoon, while more vehicles will act as platoon leaders, with a longer gap to the preceding vehicle.

The car-following algorithm is presented in Figure 4.2. It consists of three following modes—speed regulation, gap regulation, and hysteresis—for regulating a CAV's speed and/or gap to a preceding vehicle. The speed regulation mode maintains the user-desired speed when the preceding vehicle is beyond the range of V2V communication and beyond the detection range of the subject vehicle's on-board equipment. The gap regulation mode controls the dynamics of vehicles in an active CACC platoon. At a given time, a CAV can be either a platoon leader or a follower. All model assumptions and parameters used in this study are the same as provided in Milanés & Shladover (2014) and interested readers can explore the algorithm further.

The *Advanced Merging* (A.M.) algorithm used in this study is adapted from the VISSIM 11 advanced merge function and described next. The objective of the A.M. algorithm is to coordinate the mainline and merging traffic using V2V and V2I technologies. When a merging vehicle is detected, a gap is created on the mainline that can accommodate the merging vehicle. The system informs the mainline vehicles to cooperatively move out of the merging vehicle's targeted lane or to slow down slightly to create the required gap.

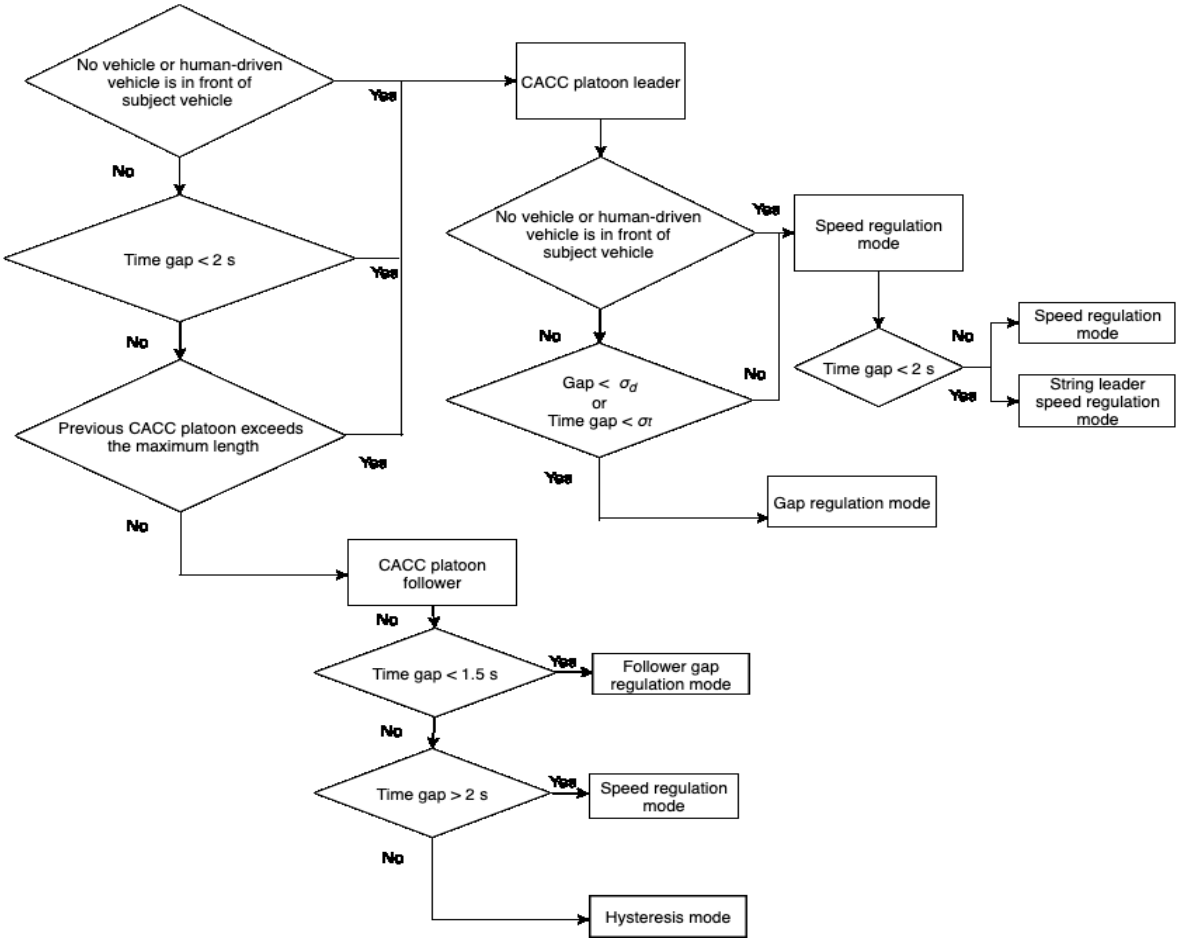

Figure 4.2: CACC car-following logic

4.2.3 Experiment Design

As previously discussed, the simulation network was first calibrated to match the HCM's capacity values. Capacity, being the performance measure of interest in this study, was estimated for different scenarios. For all scenarios tested, the market penetration rate (MPR) (used here to represent the proportion of CAVs in the traffic stream on the subject facility) was varied from 0% to 100% at 20% increments. The simulated traffic stream consisted of 100% passenger cars (i.e., no trucks or other heavy vehicles).

Three levels of intra-platoon gap were available in the simulation: aggressive (0.6 s), normal (following a distribution), and conservative (1.1 s). All three gap settings were tested in the BFS network evaluation. However, to limit the total number of simulations runs, only the "normal"

gap setting was used for FMS and FWS because this setting represents the most likely scenario. The "normal" gap settings were developed from the intra-platoon gap distribution specified by Nowakowski et al. (2010), where drivers in a test chose a 0.6-s time gap 57% of the time they were in car-following mode, a 0.7-s gap 24% of the time, a 0.9-s gap 7% of the time, and a 1.1-s gap 12% of the time.

The scenarios tested for BFS consisted of 2- and 3-lane mainline configurations and base capacities of 2,400, 2,100, and 1,800 pc/h/ln. In addition, we evaluated the impact of ACC-equipped vehicles, i.e., isolated AVs that adopt commercial automated following behavior, using empirical models calibrated by Goñi-Ros (2019). The FMS tested a 2-lane mainline with a single lane on-ramp with mainline volume-to-capacity (v/c) ratios of 0.8 and 1.0and with on-ramp volumes starting at 300 veh/h and increasing in 200 veh/h increments until a stable capacity was reached for each scenario. Finally, the FWS tested a 3-lane weaving segment with weaving volume ratios (VRs) of 0.2, 0.3, and 0.4. The VR is the ratio of weaving traffic to non-weaving traffic, given in the HCM as follows:

$$\boldsymbol{VR} = \frac{\boldsymbol{V_{RF} + V_{FR}}}{\boldsymbol{V_{RF} + V_{FR} + V_{FF} + V_{RR}}} \quad \textbf{(4-1)}$$

where:

The subscripts indicate the direction of flow, with movements from ramp to freeway denoted as RF, while movements from freeway to ramp are denoted as FR.

All the FMS and FWS scenarios were evaluated with and without the advanced merging algorithm. For each scenario, five simulation runs were performed with different random seeds. Capacity was estimated using the maximum 15-minute average moving hourly flow rate observed in the simulation, consistent with the HCM method for estimating capacity.

4.2.4 CAF Estimation

The CAF is estimated as the ratio of the capacity of the evaluated scenario to that of the base (starting) capacity. HCM Exhibit 12-6 provides the relationship between the base segment capacity and CAF as

$$\boldsymbol{c_{adj} = c \times CAF} \quad \textbf{(4-2)}$$

where

c_{adj} = adjusted capacity (pc/h/ln),

c = base segment capacity (pc/h/ln), and

CAF = capacity adjustment factor (unitless).

In most cases in the HCM, capacity adjustments due to the effects of recurring or non-recurring events reduce the base capacity because base capacity reflects ideal conditions (e.g., only passenger cars, clear day, level terrain). Therefore, the resulting CAF is typically less than 1.0. However, in the case of CAVs, it is expected that the shorter headways achieved through platooning will increase capacity; therefore, the expected CAF would be greater than 1.0.

4.3 RESULTS

4.3.1 Effects of CACC on Traffic Flow

The fundamental diagram (FD) has been used to understand traffic flow for decades. It spells out the basic principles behind the operations of freeway traffic and can also serve as a means for capacity estimation. While past studies (Talebpour & Mahmassani, 2016; Ghiasi et al., 2019) have studied the effect of CAVs on the FD and established the potential of removing the congested region due to CAV stability and coordination, we investigate the question from a different perspective. With different roadway starting capacities, we hypothesize that even though introduction of CAVs can remove congestion in regions that are congested at 0% MPR, the presence of human drivers in the traffic stream will have an effect on what level of CAV market penetration will result in removing the congested regime. To test this hypothesis, we simulated the FMS using a lower base capacity to compare the behavior of the FD at a high starting capacity and at a lower starting capacity. The results for each starting capacity at each CAV market penetration level are provided in Figure 4.3. This figure confirms earlier findings that CAVs are able to smooth out congestion. However, the results provide additional insights and indicate that the smoothing effect of CAVs are only equal across all roadway scenarios when their market penetration equals or exceeds 80% due to the dominant presence of CACC-equipped vehicles in the traffic stream at that time.

4.3.2 Capacity Effects of CAVs on Basic Freeway Segments

Figure 4.4Figure 4.4 shows the capacity of a BFS relative to the proportion of CACC-equipped vehicles in the traffic stream (market penetration rate, MPR). First, the results show that for all the car-following values used in this study (i.e., normal, conservative, aggressive), the capacity increases with respect to MPR. More interestingly, they all follow a quadratic trend, which indicates that capacity increases faster as the MPR increases. Similar insights have been established in past studies (e.g., Liu et al, 2018b) as well. However, the aggressive CACC intra-platoon gap results in greater capacity benefits. This result is logical because tighter headways between vehicles directly and positively effect capacity. The conservative car-following scenario, in comparison, has the least effect on capacity. Comparing the capacity values for different gap settings for each MPR, at 20% MPR, the CAV effects on capacity are not much different from each other, with the aggressive scenario producing only 1.2% higher capacity than the conservative scenario. However, as the MPR increases, a gradual increase in the margin between the two extreme CACC settings is observed, and at 100% MPR, a 17% margin is obtained. Note that these results are for the scenarios with a base capacity of 2,400 pc/h/ln.

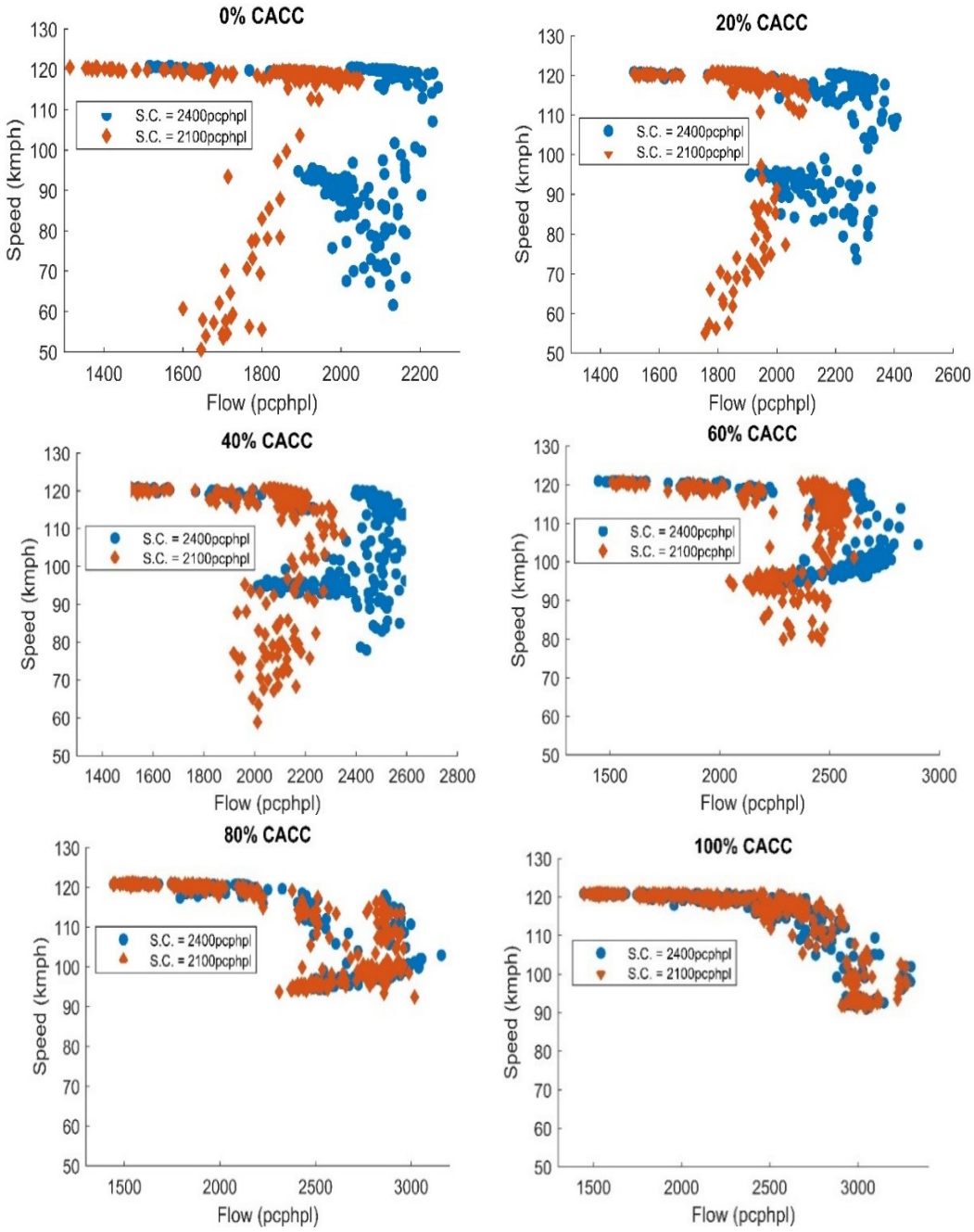

Figure 4.3: Fundamental diagrams for each CACC MPR with different mainline starting capacities

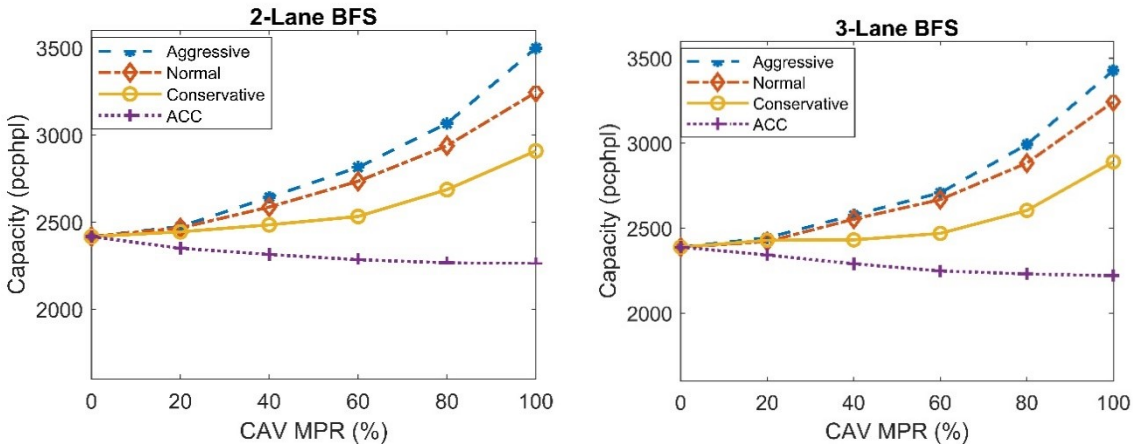

(a) Base Capacity = 2,400 pc/h/ln

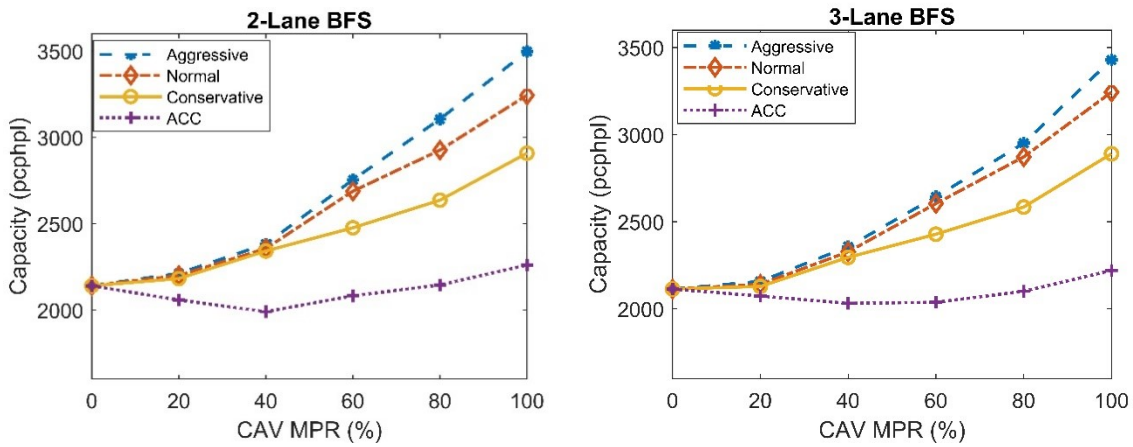

(b) Base Capacity = 2,100 pc/h/ln

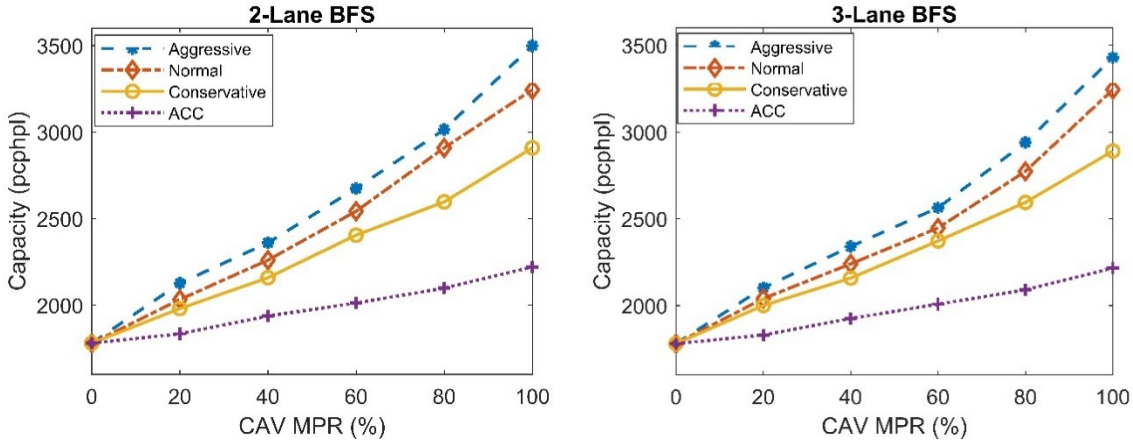

(c) Base Capacity = 1,800 pc/h/ln

Figure 4.4: CAV capacity results for basic freeway segments

Additional interesting insights can be obtained from Figure 4.4. For example, the results for a 1,800 pc/h/ln base capacity show that the initially quadratic trend of capacity improvement smoothens out to become a much linear trend. This result means that at a lower base capacity, the effects of CACCs are relatively constant as MPR increases and the CAV capacity benefits are more pronounced compared to higher base capacities, even at low MPRs.

In the 1,800 pc/h/ln base capacity scenario, instead of the 1.2% capacity difference between the conservative and aggressive car-following settings found in the 2,400 pc/h/ln base capacity scenario for 20% MPR, there is a 7% difference. However, at 100% MPR, the capacity difference between these two extreme car-following settings for the two starting capacities are the same (17%). This result further establishes the earlier statements that CACC provide higher benefits at lower MPRs for freeways with lower base capacities.

Capacity improvements were also compared for 2- and 3-lane BFS configurations. In summary, for all scenarios at all MPRs, regardless of the base capacity, the per-lane capacity of a 3-lane BFS is slightly lower than that of a 2-lane segment, all else being equal. This result can be attributed to the effect of lane changing activity and its disturbance on freeway capacity. However, the difference between the 2-lane and 3-lane scenarios is very small, partially because of the capability of CACC platoons to absorb disturbances caused by lane changes. This result provides further insights on future CACC operations in that it is preferable to limit or discourage lane changes to maintain stable traffic flow and high capacity.

While this study focuses on CAV effects on capacity due to CACC, we also conducted experiments on the effects of ACC. These results are also shown in Figure 4.4. The motivation to include ACC results is to show the importance of connectivity in enhancing capacity. First, it is observed that for a base capacity of 2,400 pc/h/ln, freeway capacity decreases as the percentage of ACC-equipped vehicles increases. This result is because ACC systems drive more conservatively than HDVs in the traffic. ACC systems are built to prioritize comfort and safety, which generally results in more conservative driving behavior. However, in the 1,800 pc/h/ln base capacity scenario, capacity increases as the proportion of ACC-equipped vehicles increases. This result occurs because even though ACC systems are designed to drive conservatively, the resulting headways are still lower than those of HDVs under low-capacity base conditions, leading to capacity improvements. This finding suggests that ACC systems can perform better than HDVs under non-ideal conditions, likely due to the deterministic behavior of ACC systems that stabilizes the traffic flow.

The result for ACC at a 2,100 pc/h/ln base capacity is also interesting. Capacity decreases at lower proportions of ACC-equipped vehicles but increases thereafter. The initial drop in capacity is a result of increased variance in driving behavior due to the distinct difference in behavior between ACC vehicles and HDVs. The eventual increase in capacity occurs because of the stability effect when ACC vehicles constitute most of the traffic stream.

4.3.3 Capacity Effects of CAVs on Freeway Merge Segments

The capacity results for FMSs are provided below in terms of CAV MPR, CACC capabilities, advanced merging (A.M.) capabilities, the mainline demand, and the on-ramp demand. As stated previously, the segment configuration evaluated consisted of a 2-lane mainline and a single-lane on-ramp. The acceleration lane was 500 feet long and started 1.5 miles downstream of the segment starting point. Table 4.1 provides capacity estimates for different combinations of MPR and technology used to assist merging. The "No on-ramp" scenario represents the segment capacity with zero ramp demand and is identical to the results of the 2-lane BFS scenario. All other scenarios were simulated by varying the on-ramp demand gradually from low (300 pc/h/ln) to high volumes. The "CACC" scenario indicates implementing only the CACC application for the CAVs in the traffic stream. The "CACC + A.M." scenarios involve equipping the CAVs with both CACC and A.M. capabilities. The "A.M." scenario indicates equipping CAVs with only A.M. capability. Each of these other scenarios was compared to the "No on-ramp" scenario and the resulting percentage difference in capacity is provided in the table.

Table 4.1: Capacity Results (pc/h/ln) for Freeway Merge Segments

	Market Penetration Rate (MPR)					
	0%	**20%**	**40%**	**60%**	**80%**	**100%**
No on-ramp (BFS)	2,416	2,466	2,586	2,734	2,938	3,244
CACC	2,206	2,242	2,371	2,556	2,932	3,296
% difference	−9%	−10%	−9%	−7%	0%	+2%
CACC + A.M.	2,206	2,353	2,439	2,662	2,976	3,306
% difference	−9%	−5%	−6%	−3%	+1%	+2%
A.M. capacity	2,206	2,231	2,280	2,330	2,346	2,353
% difference	−9%	−11%	−13%	−17%	−25%	−38%

Notes:

- All percentage differences are relative to the "no on-ramp" scenario.
- BFS = basic freeway segment, CACC = cooperative adaptive cruise control, A.M. = advanced merging.

As expected, merging traffic disturbs the traffic stream, which translates into 9% lower capacities for the fully HDV traffic scenarios (0% MPR) compared to a similar BFS. Even with increasing CAV penetration, the resulting capacity still falls below the "No on-ramp" scenario. However, upon reaching 80% CAV MPR, different results are obtained for scenarios employing CACC technology. At 80% MPR, the effect of improved vehicle capabilities allows much better coordination between mainline and merging traffic, thereby offsetting the capacity reduction as a result of the initial merging disturbance. This is because the CACC car-following behavior (i.e., control algorithms) can make vehicles react faster and stably to absorb disturbances from the downstream traffic. More specifically, the 9% reduction in capacity from merging disturbance was removed, and even at 100% MPR, the mainline was able to accommodate about 2% more vehicles merging from the ramp. In essence, as the MPR increases, the effect of merging disturbance reduces as a result of CACC coordination.

The only exception to these results is the "A.M." scenario, which involves CAVs with only advanced merging capabilities (i.e., no CACC). Although the capacity improves as the CAV

MPR increases, the effect is too low to offset the capacity reduction from the initial merging disturbances. This result further establishes the potential benefits that can be obtained from CACC vehicle operations.

With the effect of CACC already established, it is important to also examine the impact of an added advanced merging capability. This is done by comparing the "CACC" and "CACC + A.M." scenarios. The effect of A.M. is more pronounced at lower MPRs. This may be a result of more HDVs in the traffic stream, which provides more gaps for merging purposes. At high MPRs, CACC-equipped vehicles are already traveling at closer gaps with more coordination, thereby leaving many gaps for advanced merging to use. The greatest capacity improvement from A.M. capability relative to CACC is 5%, which occurs at a 20% MPR. The main capacity benefits from CAVs, as expected, come from the stable platoons operating with shorter headways.

To further explore the effect of on-ramp demand on segment capacity, we analyzed differences in capacity as functions of the on-ramp demand and enhanced vehicle capabilities. It is reasonable to assume that different on-ramp demands result in different segment capacities (e.g., the turbulence effects of an on-ramp with a demand of 100 pc/h will be less than those of an on-ramp serving 500 pc/h) (Rouphail et al., 2015). In addition, changes in mainline traffic demand may also affect downstream throughput. For instance, by setting the mainline demand to be 80% of the estimated BFS capacity for each MPR, the unused mainline capacity should be able to accommodate more merging vehicles. Figure 4.5 indicates the capacity trends as on-ramp demand increases at each CAV MPR. Both scenarios were simulated with and without advanced merging capabilities of CACC-equipped vehicles.

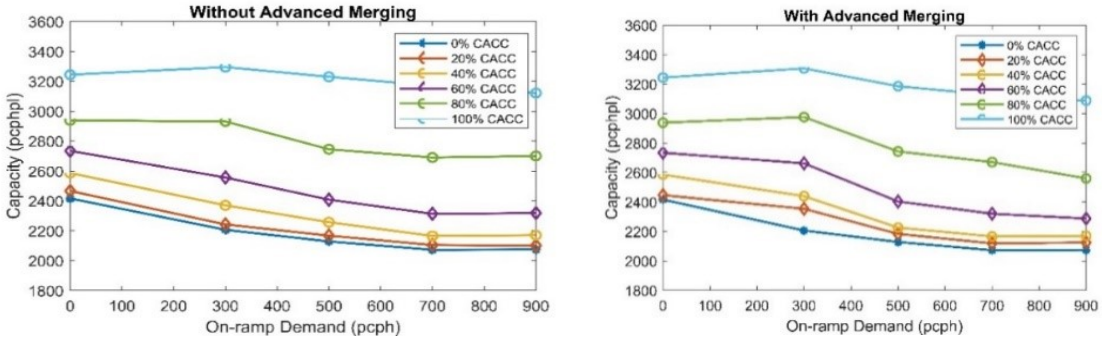

(a) 100% Mainline Demand

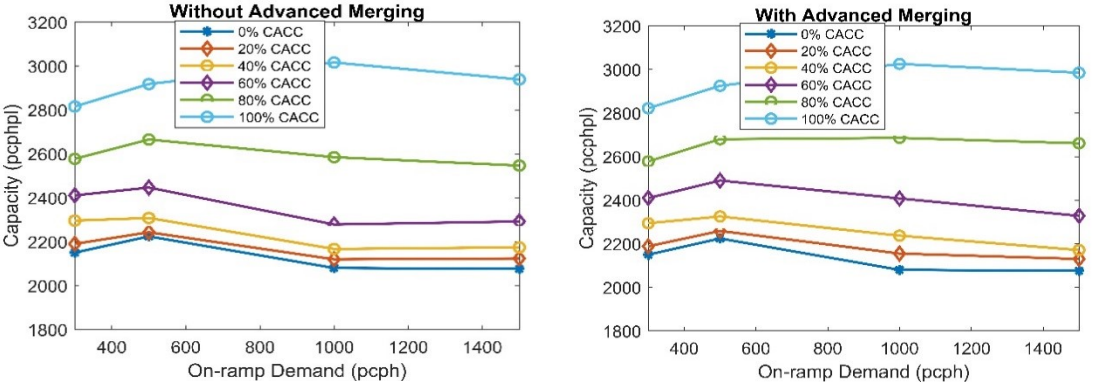

(b) 80% Mainline Demand

Figure 4.5: Capacity trend with increasing on-ramp demand by market penetration rate

In the 100% mainline demand scenario, the first interesting observation is that at low CAV MPRs, the segment capacity decreases under increasing on-ramp demand until it reaches a stable value. However, at high MPRs, the segment is able to maintain the same capacity longer under increasing on-ramp demand before reaching stable capacity conditions. These results indicate that merge segment capacity is not constant across all on-ramp demand volumes and that the capacity can decrease when on-ramp demand is high, particularly at low CAV MPRs.

In comparison, the 80% mainline demand scenario confirms the initial expectation that the unused portion of mainline capacity can accommodate more merging vehicles, and that the 20% of the volume that was removed from the mainline traffic was recovered from the merging traffic. If the 20% mainline demand is removed at 0% MPR, the segment can only accommodate about 300 vehicles, but if it is removed at 100% MPR, the segment can accommodate about 1,000 more vehicles due to CACC operations. The trend obtained at low MPRs for 80% mainline demand indicates that more vehicles can enter the mainline under this condition. However, it should also be noted that, similar to the 100% mainline demand, the capacity benefits eventually fall and then reach a stable value, also reinforcing the findings that different on-ramp demands can result in different segment capacities.

We established that at 80% mainline traffic, the merge segment can accommodate more vehicles from the on-ramp. To check the reasonableness of the result, congestion analysis was conducted on the mainline and on-ramp traffic. The results indicated that the on-ramp did not experience

any level of congestion as a result of oversaturation. The mainline traffic experienced some delay, which is as expected due to merging disturbances.

4.3.4 Capacity Effects of CAVs on Freeway Weaving Segments

Weaving segment results are provided in Figure 4.6. As stated earlier, three volume ratio (VR) levels were tested in scenarios involving vehicles with and without advanced merging capabilities. The simulation runs were performed using the "normal" gap settings for CACC-equipped vehicles.

The capacity increase in FWSs follows a quadratic trend, similar to all the other scenarios with a similar simulation setup. However, the curve's gradient is steeper due to the weaving segment's lower base capacity. The segment's capacity is 2,400 pc/h/ln without any weaving volume and capacity decreases as the VR increases, even at 0% CAV MPR. A higher VR indicates a higher volume of vehicles trying to make lane changes from the freeway to the ramp and vice versa, which results in greater traffic friction. Lane changes directly impact capacity, which was also established from the BFS analysis. At 100% CACC, the capacity reduction is as high as 8% as a result of increasing the VR from 0.3 to 0.4.

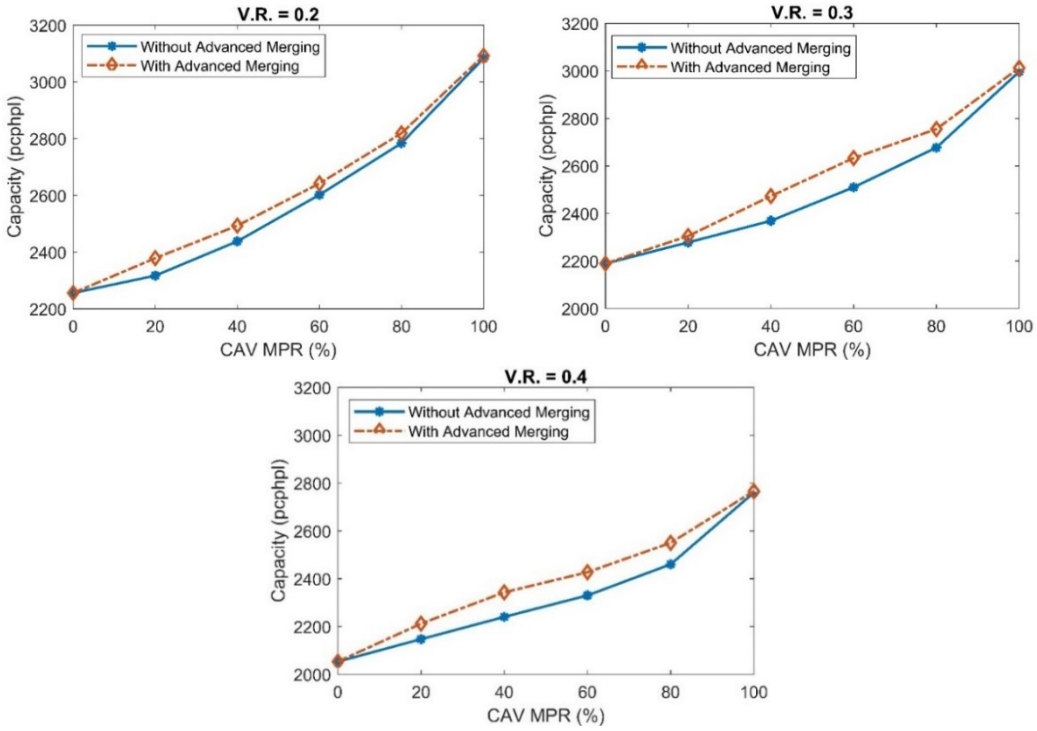

(a) Volume Ratio (VR) = 0.2, 0.3, and 0.4

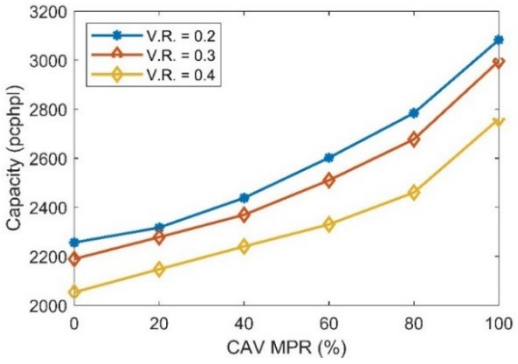

(b) All Volume Ratios Combined (Without Advanced Merging)

Figure 4.6: Freeway weaving segment capacity results with varying volume ratios

4.3.5 Capacity Adjustment Factors

4.3.5.1 Basic Freeway and Diverge Segments

Table 4.2 provides CAFs for basic freeway and freeway diverge segments where CAVs are present in the traffic stream, CAF_{CAV}. To determine the CAF value to use, first calculate the segment's initial adjusted capacity c_{adj} using HCM Equation 12-8, applying all other applicable CAFs (e.g., driver population, severe weather). Next, determine the CAF_{CAV} value from Table 4.2 based on the proportion of CAVs in the traffic stream and the initial adjusted capacity, interpolating as needed.

Table 4.2: CAFs for CAVs for Basic Freeway and Freeway Diverge Segments

Proportion of CAVs	Adjusted Segment Capacity		
in Traffic Stream	2,400 pc/h/ln	2,100 pc/h/ln	1,800 pc/h/ln
0	1.00	1.00	1.00
20	1.02	1.02	1.15
40	1.07	1.10	1.27
60	1.13	1.25	1.40
80	1.22	1.37	1.60
100	1.33	1.52	1.78

Notes:

- CAV = connected and automated vehicle, defined here as a vehicle with an operating cooperative adaptive cruise control system.
- Interpolate for other CAV proportions and adjusted segment capacities.
- Assumptions: Average intervehicle gap within CAV platoons = 0.71 s based on a distribution, CAV interplatoon gap = 2.0 s, maximum CAV platoon size = 10 pc, human-driven vehicles operate with average gaps calibrated to the given adjusted segment capacity.

4.3.5.2 Freeway Merge Segments

Table 4.3 gives CAFs for freeway merge segments where CAVs are present in the traffic stream, based on the proportion of CAVs in the traffic stream and interpolating as needed.

Table 4.3: CAFs for CAVs for Freeway Merge Segments

Proportion of CAVs in Traffic Stream	CAF_{CAV}
0	1.00
20	1.02
40	1.07
60	1.16
80	1.33
100	1.45

Notes:

- CAV = connected and automated vehicle, defined here as a vehicle with an operating cooperative adaptive cruise control system.
- Interpolate for other CAV proportions and adjusted segment capacities.
- Assumptions: Average intervehicle gap within CAV platoons = 0.71 s based on a distribution, CAV interplatoon gap = 2.0 s, maximum CAV platoon size = 10 pc, human-driven vehicles operate with average gaps calibrated to 2,200 pc/h/ln.

4.3.5.3 Freeway Weaving Segments

Table 4.4 provides CAFs for freeway weaving segments where CAVs are present in the traffic stream. The CAF value is determined from the proportion of CAVs in the traffic stream and the volume ratio (i.e., the weaving demand flow rate divided by the total demand flow rate in the weaving segment), interpolating as needed.

Table 4.4: CAFs for CAVs for Freeway Weaving Segments

Proportion of CAVs	Volume Ratio		
in Traffic Stream	0.2	0.3	0.4
0	1.00	1.00	1.00
20	1.03	1.04	1.05
40	1.08	1.08	1.09
60	1.15	1.15	1.13
80	1.23	1.22	1.20
100	1.37	1.37	1.34

Notes:

- CAV = connected and automated vehicle, defined here as a vehicle with an operating cooperative adaptive cruise control system.
- Interpolate for other CAV proportions and volume ratios.
- The volume ratio is the weaving demand flow rate divided by the total demand flow rate in the segment.
- Assumptions: Average intervehicle gap within CAV platoons = 0.71 s based on a distribution, CAV interplatoon gap = 2.0 s, maximum CAV platoon size = 10 pc, human-driven vehicles operate with average gaps calibrated to 2,200 pc/h/ln.

4.3.5.4 Regression Models

In the final part of the freeway study, we developed a simple but efficient empirical model which accepts certain inputs and predicts the capacity as a function of the inputs. The resulting value is the same as the CAFs presented in the preceding tables. The regression model can be easily integrated with any existing software implementing HCM methods. Both the CAF tables and the regression models enable analysts to make a quick but reliable estimation of future freeway segment capacity based on selected factors.

Three different empirical relationships are provided for each freeway segment. All variables included in the models are significant at a 95% confidence level. The regression result further supports that although our analysis showed slight capacity decreases for 3-lane BFS segments compared to 2-lane segments, the number of lanes is not a significant predictor (p-value = 0.16) of the resulting capacity. Advanced merging is significant for both FMSs and FWSs.

The R-square values for the three regression models are 0.89, 0.86, and 0.97 for BFS, FMS, and FWS respectively, indicating excellent fits. The relationship between the CAF and the independent variables can be expressed as

$$f_{CAV,BFS} = [1.077 + 0.043P_{PLT} \times 10^{-2} - 0.016G_{IP} - 0.031SC \times 10^{-3}]^{10} \quad \textbf{(4-3)}$$

$$f_{CAV,FMS} = [0.994 + 0.033P_{PLT} \times 10^{-2} - 0.013RD \times 10^{-2} + 0.004AM \times 10^{-2}]^{10} \quad \textbf{(4-4)}$$

$$f_{CAV,FWS} = [1.093 + 0.033P_{PLT} \times 10^{-2} - 0.051VR + 0.002AM \times 10^{-2}]^{10} \quad \textbf{(4-5)}$$

where

$f_{CAV,BFS}$= capacity adjustment factor for basic freeway segments with CAVs (unitless),

P_{PLT}= percentage of CACC-equipped vehicles in the traffic stream (%),

G_{IP}= average intra-platoon gap (sec),

SC= segment base capacity (pc/h),

$f_{CAV,FMS}$= capacity adjustment factor for freeway merge segments with CAVs (unitless),

RD= on-ramp demand (pc/h),

AM= percentage of vehicles with advanced merging capability (%),

$f_{CAV,FWS}$= capacity adjustment factor for freeway weaving segments with CAVs (unitless), and

VR= volume ratio (decimal).

In the case where G_{IP} follows a distribution, we recommend using the expected value of 0.71 sec, which represents the average of the distribution, also used in Liu et al. (*21*). The value of AM is 100% for the case with both CACC and advanced merge, 0% for the case with only CACC, and in the range of 20% to 100% for cases with only advanced merge and no CACC. Various variable interactions were tested in developing the empirical models, but they do not improve the models' performance.

4.4 FINDINGS

We analyzed the impact of CACC-equipped vehicles on freeways using different starting capacities. The results confirmed the findings of similar past studies and also provided some new findings. The capacity benefit of CACC follows a quadratic trend. However, in cases of lower starting capacities, the trend is more linear. This infers that the capacity benefits are not the same across all facility design speeds and operating conditions. We also analyzed the effect of on-ramp demand on merge segment capacity. The results indicated that different roadway capacities are achieved at different ramp demand levels. In addition, CACC coordination can potentially reduce the effect of merging disturbance at on-ramps when the market penetration rate is high enough. On weaving segments, the results showed that the capacity benefits of CACC decrease as the volume ratio increases. Weaving disturbances drastically reduce the effects of CACC coordination. Even when an advanced merging capability was provided, the effects of weaving intensity were still pronounced.

Although this research has advanced the state of knowledge about future CAV operations on freeways, further research is required. More complex freeway scenarios, such as managed lanes, higher weaving ratios, and two-lane on-ramps could be incorporated in future studies. Another area to explore is the effect of trucks (both automated and human-driven) on a traffic stream incorporating CAVs. Finally, the combined effect of other CAV applications that may potentially be implemented in the near future could be considered in future studies.

5.0 SIGNALIZED INTERSECTIONS

5.1 INTRODUCTION

This section evaluates existing HCM signalized intersection performance indicators under future CAV scenarios to obtain prevailing capacity estimates. Next, we developed saturation flow adjustment factors for each evaluated scenario. To make the framework flexible, we also developed adjustment factors for saturation headway and follow-up headway.

5.2 METHODOLOGY

5.2.1 Base Model Development

To ensure the simulation study network is realistic, we assumed a geometry that is common at signalized intersections as shown in Figure 5.1. The eastbound (EB) and westbound (WB) approaches are the major movements while the northbound (NB) and southbound (SB) approaches are minor movements. For the EB and WB approaches, there is an exclusive left-turn lane (bay length measured at 350 ft.), an exclusive through lane, and a shared through/right lane. For the NB and SB approaches, there is a shared through/right lane and an exclusive left-turn lane. The speed limit is 40 mph on the Major Street and 30 mph on the Minor Street.

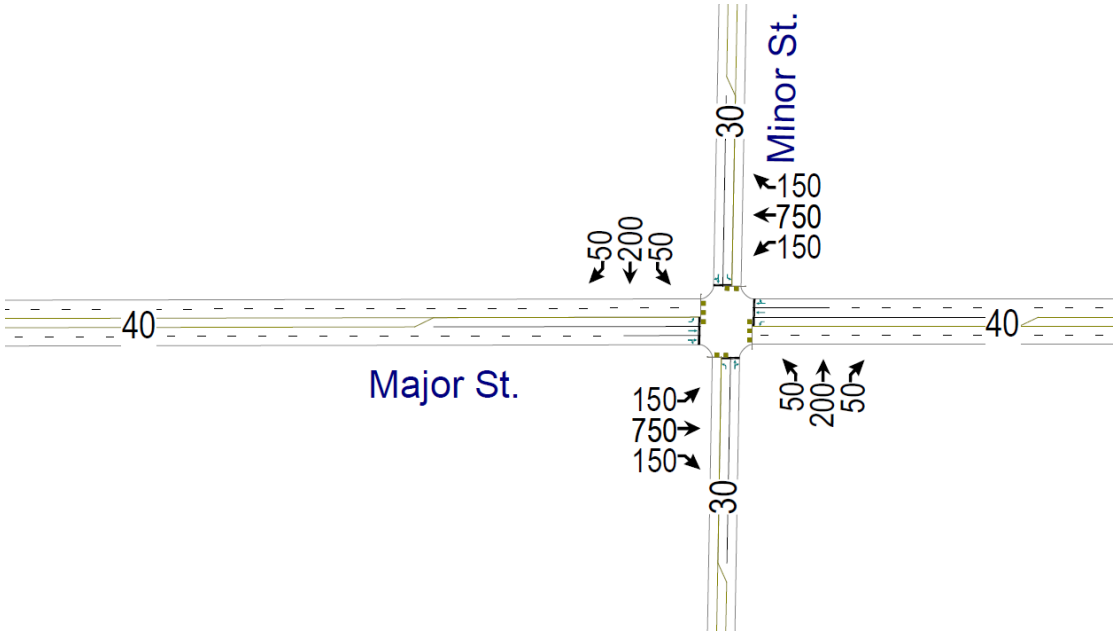

Figure 5.1: Signalized intersection study site used in VISSIM

This study focused on the analysis of exclusive lanes, similar to the procedures outlined in HCM Chapter 19 (TRB, 2016) for exclusive lanes. Therefore, we selected the through and left-turn lane on the EB approach for the analysis, and we used the results from these lanes to evaluate all

the experimental design and performance indicators. The analysis is transferable to any intersection provided that the lanes are also exclusive.

We assumed the signal timing is pre-timed with a 100-second cycle length. We developed the base signal timing using Synchro's traffic signal optimization tool assuming a volume-to-capacity ratio of approximately 0.7 for the critical phases (using the base volumes shown in Figure 5.1). To limit the number of scenarios and other confounding factors, we used only the base signal timing plan in this study while adjusting vehicle demand for the eastbound approach to create oversaturated conditions to accurately estimate capacity.

To develop CAFs for the HCM, it is critical that the base model is calibrated to the typical measures provided in the HCM for signalized intersections. This requires a systematic calibration of the simulation parameters in VISSIM and adjustments of driving behavior parameters.

For signalized intersections, HCM capacity is primarily a function of saturation flow rate (SFR). The HCM treats base saturation flow rate mostly independent to factors such as signal timing plan, so SFR was chosen as the primary calibration parameter for protected movements. Under ideal conditions, the HCM recommends a base SFR of 1,900 and 1,600 passenger cars per hour per lane (pc/h/ln) for through and left-turn movements, respectively.

To obtain the SFR from VISSIM, we followed the methodology described in the HCM Chapter 31 for collecting saturation flow rate (TRB, 2016). We increased the traffic demand on the analysis approach to oversaturated levels to ensure demand is greater than capacity. For each cycle, we subtracted the time recorded for the fourth vehicle from the time recorded for the last or the 14th vehicle (whichever is closer), and then divided by the number of headways after the 4th vehicle to obtain the average headway per vehicle under saturation flow (also called saturation headway). We obtained the SFR by dividing 3,600 with the saturation headway.

5.2.1.1 Calibration Parameters for Protected Left Turns

This study used the Wiedemann '74 model to represent driver behavior on arterials (Mahmood & Kianfar, 2019). Wiedemann '74 provides three calibration parameters for representing the behavior of drivers: average standstill distance (w74ax), additive part of safety distance (w74bxAdd), and multiplicative part of safety distance (w74bxMult). We first used the default values of each now parameter (w74ax = 6.56-ft, w74bxAdd = 2.0, and w74bxMult = 3.0) to test the base model and to obtain representative SFRs, which led to a SFR of 2,110 pc/h/ln and 1,720 pc/h/ln for the through and left-turn movements, respectively. These initial SFRs were higher than the values provided in the HCM as the baseline SFR. Therefore, we adjusted the Wiedemann '74 parameter values to match the baseline SFR. After calibration, the Wiedemann '74 parameter values used for analysis were: w74ax = 6.56-ft, w74bxAdd = 2.89, and w74bxMult = 3.89 and the SFRs were 1,910 pc/h/ln and 1,550 pc/h/ln for the through and left-turn movements, respectively, as summarized in Table 5.1.

Table 5.1: Calibrated Wiedemann '74 Driver Behavior Parameter Values for Signalized Intersections With Protected Left Turns

Wiedemann '74 Driver Behavior Parameter	Default Value	Calibrated Value
Average standstill distance (w74ax)	6.56 ft	6.56 ft
Additive part of safety distance (w74bxAdd)	2.0	2.89
Multiplicative part of safety distance (w74bxMult)	3.0	3.89
Resulting SFR for Through movement	2,110 pc/h/ln	1,910 pc/h/ln
Resulting SFR for Left-Turn movement	1,720 pc/h/ln	1,550 pc/h/ln

5.2.1.2 Calibration Parameters for Permitted Left Turns

With the analysis focusing on signalized intersections, we also designed the experiment to evaluate the performance for the permitted left turns. Performance measures and analysis for permitted left-turn movements at signalized intersections are different than the protected movements. Under this condition, the permitted left-turn green phase runs concurrently with the green phase on the conflicting through movement, and left-turning vehicles can cross the intersection based on the availability of acceptable gaps. Therefore, we recalibrated the permitted left-turn movement using VISSIM's conflict areas function to separate conflicting movements. The conflict areas also reflect the Wiedemann driver behavior using two parameters: the front gap, and the rear gap (PTV Group, 2018). We tuned these parameters until we reached the selected calibration measures for the movement.

We selected the critical headway (t_c), and the follow-up headway (t_f) as the calibration parameters for permitted left turns. The HCM recommends 4.5 sec and 2.5 sec for these parameters, respectively. To obtain these parameters in VISSIM, we used Raff's gap-acceptance method (Guo et al., 2014). We used data collection points to record gaps between vehicles on the opposing through movement and the timestamps at which left-turning vehicles crossed the opposing lanes were recorded (see Figure 5.2). By processing these two datasets, we obtained follow-up headway and number of accepted and rejected gaps. In the Raff's gap-acceptance method, the cumulative distribution frequency (CDF) of the accepted gap and the reverse CDF of the rejected gaps are plotted, and their intersection gives the c_g. The resulting c_g and t_f after calibration are 4.5 sec and 2.5 sec respectively as recommended by the HCM.

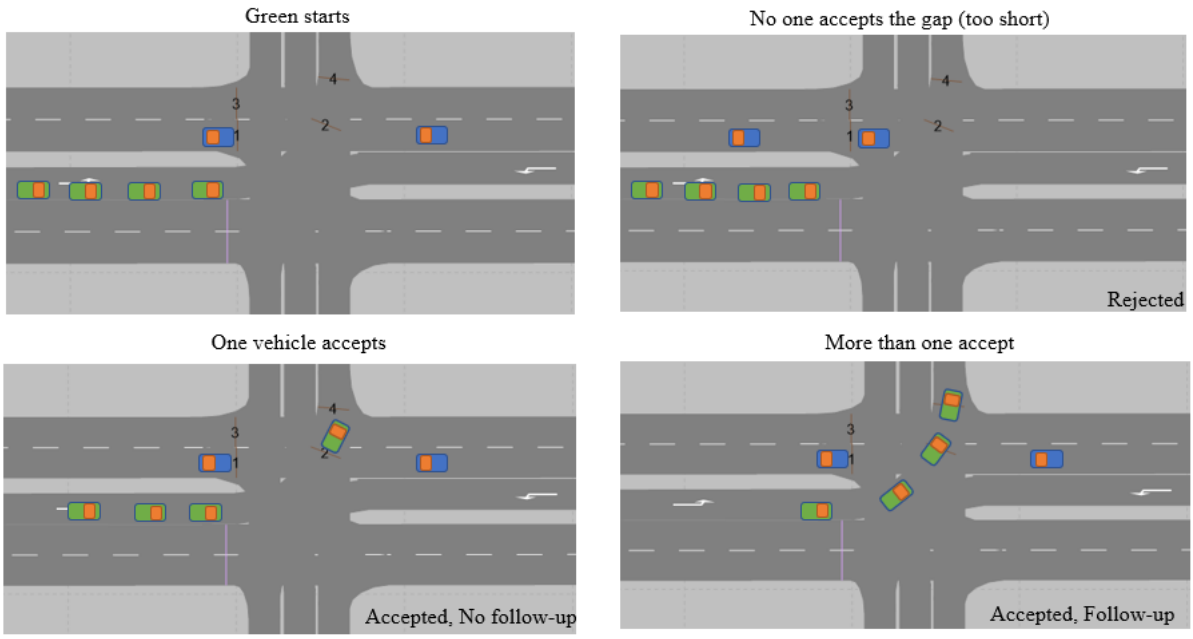

Figure 5.2: Simulation set-up to obtain gap acceptance parameters

5.2.2 CAV Modeling

As noted above, the CACC car following model developed in this study was based on a well-accepted study by Milanés & Shladover (2014), which has been previously used (Liu et al., 2018a and 2018b; Guo & Ma, 2020). We adapted their model in VISSIM to include testing various settings of intra-platoon gaps for sensitivity analysis. We also developed additional CACC protocols in VISSIM API for operations of CACC vehicles to form or leave platoons and perform lane following under various conditions, as shown in Figure 5.3. We assumed a maximum platoon length of 5 or 8 vehicles (Guo & Ma, 2021). Below, we present a basic introduction of the logic, and more detail can be found in Milanés & Shladover (2014). All model assumptions and parameters used here are within the ranges recommended in the same study.

As shown in Figure 5.3, the CACC protocol consists of two modes (speed regulation and gap regulation) in which the switching conditions within each following mode are based on the regulation of the gap and speed between consecutive CAVs. The purpose of the speed regulation mode is to maintain the user-desired speed when the preceding vehicle is beyond a pre-set gap (i.e., a time gap larger than 2 seconds from the preceding vehicle). The gap regulation mode controls the dynamics of vehicles in an active CACC platoon. The system assumes a vehicle can either be a platoon leader or a follower. A detailed discussion of the algorithm and its working equations are also provided in Section 4, which discusses the development of adjustment factors for freeways.

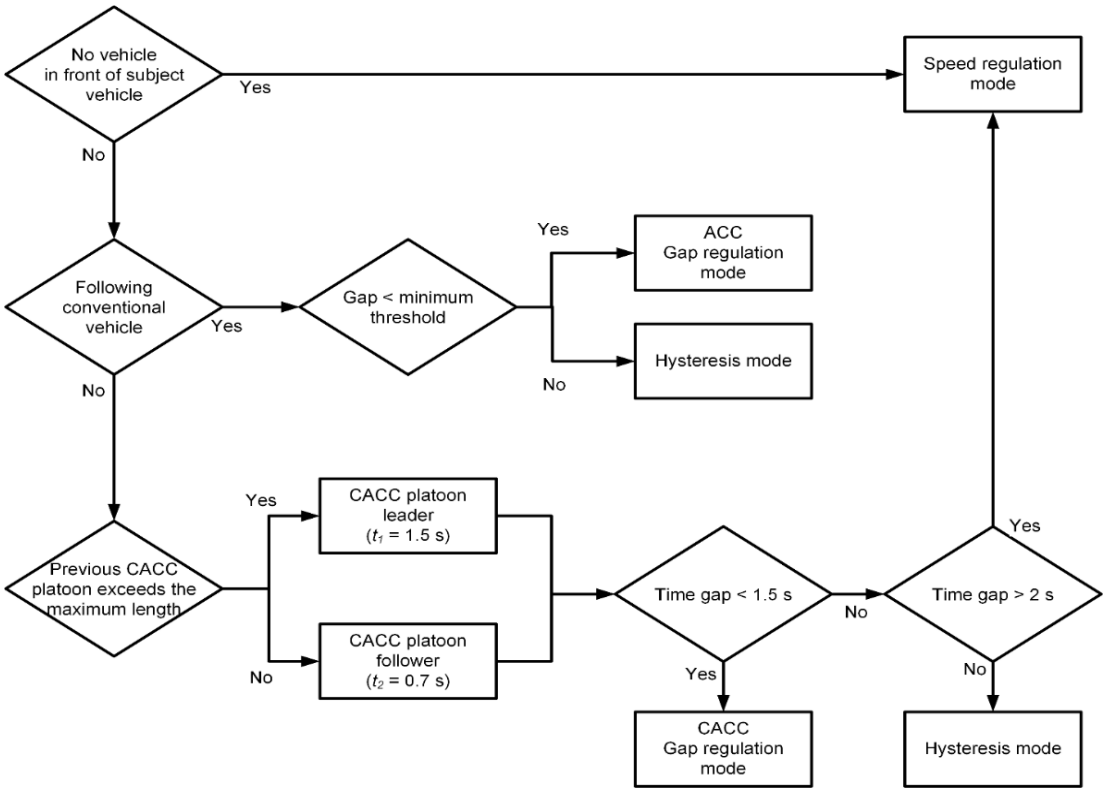

Figure 5.3: CACC protocol

Finally, to enhance their gap-acceptance behavior, CAVs are prompted to switch to VISSIM's internal logic when approaching the intersection conflict area. This means VISSIM's internal behavior controls the gap-acceptance logic for the CAVs in the conflict areas. However, the CAV's behavior was calibrated to be different from that of human-driven vehicles (HDVs). If the CAV vehicle detects an opposite conflict vehicle, it stops at the conflict area; otherwise, it will cross the intersection. Each CAV can look farther ahead than HDVs and can follow a preceding crossing vehicle by maintaining a lower following gap, similar to those maintained when traveling in CAV mode. With this, more CAVs can potentially accept a single available gap than HDVs would, meaning that CAVs can platoon through the intersections (captioned "Accepted, Follow-up" in Figure 5.2). This is particularly beneficial for improving the permitted left-turn movement capacity.

5.2.3 Performance Indicators and Capacity Estimation

For the through and left-turn-protected movements, the HCM provides the capacity estimation calculation, as shown in Equation 5-1. The effective green time (g) specifies the total time being effectively used by vehicles. It is obtained as the total lost time (the sum of start-up and end lost times) subtracted from the summation of the green time, yellow interval, and red clearance. The SFR has been described earlier and is also used in calculating the capacity from the obtained saturation headway. Therefore, we used the saturation headway, start-up lost time, and end lost time to assess the effects of CAVs for these movements.

$$\boldsymbol{c = s \times \left(\frac{g}{C}\right)}$$

(5-1)

where:

c = capacity (veh/h/ln),

s = saturation flow rate (veh/h/ln),

g = effective green time (s), and

C = cycle length (s).

For the left-turn permitted movement, the HCM also provides Equations 5-2 and 5-3 for estimating capacity for an exclusive lane. There are four main parameters controlling the permitted left-turn capacity: the critical gap, the follow-up headway, the unblocked green time in the opposing through movement, and the number of sneakers per cycle. We extracted the data in VISSIM using the signal change protocol and the queue counter measurement files, similar to our methods for protected left turns. While we investigated these measures, we also directly obtained capacity data from VISSIM to later compare the HCM model with actual simulation results for the left-turn-permitted mode. The HCM does not account for CAV behaviors, so it is possible that HCM models do not appropriately estimate the prevailing capacity under mixed conditions.

$$\boldsymbol{c_{l,e} = s_p \frac{g_u}{C} + \frac{3600}{C} n_s}$$

(5-2)

$$\boldsymbol{s_p = \frac{v_o e^{\frac{-v_o t_{cg}}{3600}}}{1 - e^{\frac{-v_o t_{fh}}{3600}}}}$$

(5-3)

where:

$c_{l,e}$ = exclusive permitted left-turn lane capacity (veh/h/ln),

s_p = the saturation flow rate for permitted left turn movement (veh/h/ln),

g_u = unblocked green time (s),

n_s = sneakers per cycle (veh),

v_o = opposing demand (veh/h),

t_{cg} = critical gap time (s), and

t_{fh} = follow-up headway time (s).

5.2.4 Experiment Design

Table 5.2 provides the experimental design. For all scenarios, we conducted five simulation replications using different random seeds. We used the average of the replication results to evaluate the system. We set simulation duration to 1 h (3,600 sec) with the first 15 minutes used for warm-up and the remaining 45 minutes for data collection. We used VISSIM's default random vehicle arrivals. We changed the vehicle types and distribution from the default and set to North American standard to ensure consistency with local traffic conditions in the United States. We did not include trucks in the vehicle mix, which is consistent with the HCM base capacity estimation as well as the freeway models discussed previously. Further, on entering the network, we made all vehicles assume the same desired speed distribution. However, depending on the position and operating mode of the CAVs, a typical stand-alone CAV can sometimes try to join the preceding platoon if the maximum platoon length is unreached. In this case, the subject CAV may travel slightly above the speed limit and merge with the platoon.

Table 5.2. Summary of Experimental Design for Signalized Intersections

Factor	Level	Comments
CAV MPR	0%, 20%, 40%, 60%, 80%, and 100%	• CAV MPR for all approaches is kept the same thus 100% CAV MPR would imply 100% CAV on all the lanes for all approaches.
Maximum Platoon Size	5 and 8 vehicles	• Maximum allowed platoon (CACC) size for each platoon in the network. • ACC vehicles are stand-alone and do not platoon.
Intra-Platoon Gap	0.6, 0.7, and 1.1 sec	• 0.6-sec intra-platoon gap represents a scenario where the driver population is comfortable with aggressive gaps (considered as the "*Aggressive*" scenario) • 0.7-sec intra-platoon gap is the average gap with the following distribution of gap settings: 57% CAVs use 0.6 s, 24% use 0.7 s, 7% use 0.9 s, and 12% use 1.1 s (24). This represents a scenario with variation in driver gap preference (considered as the "*Normal*" scenario) • 1.1-sec intra-platoon gap represents a conservative driver population (considered as the "*Conservative*" scenario)

5.3 RESULTS

5.3.1 Effects of CAVs on Protected Movement Performance

Figure 5.4 provides the saturation headway (SH), start-up lost time, and end lost time results under varying MPRs. The left column is for protected left turns; the right column is for the through movement.

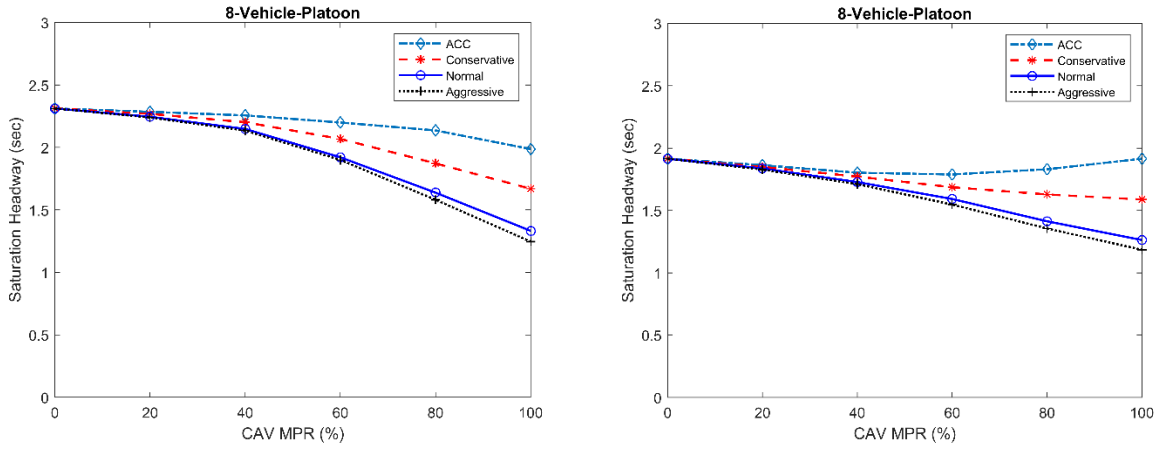

(a) Saturation Headway

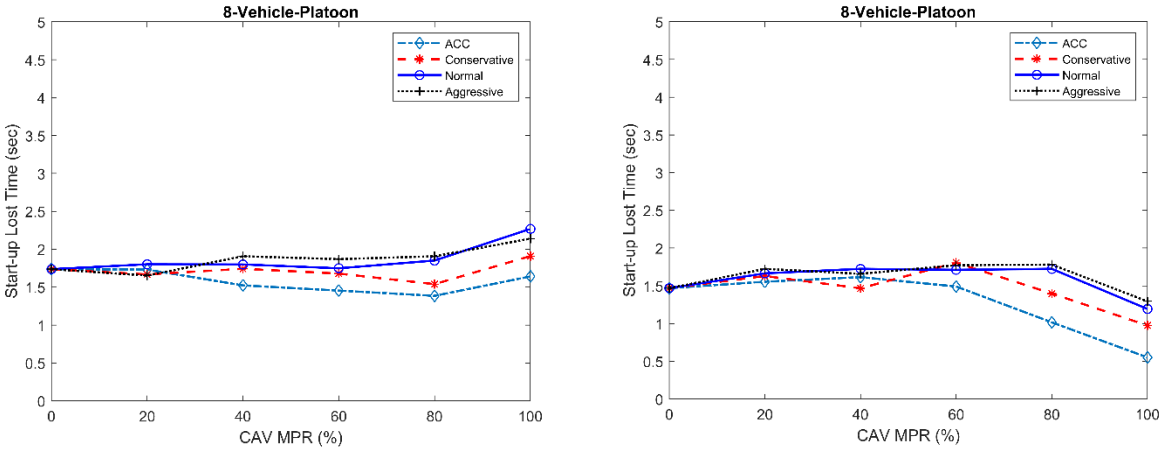

(b) Start-up Lost Time

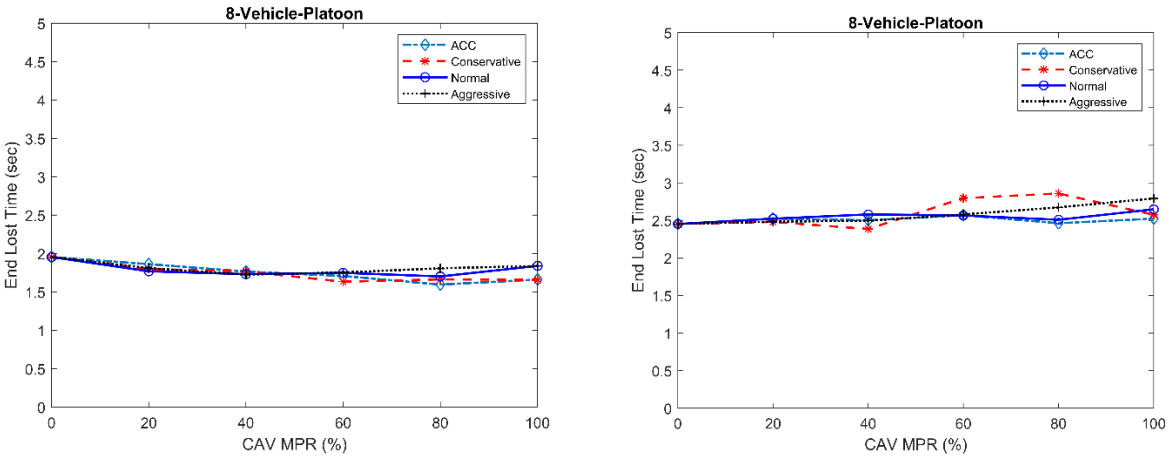

(c) End Lost Time

Figure 5.4: Left-turn movement (left) and through movement (right) performance

5.3.1.1 Saturation Headway with Platooning (CACC)

The results show a decreasing trend in SH (therefore increasing capacity) as a result of vehicle platooning and reduced gap under all scenarios. Vehicle platooning has the greatest impact in the "aggressive" scenario (up to 40% decrease) at 100% CACC MPR.

We show the results from the 8-vehicle platoon (8-VP) scenario only; however, findings from the 5-vehicle platoon (5-VP) are similar. We attribute these similar results to the fact that the SH is measured based on maximum 10 vehicles in the queue. This means for both 5-VP and 8-VP scenarios under 100% MPR, we have the inter-platoon gap (1.5 sec) occurring at most twice for both scenarios depending on vehicle arrival. Therefore, there is not much difference in operations. Additionally, the operation results for "aggressive" and "normal" CACC gap settings are close. This is due to small difference (0.1 s) in the average intra-platoon gap of "normal" (0.7 s) and the "aggressive" (0.6 s) gap settings scenarios.

Observing the trends based on the movement type, we find the left-turn-movement SH was reduced by 40% in some cases, compared to the through-movement SH reduction of 30% in the same cases. The base SH of left-turn was higher than the base SH of the through movement, which indicates that the potential benefits of CAVs could be greater under conditions where the base SH are higher, that is, conditions where the operations are initially worse. This is also consistent with the freeway findings discussed earlier.

5.3.1.2 Saturation Headway without Platooning (ACC)

The ACC scenario provides more interesting results. For the through movement, we observe an initial downward SH trend followed by an upward trend as the CAV MPR increases. This means ACC first slightly improves the capacity but then the improvement gradually drops. Past studies have observed relatively similar results. For example, Vander Werf et al. (2002) showed an initial improvement in operations, then a drop in improvement at high ACC MPR. Thus, we expect ACC would reduce SH only at low MPRs, and the improvement will gradually reduce at high MPR due to the ACC vehicles maintaining a conservative gap (1.5 sec for this study). ACC vehicles have a conservative gap setting due to safety reasons as ACC is not string stable (Milanés & Shladover, 2014).

When we examine the results for the left-turn movements, we find a rather consistent trend that is similar to the results observed in CACC mode. Therefore, we explored the study network in terms of geometry, traffic, and vehicle behavior characteristics to obtain insights on the new results obtained for left turns. We found that the effect of the reduced speed area traveled by left-turning vehicles as they traverse the intersection potentially improves the performance of ACC by providing more behavioral stability at high MPRs. The reduction in speed causes approaching vehicles to slightly decelerate on traversing the intersection. Since ACC vehicles are much more conservative than CACC vehicles, the speed reduction towards the intersection tends to enhance the operations of ACC vehicles at high MPR.

5.3.1.3 Start-Up Lost Time

Figure 5.4 provides the start-up lost time (SLT) for each scenario. Generally, the results obtained for SLT and ELT are marginal and negligible.

For the through movement, the SLT results stay relatively constant across low MPRs and drop slightly at high MPRs (60%-100%). Since the SLT measure is dependent on the first four vehicles in the queue, and the arrival pattern of vehicles is random, it is unlikely to always have CAVs in those positions at low MPRs. Therefore, under low MPR, the flat trend is expected as each signal cycle has random arrivals. However, at high MPR, the traffic approaches homogeneity, and it is more likely to have CAVs in the first four positions even with the random arrivals.

Comparing different CAV applications, the SLT is slightly lower when there is a high MPR of ACC-equipped vehicles than when there is a high MPR of CACC-equipped vehicles.

In the case of the left-turn movements, we observe a slightly different trend from that of the through movements. At low CAV MPRs, the SLT is similar to that obtained for HDVs. At high CAV MPRs (80% and 100%), the SLT slightly increases. The only observable difference between the operations of the two movements is the reduced speed area ahead of vehicles approaching the left-turn stop line, this reduced speed area affects the potential effects of vehicle technology from the first few vehicles in the queue at high MPRs. The results for both movements show the effect of the reduced speed on the operations of CAVs when starting from an initial stop.

5.3.1.4 End-Lost Time

The end-lost time (ELT) results are also provided in Figure 5.4. For both movements, we obtained a relatively flat trend in all scenarios. This signifies that the behavior of both HDVs and CAVs to traverse the intersection at the end of the green phase is relatively similar. Since end-lost time is highly dependent on the number of vehicles clearing an intersection after the green phase is terminated, this measure is affected by only one or two vehicles that are willing to traverse the intersection after the green phase. This action happens in a very short timeframe and is not expected to have a significant change. Moreover, CAV trajectory optimization is not a part of this study, and it is reasonable that there is no difference under mixed traffic conditions.

5.3.1.5 Capacity Impacts

Generally, the results obtained for SLT and ELT are marginal and negligible, showing that their effects on estimating movement capacity when incorporated into Equation 5-1 are also negligible. This is because the magnitude of the changes is marginal when compared to the cycle length (e.g., for a phase that has 50 seconds of green time, even with 100% MPR, SLT decreases by approximately one second, increasing effective green time by only about 2%). Therefore, regardless of the CAV MPR, SLT and ELT can be assumed unchanged when estimating capacity and the total lost time value for fully HDV traffic can be used for estimation across all CAV MPRs.

5.3.2 Effects of CAVs on Permitted Movement Performance

5.3.2.1 Critical Headway

Figure 5.5 provides the critical headway (t_c) results, as well as a typical CDF curve intercept obtained from Raff's method for evaluating the t_{cg}. The 0% MPR result represents the calibrated critical gap value of 4.5 sec. The results are the same for 5-VP and 8-VP for 0% MPR, so we provide only one set of results. We found relatively similar t_{cg} values for all CAV aggressiveness scenarios, even for ACC.

Note that t_{cg} values are reflections of the available gaps in the opposing movements and are dependent on the behavior of only the first vehicle in the queue during a gap-acceptance event. At low MPRs and low opposing demand, there would be more acceptable gaps for the queue leader to accept. As opposing demand increases, the platooning effect on the opposing traffic movement reduces the number of acceptable gaps. This tends to limit the reduction in t_{cg} that may be expected from increasing CAV penetration. The gap-acceptance algorithm in this study might have more effect on the follow-up headway than the critical gap, because the gap-acceptance algorithm we used does not reduce the gap size that is acceptable by the queue leader but instead allows more queued vehicles to accept the same gap.

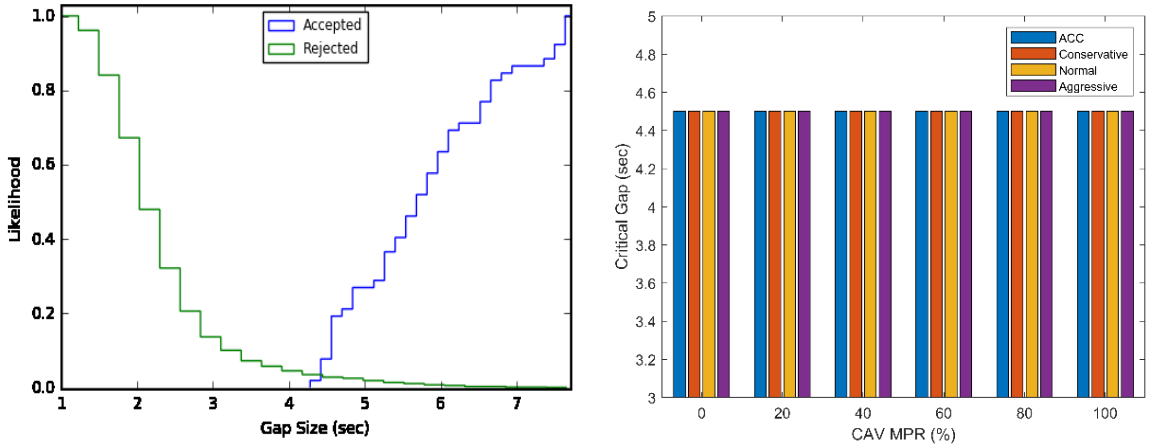

Figure 5.5: Gap acceptance results with varying CAV market penetration rate: Critical headway

5.3.2.2 Follow-up Headway

Figure 5.6 shows the results for the follow-up headway (t_{fh}) under all scenarios. The 0% MPR result represents the calibrated t_{fh} values of 2.5 sec. We observe a generally decreasing trend as CAV MPR increases, leading to more vehicles using the same mainline gap more effectively and traveling more closely as a result of their improved capability. Once a queue leader accepts a gap, the follower has a reduced following headway and does not have to wait for another gap to initiate a new gap-acceptance event.

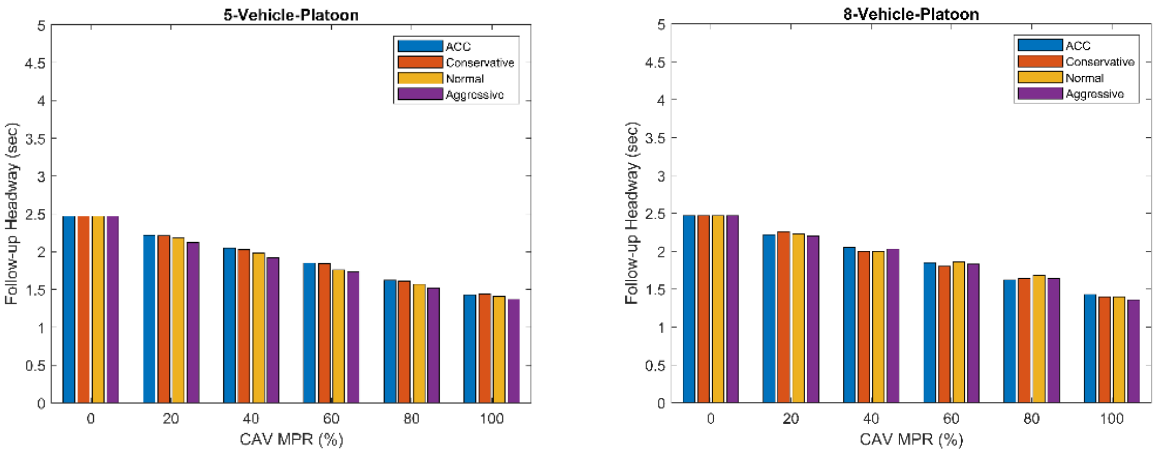

Figure 5.6: Gap acceptance results: Follow-up headways

Comparing the t_{fh} behavior for 5-VP and 8-VP scenarios, there are no observable differences in performance. This stems from two reasons: (1) the number of vehicles that can use an available gap, and (2) the number of vehicles in a queue during a gap-acceptance event. A queue on the permissive left-turn movement means there are not enough gaps in the opposing movement to allow vehicles to traverse, and only a few vehicles can use the same gap at a time. It is unlikely that more than 5 vehicles can find a single gap that is large enough to accept under such queuing conditions. On the other hand, if there are many vehicles in a queue during an event, it is also likely that the demand on the opposing traffic is close to saturation, which may lead to vehicles unable to find any gap. In that case, only a few left turn vehicles usually clear the intersection after the green phase ends (also known as "sneakers"). Therefore, there are no differences between having a 5-VP or an 8-VP.

While ACC and CACC vehicles show relatively similar trends, the t_{fh} reduction obtained from ACC is slightly less than CACC due to the platooning and headway settings.

5.3.2.3 Unblocked Green Time

Finally, the unblocked green time (g_u) results are provided in Figure 5.7 for each opposing demand level considered for the permitted left-turn lane. Since earlier findings have illustrated insignificant differences between the 5-VP and the 8-VP for permitted left turns, we only show the g_u results for 8-VP. Each line shows different CAV MPR considered herein.

The figure shows how the g_u for the permitted left-turn movement is reduced as the opposing demand increases. This is because as demand increases, the queue on the opposing approach increases, which takes the opposing approach longer to clear the initial queue.

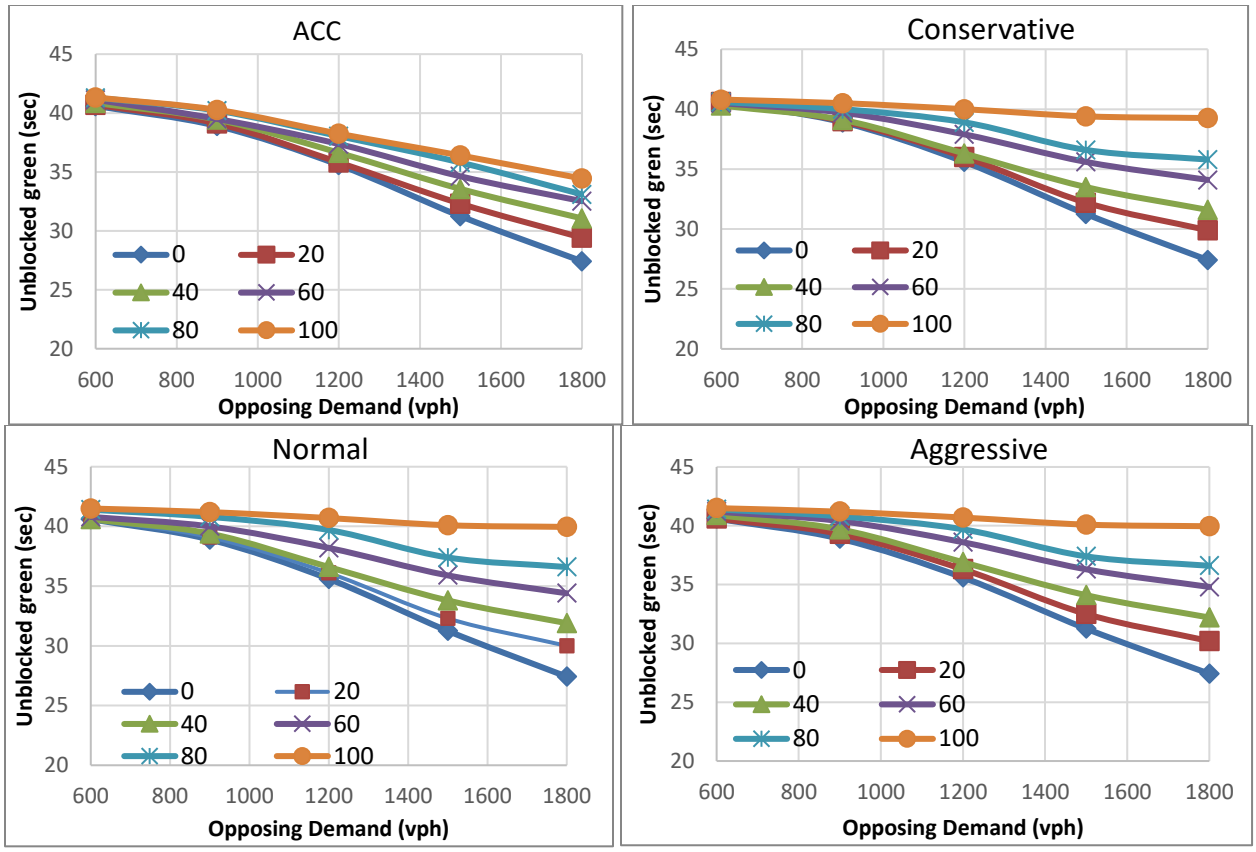

Figure 5.7: Unblocked green time results

The results also show that as CAV MPR increases, the magnitude of g_u increases, even under the same opposing demand level. This is attributed to the reduced discharged headways of CAVs for the opposing through movement compared to HDVs as discussed in the protected movement results. Under high CAV MPRs, queues dissipate more quickly compared to traffic with all HDVs. The faster dissipation of queues under high CAV MPRs provides longer unblocked green time for the left-turn movements.

Comparing CACC to ACC, the CACC platooning results in longer unblocked green time than the ACC behavior due to the ACC's conservative gap setting. However, there are still improvements when ACC is compared to HDV traffic.

The number of sneakers per cycle, n_s, as provided in Equation 5-2 was also evaluated for all scenarios and found to be 2 vehicles. This value did not change for all the simulated scenarios, and we used the same value for computing the HCM capacity shown in the following section.

5.3.2.4 Investigating Left-Turn Capacity Relative to Opposing Demand

To explore the sensitivity of the capacity estimates to the obtained t_{cg}, t_{fh}, g_u, and n_s values, we obtained the prevailing (VISSIM) capacity under the simulated opposing demand levels and compared them with the values obtained by using HCM models using the obtained t_{cg}, t_{fh}, g_u, and n_s values. Figure 5.8 shows the results.

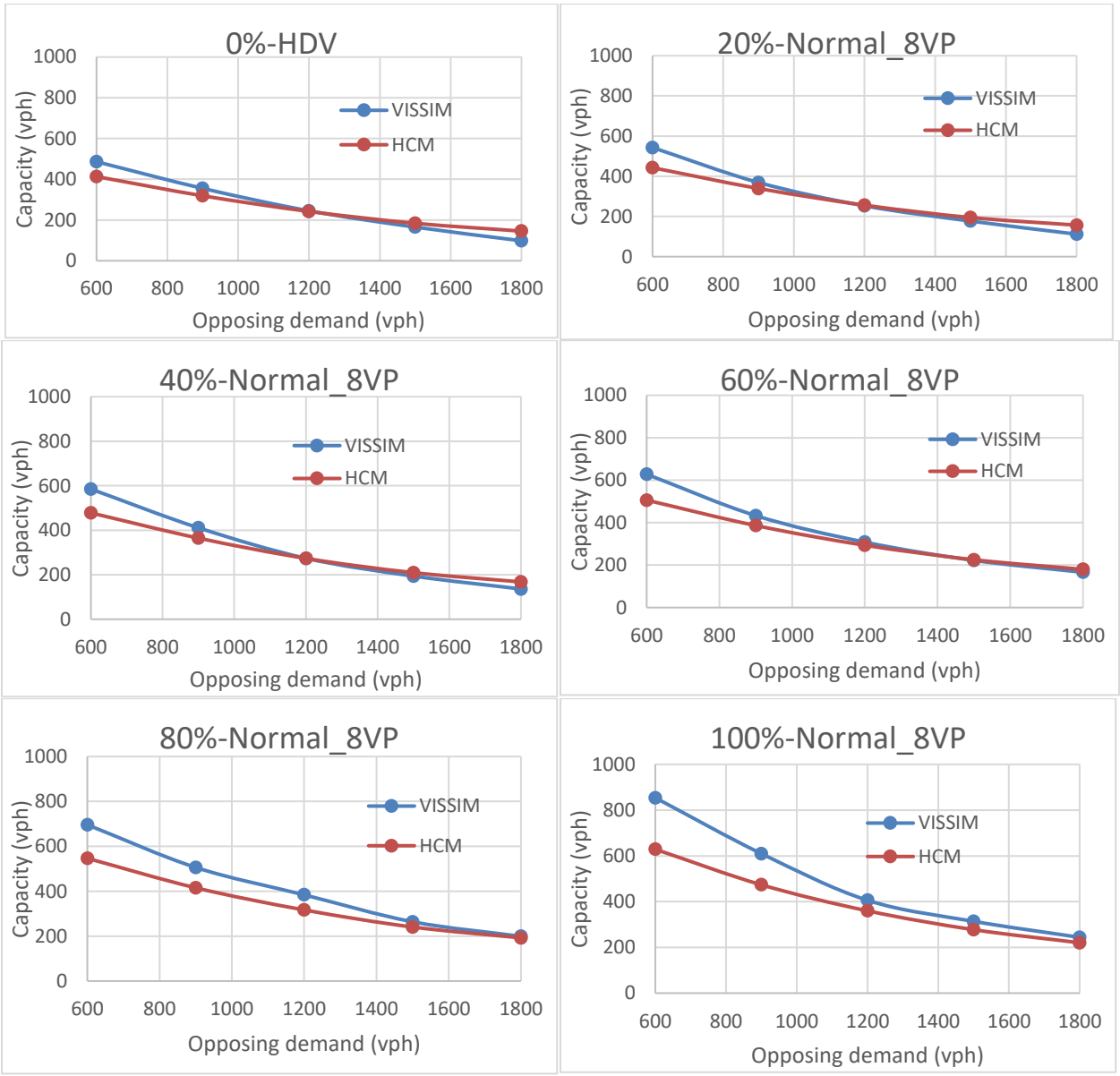

Figure 5.8: Comparison of simulation capacity results with HCM capacity estimates

For HDV traffic (0% MPR), the HCM model slightly underestimates the actual capacity at low opposing demand and slightly overestimates at high opposing demand. This is consistent with past studies that have investigated the accuracy of the HCM models under various fully HDV traffic (Ren et al., 2016).

With increasing CAV MPR, the estimation difference between the actual capacity and HCM models at high opposing demand reduces. This is due to the increased capacity from the CAVs. Since the HCM model initially overestimates capacity, the capacity increase from CAVs eventually reduces the HCM model estimation error. However, this is not the case at low opposing demand. The HCM initially underestimates with the 0% MPR, and as the prevailing capacity increases from CAVs, the HCM estimation error continues to increase. The difference is most pronounced at 100% MPR, where the HCM model and the prevailing capacity are easily distinguishable (more than 200 vehicles). With 100% MPR, the HCM model completely underestimates capacity at all opposing demand levels. This is because the HCM equations were based on the HDV and are unable to consider the effects of CAVs.

We show the results for the "normal" CAV gap-settings with 8-VP only. The results were similar for all scenarios.

5.3.3 Saturation Flow Adjustment Factors

As shown in Equations 5-1 and 5-2 the capacity of traffic movements at signalized intersections is a function of the saturation flow rate. Therefore, unlike the other HCM facility types discussed in this report, this portion of the study developed saturation flow adjustment factors instead of direct capacity adjustment factors.

5.3.3.1 Through Movements

Table 5.3 provides base saturation flow rates for through movements at signalized intersection approaches where CAVs are present in the traffic stream. The base saturation flow rate is applied in HCM Equation 19-8 along with a variety of adjustment factors to determine an adjusted saturation flow rate. Most of these adjustments also apply with CAVs; however, the adjustment for lane width should not be applied when CAVs are present.

Table 5.3: CAFs for CAVs for Through Movements at Signalized Intersections

Proportion of CAVs in Traffic Stream	Base Saturation Flow Rate (pc/h/ln)
0	1,900
20	2,000
40	2,150
60	2,250
80	2,550
100	2,900

Notes:

- CAV = connected and automated vehicle, defined here as a vehicle with an operating cooperative adaptive cruise control system.
- Interpolate for other CAV proportions.
- Assumes no interaction with non-motorized road users, no adverse weather impacts, and a facility without driveways or access points impacting saturation flow rates.

5.3.3.2 Protected Left Turns

Table 5.4 provides values of the saturation flow rate adjustment factor for protected left turns as a function of increasing proportion of CAVs in the traffic stream. This factor should be used as an additional adjustment in HCM Equation 19-8 to estimate the adjusted saturation flow rate for protected left turns. It should also be applied as an additional adjustment in HCM Equation 31-112 to estimate the adjusted saturation flow rate for the protected portion of protected-permitted phasing. Note that the factors in Table 5.4 are adjustments to the base saturation flow rate (with 0% CAVs). These factors should not be used in addition to the values in Table 5.3.

Table 5.4: CAFs for CAVs for Protected Left Turns at Signalized Intersections

Proportion of CAVs in Traffic Stream	Saturation Flow Rate Adjustment for Protected Left Turns
0	1.00
20	1.01
40	1.07
60	1.11
80	1.21
100	1.56

Notes:

- CAV = connected and automated vehicle, defined here as a vehicle with an operating cooperative adaptive cruise control system.
- Assumptions: Average intervehicle gap within CAV platoons = 0.71 s, CAV interplatoon gap = 1.5 s, maximum CAV platoon size = 8 pc, human-driven vehicles operate with through movement saturation flow rates calibrated to 1,900, assumes no interaction with non-motorized road users, no adverse weather impacts, and a facility without driveways or access points impacting saturation flow rates.
- Interpolate for other CAV proportions.

5.3.3.3 Permitted Left Turns

Table 5.5 provides values of the CAV saturation flow rate adjustment factor for permitted left turns as a function of the total opposing through volume per lane. This factor should be used as an additional adjustment in HCM Equation 31-100 to estimate the adjusted saturation flow rate for permitted left turns. The factors in Table 5.5 are adjustments to the base saturation flow rate (with 0% CAVs) and should not be used in addition to the values in Table 5.3 or Table 5.4.

Table 5.5: CAFs for CAVs for Permitted Left Turns at Signalized Intersections

Proportion of CAVs in Traffic Stream	Saturation Flow Rate Adjustment for Permitted Left Turns by Opposing Through Volume Per Lane (pc/h/ln)			
	300	450	600	750
0	1.00	1.00	1.00	1.00
20	1.12	1.04	1.03	1.07
40	1.20	1.16	1.12	1.18
60	1.29	1.22	1.26	1.36
80	1.43	1.43	1.57	1.60
100	1.76	1.72	1.66	1.90

Notes:

- CAV = connected and automated vehicle, defined here as a vehicle with an operating cooperative adaptive cruise control system.
- Assumptions: Average intervehicle gap within CAV platoons = 0.71 s, CAV interplatoon gap = 1.5 s, maximum CAV platoon size = 8 pc, human-driven vehicles operate with through movement saturation flow rates calibrated to 1,900 pc/h, assumes no interaction with non-motorized road users, no adverse weather impacts, and a facility without driveways or access points impacting saturation flow rates.
- Interpolate for other CAV proportions.

5.4 FINDINGS

We considered a realistic simulation network with exclusive left-turn lanes to investigate the effects of CAVs on signalized intersection capacity. We investigated three exclusive movement setups (through movement, protected left-turn, and permitted left-turn) to obtain changes in performance measures under the impact of CAVs.

For through movements, the result suggest an increase in the saturation flow rate with increasing proportion of CAVs in the traffic stream. The calibrated saturation flow rate of 1,900 pc/h/ln at 0% CAVs increased to 2,900 pc/h/ln at 100% CAVs, a more than 50% increase.

For the protected left-turn movement, results indicate that saturation headway decreases considerably with increasing CAV MPR, thereby improving the saturation flow rates and capacity for protected movements. With increased CAV MPR, there were no significant changes in lost times.

For the permitted left-turn scenario, we observed no changes in the critical gap relative to the conventional HDV traffic. However, by enhancing CAVs with platooning capabilities, the follow-up headway decreases as the CAV MPR increases. Also, due to the reduced discharge headway of CAVs, queues on the opposing approach were more quickly dissipated, thereby providing more unblocked green time for permitted left-turn movement, and subsequently increasing the permitted left turn capacity. These results were combined to develop capacity adjustment factors in the form of lookup tables that could be used as a quick evaluation tool for planning projects to assess the effects of CAVs, similar to those used in the HCM.

For permitted left-turn movements, the CAF table obtained from this study provides capacity adjustments by considering factors such as the CAV market penetration rate, the opposing traffic demand, and the type of vehicle automation in the traffic stream (CACC or ACC). For the protected movements, the table only considers the CAV market penetration and the type of vehicle automation. Additionally, adjustment factors are included for saturation headway (for protected movements) and follow-up headway (for permitted movement). This gives HCM users more flexibility while applying the CAFs. These values can be directly used as multipliers for existing HCM equations to account for CAV impacts, a new resource which was not available before.

While this study evaluated the impacts of CAVs at signalized intersections for exclusive lanes, scenarios of shared lanes with more complex configurations can be a subject of future research. We also considered only CACC and ACC-equipped vehicles. However, there are other enhancements such as trajectory and signal optimization that are likely to accompany CAV penetration. These hybrid strategies can also be considered and evaluated in future studies.

6.0 TWO-WAY STOP-CONTROLLED INTERSECTIONS

6.1 INTRODUCTION

This section explored development of capacity adjustment factors (CAFs) for CAVs on the minor movements of a two-way stop-controlled (TWSC) intersection at different levels of traffic demand and market penetration. This section also compares simulation results with the HCM capacity model for estimating movement capacities, to assess the accuracy of the current HCM model in estimating CAV traffic conditions.

The original intent behind the modeling of TWSC intersections in a sequence after signalized intersections and before roundabouts was to provide an incremental bridge in knowledge between permissive left-turn movements at signalized intersections, which share some gap acceptance parameters but within a cyclically interrupted environment from the traffic signal, and the yield-at-entry movements at roundabouts, which share the gap acceptance characteristics of a TWSC intersection but with a different set of priorities and spatial arrangement. In retrospect, the work towards calibrating the VISSIM model for roundabouts proved simpler than for TWSC intersections, thus allowing the team to bypass this originally anticipated intermediate step. Modeling discussion and results for roundabouts are presented in the next section.

This section presents some of the modeling considerations for CAVs at TWSC intersections and some items for further research in this area.

6.2 METHODOLOGY

6.2.1 Base Model Development

The TWSC intersection used in this study is a hypothetical intersection designed to allow each turning movement to be calibrated relative to the HCM. The network was modeled using the traffic microscopic simulation tool VISSIM. The eastbound (EB) and westbound (WB) approaches are the major street approaches, while the northbound (NB) and southbound (SB) approaches are the minor street approaches. The major street approaches have three lanes in each direction: shared through-right lane, an exclusive through lane, and an exclusive left-turn lane with a 345-ft storage bay length. The minor street approaches have three exclusive lanes in each direction: left-turn, though, and right-turn. The major street was assigned a speed limit of 40 mph, while the minor street had a speed limit of 30 mph. Stop signs were also assigned to all minor street lanes to bring vehicles to a complete stop on approaching the intersection.

The movements studied were the major-street left, minor-street right, minor-street through, and minor-street right. Vehicles from these movements must wait for vehicles of a higher rank to pass through the intersection. HCM Chapter 20 provides details about the relative priority of the movements at a TWSC intersection.

VISSIM's built-in Wiedemann '74 driver behavior model was used, because it is more suitable for urban roads (PTV Group, 2018). Because a TWSC intersection was being studied, the gap-acceptance behavior of vehicles should be calibrated for the conflicting movements. This was achieved by using a combination of VISSIM's Conflict Area (CAs) and Priority Rule (PRs) functions. Due to the complexities involved in modeling TWSC intersections, using only PR or CA is insufficient for to maintain a correct relative priority of the various movements. Therefore, the combination of CAs and PRs were used to replicate driving behaviors when the vehicles were making a gap-acceptance maneuver. As a result, a total of three driving behavior functions were used in this study: car-following behavior, CAs, and PRs.

Three calibration parameters are provided for the car-following behavior: average standstill distance, additive part of safety distance, and multiplicative part of safety distance. Four parameters are provided for CAs: front gap default (FrontGapDef), rear gap default (RearGapDef), safety distance default (SafDisFactDef), and additional stop distance (AddStopDist). Finally, two parameters are provided for PRs: minimum gap time (MinGapTime) and minimum headway (MinHeadway). More details on these parameters can be found in the PTV VISSIM user's manual (PTV Group, 2018). In this study, car-following behavior parameters were left as the default values, while the calibration process focused on PRs and CAs.

The project team was unable to achieve calibration of the VISSIM model to the HCM model over the entire range of conflicting flows for each of the minor movements. Calibration was especially difficult at low conflicting flows where follow-up time is the dominant gap acceptance parameter in the HCM models.

6.2.2 CAV Modeling

6.2.2.1 ACC/CACC Modeling

The cooperative adaptive cruise control (CACC) car-following model was based on one developed by the California PATH program (Milanés & Shladover, 2014; Liu et al., 2018a & 2018b). The maximum platoon size was set at 8. CACC can operate in either speed regulation mode or gap regulation mode. Speed regulation maintains the speed limit when the gap from the preceding vehicle is larger than the catch-up distance threshold (set at 2 sec in this study). In speed regulation mode, the vehicle's acceleration is given by Equation 6-1.

$$\boldsymbol{a_{sv} = 0.457\left(v_f - v_{sv}\right)} \quad \textbf{(6-1)}$$

where

a_{sv} = acceleration recommended by the controller to the subject vehicle (m/s^2),

v_f = free-flow speed (m/s), and

v_{sv} = current speed (m/s).

If the preceding vehicle is an HDV, the subject CAV will switch to adaptive cruise control (ACC) mode to regulate its driving behavior. If the gap between the subject vehicle and the preceding vehicle is smaller than the given minimum following threshold (1.5 sec in this study), the controller will switch to the ACC gap regulation mode to maintain a safe following time gap t_{hw}. The gap regulation mode is described by Equation 6-2:

$$\boldsymbol{a_{sv} = 0.23 \times (d - t_{hw} v_{sv} - L) + 0.07 \times (v_l - v_{sv})} \quad \textbf{(6-2)}$$

where

d = headway between the subject vehicle and the preceding vehicle (m),

t_{hw} = desired time gap of the ACC controller (s),

L = length of the preceding vehicle (m),

v_l = current speed of the preceding vehicle (m/s), and other variables are as described previously.

When the clearance gap is between the catch-up distance threshold and the minimum following threshold, the controller will continue implementing the control logic used in the previous time (hysteresis mode). This setting can help provide smooth transitions between speed regulation mode and gap regulation mode.

When the preceding vehicle is a CAV, the size of the previous CACC platoon is smaller than the maximum platoon size, and the distance from the subject CAV is shorter than the catch-up threshold, the subject CAV will switch to CACC gap regulation mode, to catch up with the preceding platoon and become a follower. In this situation, an intra-platoon gap is applied to control the behavior of a follower. If the subject vehicle is a CACC platoon leader and its preceding vehicle is the last in the preceding platoon, an inter-platoon gap is applied to maintain the distance between platoons. Finally, if the time gap to the preceding platoon is larger than the catch-up distance threshold, the subject CAV will switch back to the speed regulation mode given by Equation 6-1. Otherwise, the subject CAV will apply gap regulation mode to keep a safe following distance, following Equation 6-3 and 6-4.

$$\boldsymbol{a_{sv} = 0.23 \times (d - t_{hw} v_{sv} - L) + 0.07 \times (v_l - v_{sv})} \quad \textbf{(6-3)}$$

$$\boldsymbol{a_{sv}(t) = \frac{\left(v_{sv}(t) - v_{sv}(t - \Delta t)\right)}{\Delta t}} \quad \textbf{(6-4)}$$

where:

Δt = time step updating (s), e_k = time gap error given by Equations 6-5 and 6-6, and all other variables are as defined previously.

$$\boldsymbol{e_k(t) = d(t - \Delta t) - t_1 v_{sv}(t - \Delta t) - L} \quad \textbf{(6-5)}$$

$$\boldsymbol{\dot{e}_k(t) = v_l(t - \Delta t) - v_{sv}(t - \Delta t) - t_l \dot{v}_{sv}(t - \Delta t)} \quad \textbf{(6-6)}$$

where:

t_1 = the constant time gap between the last vehicle of the preceding CACC platoon and the subject vehicle (1.5 sec in this study), and all other variables are as defined previously.

Followers catching up to a preceding platoon were allowed to temporarily exceed the desired speed by up to 1.1 × speed limit. Simultaneously, a forward-collision warning system (Kiefer et al., 2003) developed by the Collision Avoidance Metrics Partnership (CAMP) was utilized in C/ACC car-following models to detect whether the gap between the subject vehicle and the preceding vehicle was sufficient for a safe car-following distance. If a collision warning was activated, the system changed back to the internal car-following (W74) model to provide a reasonable deceleration suggestion for the study vehicle to avoid a crash. CAVs would also switch back to the internal car-following model while crossing the intersection, to provide reasonable behavior and to avoid crashes. The parameters of this car-following model fit the all-knowing model provided by VISSIM.

6.2.2.2 Major Road Left-Turn Gap Acceptance Behavior

V2V communication can provide extra efficiency for CAVs on the major left. Major-Left Gap Acceptance Behavior was applied for major left CAVs approaching the intersection to generate the operational suggestions to ensure they could cross the intersection without stopping, as shown in Figure 6.1:

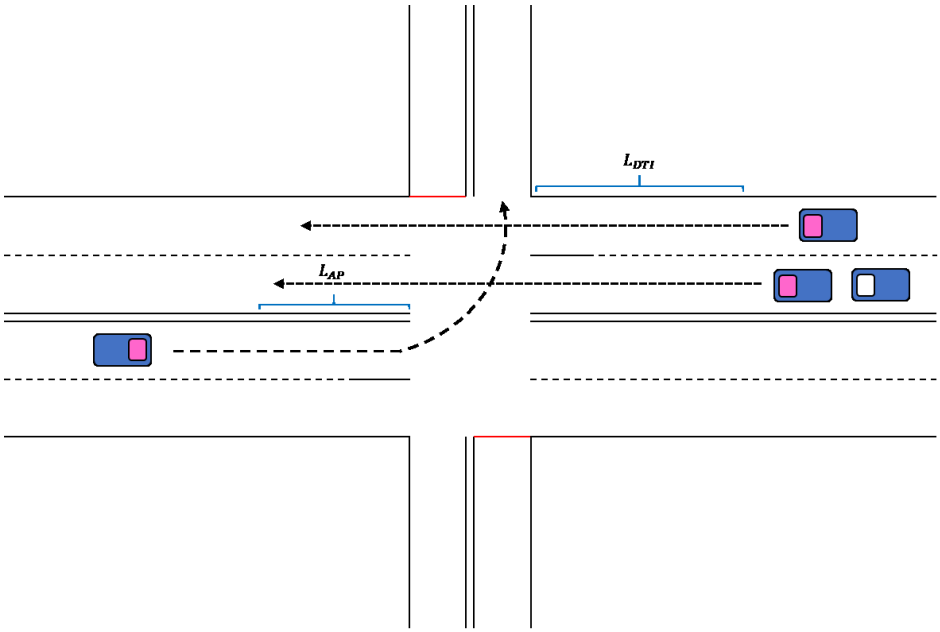

Figure 6.1: Distance illustration of Major-left V2V Gap Acceptance Behavior

Major-left V2V Gap Acceptance Behavior relies on the communication between the left-turning CAV and the nearest conflicting vehicles approaching the intersection. The approach area length L_{AP} is determined with the aim of keeping the left-turn CAV from decelerating from the road speed limit to zero within this area. The minimum approach area length is determined by Equation 6-7 (Chai et al., 2018):

$$\boldsymbol{L_{AP} \geq v_{limit}^2 / 2a_B} \quad \textbf{(6-7)}$$

where:

L_{AP} = minimum approach area length (m),

v_{limit} = maximum vehicle speed on the major street (m/s), and

a_B = braking deceleration (m/s^2).

In this study, the maximum vehicle speed on the major street was 19.68 m/s, equivalent to 1.1 × 40 mph, due to the ability of following vehicles to temporarily exceed the speed limit by 40 mph while catching up to a preceding platoon. The assumed braking deceleration was 3.5 m/s^2. Based on these values, the minimum approach area length is 56 m. However, to provide a comfortable deceleration process while keeping the left-turning vehicle safe, L_{AP} was set at 80 m.

When Major-left V2V Gap Acceptance Behavior was activated, left-turn CAVs could cross the intersection without stopping, as given by Equation 6-8:

$$\frac{L_{DTI} + \partial}{V_{tr}} > \frac{L_{AP} + L_{DTC_l}}{V_l} \quad \textbf{(6-8)}$$

where:

L_{DTI} = conflicting vehicle's distance to the conflict point (m),

∂ = security coefficient (m),

V_{tr} = speed of the conflicting vehicle (m/s^2), and

L_{DTC_l} = distance from entering the intersection to the conflict point for left-turn CAVs (18m in this study), and

V_l = speed of the left-turn vehicle (m/s).

The value of L_{DTC_l} is measured directly in the VISSIM network. The security coefficient ∂ is used for ensuring the safety of the system; after testing several values, it was set at 30 m. The detailed Major-Left Gap V2V Acceptance Behavior protocol is shown in Figure 6.2.

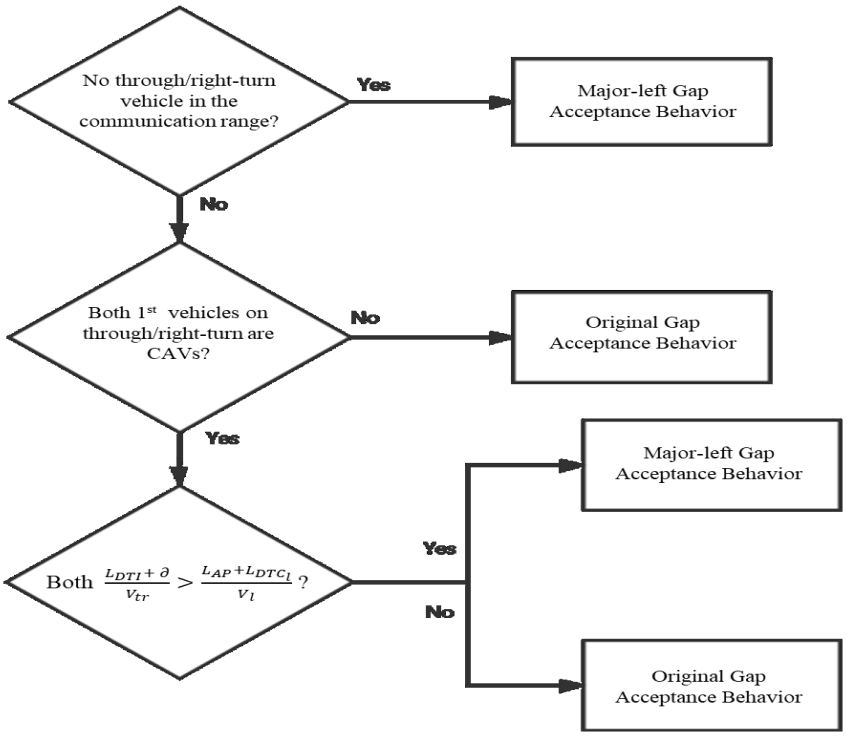

Figure 6.2: Major-left Gap Acceptance Behavior protocol

6.2.2.3 Critical Headway and Follow-up Headway

The gap-acceptance model aims to provide appropriate instruction for vehicles on movements with priority ranks greater than 1. Gap acceptance theory includes three basic elements: the distribution of gaps in the conflicting flow, the utilization of these gaps, and the relative priority of the movements. More details are provided in HCM Chapter 20. Critical headways and follow-up headways reflect drivers' behavior to the gaps.

Critical headway is the minimum time interval in the major-street traffic stream that allows one minor-street vehicle to enter the intersection (Troutbeck, 2016). Three statistical methods are commonly utilized in most research to calculate the critical headway (McGowen & Stanley, 2012): the Raff method (Raff, 1950), the logistic regression method, and the maximum-likelihood method (Troutbeck, 1992; Kyte et al., 1996). This paper uses the Raff method as modified by Troutbeck (2016) to calculate the critical headway.

The Raff method regards the intersection of the cumulative distribution of gaps accepted and the inverse of the cumulative distribution of gaps rejected as the critical gap. The Raff method has been used because it is simple and does not require the analyst to set any distributional form. However, it still has its shortcomings. The results of the Raff method can be affected by the gap size, especially when there are extra-long gaps, which may lead to overestimation of the results. To minimize this bias, gaps over 12 sec were ignored because these gaps can be accepted by almost all drivers (Troutbeck, 2016). Simultaneously, only the largest gap rejected by a single vehicle should be taken into consideration. This limitation can balance the number of accepted and rejected gaps.

Follow-up time is the time between the departure of one vehicle from the analysis movement and the next vehicle utilizing the same gap in the conflicting flow, under conditions of continuous queuing. In the microscopic analysis, the follow-up headway was calculated as the average value of the set of following headways (Li et al., 2013).

6.2.3 Capacity Estimation

This section briefly describes the HCM's process for calculating the capacity of each analysis movement by using the HCM method. A detailed description, including the calculation of movement capacities from potential capacities, is provided in HCM Chapter 20. Calculating the potential capacity is the starting point for determining the capacity of each movement, as shown in Equation 6-9.

$$c_{p,x} = v_{c,x} \frac{e^{-v_{c,x} t_{c,x}/3{,}600}}{1 - e^{-v_{c,x} t_{f,x}/3{,}600}} \quad \textbf{(6-9)}$$

where:

$c_{p,x}$ = potential capacity of movement x (veh/h),

$v_{c,x}$ = conflicting flow rate of movement *x* (veh/h),

$t_{c,x}$ = critical headway of movement *x* (s), and

$t_{f,x}$ = follow up headway of movement *x* (s).

The HCM provides a detailed procedure to calculate the conflicting flow rate of each movement when converting the traffic volume into the conflicting flow rate. In the simulation, the conflicting volume can be collected directly from VISSIM; the conflicting 15-min flow rate is determined by multiplying the peak 15-min volumes by four.

The CAF is the ratio of the capacity of the evaluated scenario to that of the base capacity without CAVs, as given by Equation 6-10.

$$\boldsymbol{c_{adj} = c \times CAF} \quad \textbf{(6-10)}$$

where:

c_{adj} = adjusted capacity (pc/h/ln),

c = base capacity (pc/h/ln), and

CAF = capacity adjustment factor.

In the HCM, the base capacity is always assumed as the capacity under ideal conditions, without heavy vehicle, severe weather, incidents, or other effects. The only variables considered in this study are the conflicting flow rate and CAV market penetration rate (MPR).

6.3 RESULTS

The project team found it difficult to achieve calibration of the VISSIM models to the HCM model across each of the minor movements. In particular, the VISSIM model for the major-street left-turn movement produced capacities that were substantially higher than the minor-street right-turn movement under low conflicting flows but substantially lower than the minor-street right-turn movement under high conflicting flows. These differences are not easily explained or adjusted with simple calibration factors. The causes are unknown but may be due in part due to the way VISSIM models yield-controlled movements (i.e., the major-street left-turn movement) versus stop-controlled movements (i.e., each of the minor-street movements). Budget constraints prevented further exploration of these discrepancies.

Due to challenges in developing reasonable calibrations between the VISSIM modeling and the current HCM model, no capacity adjustment factors were developed for TWSC intersections. For many planning applications, the lack of CAV adjustments factors is unlikely to adversely affect the modeling of urban street segments that usually have termini of either signalized intersections or roundabouts. In the absence of CAV factors, similar behavior expected for human drivers can be used as a conservative assumption.

The following recommendations for further research on the CAV effects for TWSC intersections are suggested:

- Further exploration of modifying the VISSIM stop-controlled model to better match HCM follow-up times for both major-street left-turn movements and each of the stop-controlled minor-street movements.

- Modeling of a simpler base lane configuration with only a single through lane in each direction. This should minimize potential differences between the minor-street right-turn movement that seeks a gap in the near lane and the other movements that seek gaps across all lanes.

7.0 ROUNDABOUTS

7.1 INTRODUCTION

This section explores the impact of CAVs on the capacity of both single-lane and double-lane roundabouts and develops capacity adjustment factors (CAFs) for CAVs over various market penetration rates to modify the HCM capacity results.

7.2 METHODOLOGY

7.2.1 Base Model Development

In this study, the research team conducted a set of microscopic simulations to study the impact of CAVs on the roundabout capacity. PTV has multi-resolution traffic modeling platforms that include macroscopic, mesoscopic, microscopic, and hybrid mesoscopic-microscopic modeling engines. As shown in Figure 7.1, the research team coded two roundabout models in VISSIM: a single-lane roundabout and a double-lane roundabout. The single-lane roundabout consists of four single-lane entries, each conflicted by one circulating lane. The double-lane roundabout has four double-lane entries, each conflicted by two circulating lanes. The diameters of the single-lane and double-lane roundabout assumed for this evaluation are 147 ft and 185 ft, respectively.

(a) Sketch of single-lane roundabout (b) Sketch of two-lane roundabout

Figure 7.1: Roundabout models

The HCM provides different capacity models for different types of entry lanes in roundabouts. To investigate the impact of different CAV market penetration rates (MPR) on the entry capacity, the research team calibrated the models developed in this study by the HCM models.

Previous studies have summarized that the settings of three elements in VISSIM have a critical impact on the operational performance of roundabout simulation models (Schroeder, 2012; Wei et al., 2012). These elements include:

- Priority Rules (PR) or Conflict Areas (CA), which control the yielding logic;

- Reduced Speed Areas (RSA), which provide temporary speed control over a short roadway distance; and

- Wiedemann ’74 and ’99 car-following models, which control the simulated car-following behavior.

In this study, the conflict area (CA) is adopted to control the yielding logic at the roundabout entrances. The research team calibrated the simulation networks by adjusting the simulation parameters in VISSIM and compared the capacity curves generated by the simulation results with the HCM capacity curves to ensure the calibrated simulation models have acceptable goodness of fit with the HCM models. The calibration results are shown later in this chapter.

7.2.2 CAV Modeling

7.2.2.1 CACC and Platooning Modeling

The CACC control logic the research team adopted in this study was developed by Milanés and Shladover (2014) and Liu et al. (2018) The lateral behaviors of CAVs were modeled using the same logic as for human-driven vehicle behavior because this study focuses on the impact of the car-following behavior of CACC operations at the early stages of deployment and does not explicitly consider lane changes for platooning.

No Vehicle in Front of CAV

As shown in Figure 7.2, if no vehicle is in front of the subject CAV, the subject vehicle will apply the *speed regulation mode* to regulate the driving behavior. This mode keeps the subject CAV cruising with a target speed to reduce unnecessary oscillations, as shown in Equation 7-1 (Liu et al., 2018a).

$$\boldsymbol{a_{sv} = k_1(v_f - v_{sv})} \quad \textbf{(7-1)}$$

where:

k_1 is the control gain of the difference between current speed v_{sv} and free-flow speed v_f and determines the acceleration a_{sv}. The control gain k_1 is set to $0.4\ \text{sec}^{-1}$ in this study (Liu et al., 2018a).

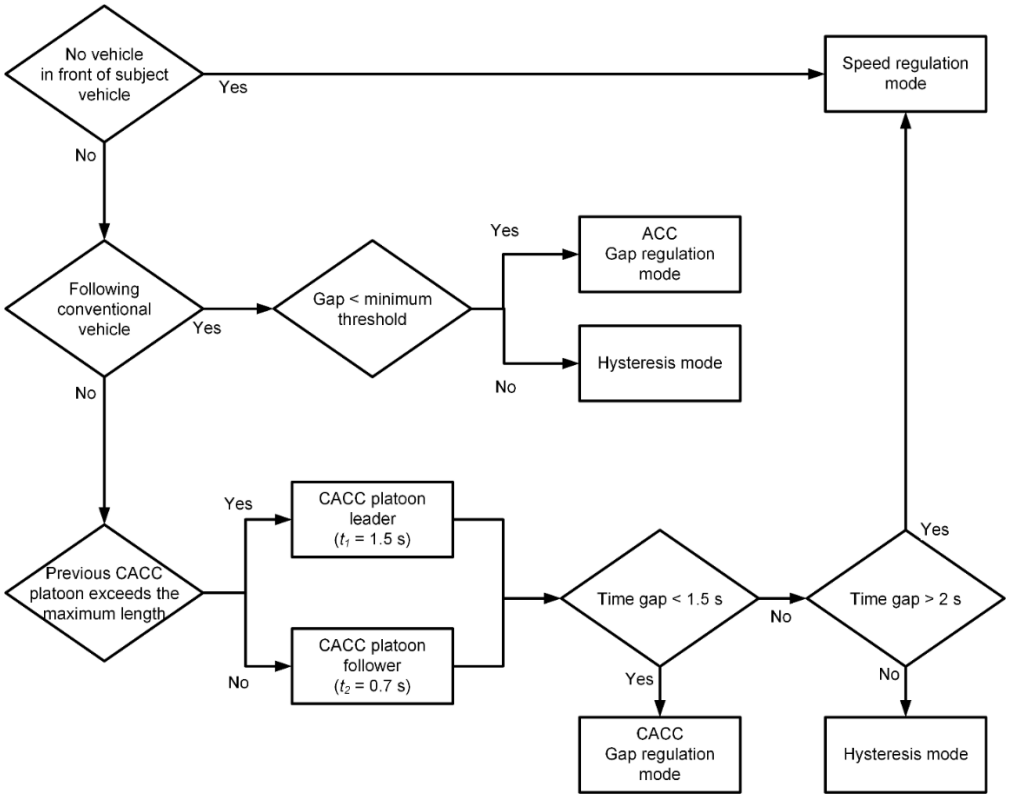

Figure 7.2: CACC protocol

CAV Following a Human-Driven Vehicle

In the case where the vehicle in front of the subject vehicle is a human-driven vehicle, the subject CAV will switch to the *ACC mode* to regulate the driving behavior. If the subject CAV is too close to the preceding vehicle (i.e., the detected clearance distance is smaller than a given minimum following threshold), it will switch to the *ACC gap regulation mode* to maintain a safe following time gap t_{hw}, as shown in Equation **Error! Reference s ource not found.**. Otherwise, the CAV will repeatedly implement previous control logic to ensure consistent driving behavior.

$$\boldsymbol{a_{sv} = k_2(d - t_{hw}v_{sv} - L) + k_3(v_l - v_{sv})} \quad \textbf{(7-2)}$$

where:

$k_2 = 0.23\ \text{sec}^{-2}$ and $k_3 = 0.07\ \text{sec}^{-1}$ are control gains on following distance difference and speed difference, respectively (Liu et al., 2018a).

The headway d, preceding vehicle length$L$, and preceding vehicle speed v_l are considered in Equation 7-2.

CAV Following Another CAV

If the vehicle in front of the subject vehicle is a CAV, the subject vehicle will switch to the *CACC mode* and communicate with the vehicle in front to exchange critical information (e.g., speed, location, platoon size). If the length of the previous CACC platoon is less than the maximum allowable platoon length, the subject CAV will catch up with the preceding CACC platoon and become a platoon follower; therefore, the intra-platoon gap t_2 (0.7 sec in this study) is applied to tightly follow the preceding CAV. Otherwise, the subject CAV becomes a CACC platoon leader and applies the inter-platoon gap t_1 (1.5 sec in this study) to follow the preceding CAV. The specific regulation mode depends on the actual time gap between the subject CAV and its preceding CAV. If the time gap is larger than a given threshold (2 sec in this study), the subject CAV will apply the *speed regulation mode*, as shown in Equation 7-1. Otherwise, it will apply the *CACC gap regulation mode* to keep a safe following distance with the determined following gap (i.e., inter-platoon gap or intra-platoon gap) by implementing Equations 7-3 through 7-6 (Liu et al., 2018a).

$$\boldsymbol{v_{sv}(t) = v_{sv}(t - \Delta t) + k_p e_k(t) + k_d \dot{e}_k(t)} \tag{7-3}$$

$$\boldsymbol{a_{sv}(t) = \frac{\left(v_{sv}(t) - v_{sv}(t - \Delta t)\right)}{\Delta t}} \tag{7-4}$$

$$\boldsymbol{e_k(t) = d(t - \Delta t) - t_1 v_{sv}(t - \Delta t) - L} \tag{7-5}$$

$$\boldsymbol{\dot{e}_k(t) = v_l(t - \Delta t) - v_{sv}(t - \Delta t) - t_l v_{sv}(t - \Delta t)} \tag{7-6}$$

where:

$k_p = 0.45$ sec^{-1} and $k_d = 0.0125$ are gap error control gains.

Emergency Braking Considerations

Due to the linearity of the above models, the vehicles cannot handle emergency braking to avoid collisions. The forward collision warning algorithm (Kiefer et al., 2003) developed by the Collision Avoidance Metrics Partnership (CAMP) is included in the CACC car-following modes to determine whether the gap between the subject vehicle and the preceding vehicle is sufficient for safe car following. If the crash warning is activated, it implies that a crash will happen if both the subject vehicle and the preceding vehicle keep their current acceleration rates for the next few seconds.

7.2.2.2 Route Conflict Anticipation

A driver's decision to enter the roundabout is primarily influenced by the conflicting traffic, i.e., the circulating flow that directly passes in front of the vehicle on the subject entry. In some cases, however, other flows might also affect a driver's entry decision, such as the upstream exiting flow or particular turning movements of circulating vehicles.

As illustrated in Figure 7.3, for a human-driven vehicle at the entrance line of the northbound entry lane, the conflicting vehicle's routing decision is uncertain until it commits to a circulating or exiting maneuver. Such uncertainty could create unnecessary waiting time for the entering vehicle, thus reducing the entry capacity. Unlike human-driven vehicles, if the yielding vehicle and incoming vehicle are both CAVs, the two CAVs could share routing information through vehicle-to vehicle (V2V)-communication. If the paths of the two CAVs do not conflict, the CAV at the entry could enter before the incoming CAV shows a visible intention to circulate or exit.

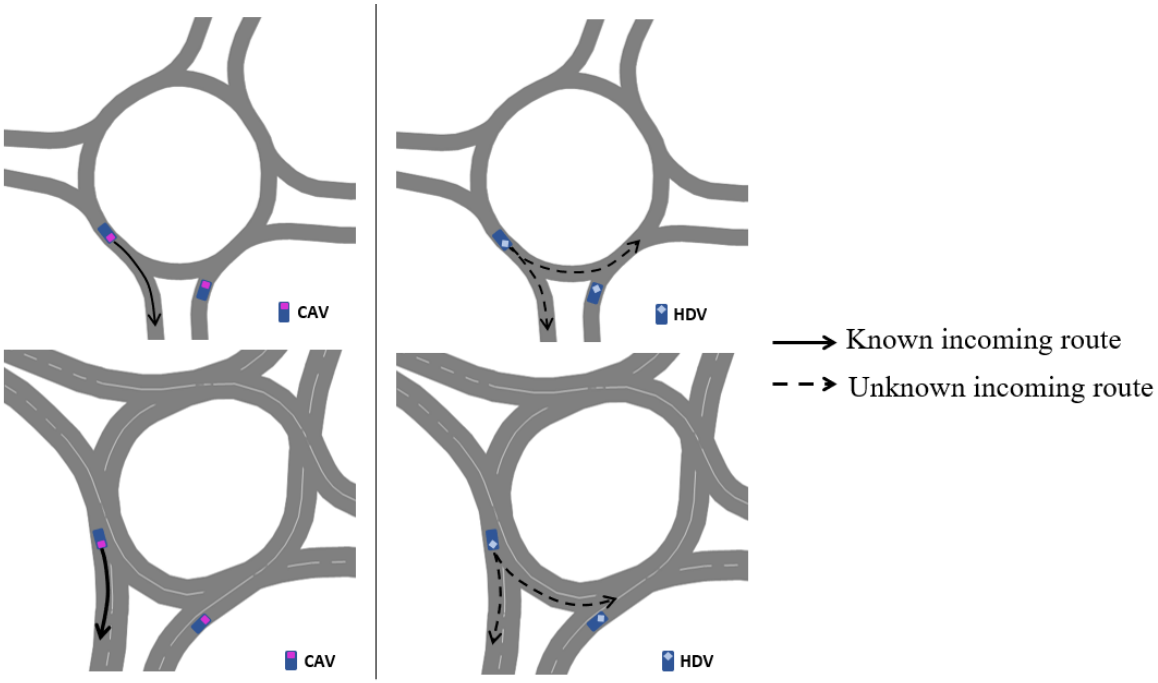

Figure 7.3: Route conflict anticipation

When a CAV approaching the roundabout is within 30 m (98.4 ft.) of the entrance line, it automatically searches for the incoming vehicles on the circulating lane(s) via V2V communication. Once the V2V communication is established, the CAVs on the entering lane(s) and on the circulating lane(s) share critical information such as location, speed, acceleration, and routing decisions. By sorting the incoming CAVs by distance, the entering CAV targets the closest incoming CAV on each circulating lane and determines whether the route of the target CAV conflicts with its own intended path. If the routes (paths) do not conflict, the entering CAV enters without yielding. Note that if the first

vehicle in the upcoming traffic stream is not a CAV or if its route conflicts with the subject vehicle, then the entering CAV's behavior will be controlled by gap acceptance criteria, similar to regular roundabout entering behavior in human-driven vehicle traffic.

7.2.2.3 Gap Acceptance

Data Collection Points

Figure 7.1 illustrated the locations of the data collection points that were placed to facilitate the collection of traffic flow data as well as timestamps of vehicles' gap acceptance events. The timestamps are used to estimate the critical headways and follow-up headways. Gaps were calculated as the time difference between the timestamps of vehicles crossing data collection points.

From the data collected by the data collection points in the simulation network, critical and follow-up headway calculations were extracted to use in the analysis of the roundabout capacity. *Critical headway* is the mean minimum headway between circulating vehicles that an entering driver can safely use to enter the roundabout. *Follow-up headway* is the mean time between consecutive queued vehicles entering the roundabout before being interrupted by a circulating vehicle.

Estimation of Critical Headways and Follow-Up Headways

Raff's method (Raff, 1950) is a common procedure for estimating critical headways and has been shown by Troutbeck to be a reasonable substitute with modification for the Maximum Likelihood Method used for model development in the HCM (Troutbeck, 2016). It requires accepted and rejected headways. A rejected headway is any headway between circulating vehicles not taken by an entering vehicle waiting at the approach. These headways are based on driving behavior and can vary among drivers and locations. A graphical method, based on Raff's definition (Raff, 1950), was used to estimate critical headway. The concept of the *critical gap* was used by Raff, who defined it as the gap that has the number of accepted shorter gaps equal to the number of longer rejected gaps. Using this graphical method, two cumulative distribution curves are drawn: one of them relates gap lengths t with the number of accepted gaps less than t and the other relates t with the number of rejected gaps greater than t. The intersection of these two curves gives the value of t for the critical gap. Examples of this graphic method are shown later in this chapter.

The estimation of the follow-up headway is a much simpler process. First, the research team measured the headway between consecutive queued vehicles entering the roundabout within the same gap. Then the research team obtained the follow-up headway for each simulation run by averaging the measured follow-up headways among all the entering vehicles.

7.2.3 Capacity Estimation

Capacity at a roundabout entry is commonly measured one of two ways: direct empirical measurement, or estimation using models from gap acceptance theory with field-measured parameters. For *direct empirical measurement*, the capacity of the subject entry can be directly measured by the flow data collected from the data collection points set at the end of the entering approach, provided that the subject approach is loaded to a constant queue. To reduce the oscillation caused by the randomness of the traffic flow, the maximum 15-minute flow rate is used to calculate the hourly capacity. The two-hour simulation period is divided into eight 15-minute intervals, and the interval with the peak flow is the maximum 15-minute flow. Then the capacity is obtained by multiplying the maximum 15-minute flow by four.

For *estimation using models from gap acceptance theory*, the HCM offers a generalized form of the formula based on Siegloch (1973) model as follows:

$$\boldsymbol{C_{pce} = Ae^{-B \cdot v_C}} \tag{7-7}$$

$$\boldsymbol{A = \frac{3,600}{t_f}} \tag{7-8}$$

$$\boldsymbol{B = \frac{t_c - (t_f/2)}{3,600}} \tag{7-9}$$

where:

C_{pce} = lane capacity (pc/h),

v_c = conflicting flow (pc/h),

t_c = critical headway (s), and

t_f = follow-up headway (s).

Parameter *A* is the intercept, determined by the inverse of the follow-up headway. A shorter follow-up headway results in a larger intercept. Parameter *B* is the slope, determined by both critical headway and follow-up headway. A larger critical headway results in a lower capacity. For a given location, critical headway and follow-up headway typically move in the same direction as a measure of driver aggressiveness.

In each test scenario, the follow-up headway and the critical headway are measured, then the capacity formula for this test scenario as well as the capacity parameters *A* and *B* are determined

using Equations 7-7 through 7-9. In this study, the capacity curve parameters *A* and *B* generated from the three basic simulation models are regarded as *baseline capacity parameters*, while the parameters *A* and *B* calculated from extended CAV simulation scenarios are considered as *adjusted parameters*. The adjustment factor for baseline *A* and *B* can be derived by dividing the adjusted parameters by the baseline parameters, as shown in Equations 7-10 through 7-12.

$$\boldsymbol{C_{adj} = A_{adj} \cdot e^{-B_{adj} \cdot v_C}} \quad \textbf{(7-10)}$$

$$\boldsymbol{f_A = \frac{A_{adj}}{A}} \quad \textbf{(7-11)}$$

$$\boldsymbol{f_B = B_{adj}/B} \quad \textbf{(7-12)}$$

where:

f_A = adjustment factor for parameter *A*,

f_B = adjustment factor for parameter *B*, and

C_{adj} = adjusted entry capacity (pc/h).

7.2.4 Experiment Design

In the current HCM capacity methods, the calculation of *entry capacity* is specified by the number of entry lanes and the number of conflicting circulatory lanes. The capacity of each entry lane is expressed as an empirical function of conflicting flow, i.e., the circulatory traffic flow that directly passes in front of the subject entry lane. Three cases were studied using simulation: one entry lane opposed by one circulating lane (i.e., a single-lane roundabout), and separate formulas for the left and right entry lanes of a two-lane entry opposed by two circulating lanes (i.e., a full double-lane roundabout). The HCM also presents capacity formulas for two additional cases: a single lane opposed by two circulating lanes, and two lanes opposed by one entry lane. However, due to the time and effort needed for the three studied cases and the other interrupted flow models (signalized and stop-controlled intersections), these two additional roundabout cases were not studied explicitly in this research through simulation modeling. Instead, the research team has used the simulation results for the three modeled roundabout cases to estimate parameters for these two other roundabout cases. This process is discussed further in the findings.

Three basic simulation models are created for the single-lane and double-lane roundabout in this study. For each basic model, six variant models representing CAV market penetration rate (MPR) ranging from 0% to 100% at 20% increments were built.

All simulation experiments performed in this research were based on simulation runs of 7,500 sec (125 minutes) at a resolution of 10 time steps per simulation second. A 5-minute warm-up time was included in each run to allow traffic to stabilize before collecting data between 300 sec and 7,500 sec (120 minutes). Each run was used to obtain the entering flow under one regime of circulating flow. A total of seven (fourteen for double-lane cases) conflicting flow regimes were used to generate data throughout a range of practical circulating flows, with five simulation runs using different random seeds per conflicting flow rate. The flow regimes start from the circulating flow of 0 pc/h. For each subsequent regime, 200 pc/h were added for both the single-lane and double-lane roundabout cases.

Both the single-lane roundabout and the double-lane roundabout VISSIM models were calibrated by the HCM capacity models, with the left and the right entry lane of the double-lane roundabout calibrated separately. The simulation models were calibrated by adjusting the parameters regarding the conflict area (CA), the Wiedemann '74 driving model, and the reduced speed area. The calibration results are illustrated in Figure 7.4.

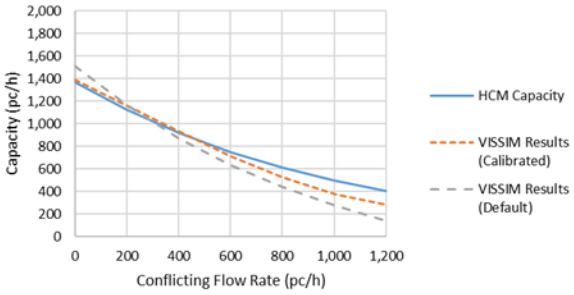

(a) Single-Lane Roundabout

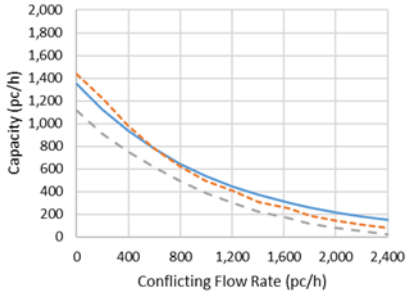

(b) Left Lane of Two-Lane Entry

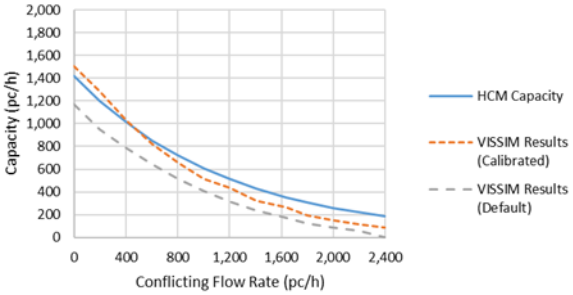

(c) Right Lane of Two-Lane Entry

Figure 7.4: Roundabout calibration results

Figure 7.4 shows the capacity curves derived by the HCM capacity models, the calibrated VISSIM models, and the default VISSIM models, respectively. As shown in Figure 7.4, the calibration reduces the error between the VISSIM capacity curves and the HCM capacity curves. The R-squared values for the VISSIM capacity curves and the HCM capacity curves under three simulation models were calculated to evaluate the calibration performance. The R-squared values of the default VISSIM models are 0.83, 0.85, and 0.82, respectively, while the R-squared values of the calibrated VISSIM models are 0.92, 0.94, and 0.91. These results indicate that the test models were calibrated to a sufficient level for this study. These calibrated models were treated as the base models in this study.

7.3 RESULTS

7.3.1 Effects of CAVs on Entry-Lane Capacity

In each of the three base case models, six CAV MPR scenarios (i.e., 0%, 20%, 40%, 60%, 80%, and 100%) were tested to generate a capacity curve. The comparison of capacity curves in different MPR scenarios are shown in Figure 7.5 where it can be seen that the impact of CAV on entry capacity is significant for both single-lane and double-lane roundabouts. At each conflicting flow rate, the capacity of an entry lane increases with the increase of CAV MPR. Specifically, we use 0% and 100% MPR scenarios for detailed comparison. When the conflicting flow rate is 0 pc/h, the increase in capacity from 0% to 100% MPR is 36%. As the conflicting flow rate increases, the proportion of the capacity increase keeps rising and can be as large as 116% when the conflicting flow rate is 1,200 pc/h.

Similar characteristics can be found in the double-lane roundabout cases in Figure 7.5 for the left entry lane, the capacity increase between 0% and 100% MPR is in the range of 38% to 123%; for the right entry lane, the capacity increase is in the range of 29% to 110%.

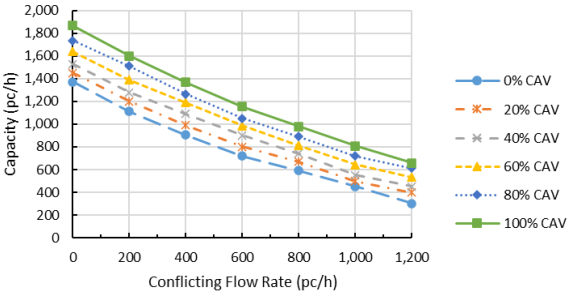

(a) Single-Lane Roundabout

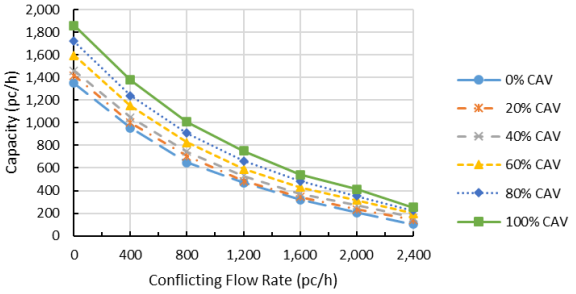

(b) Left Lane of Two-Lane Entry

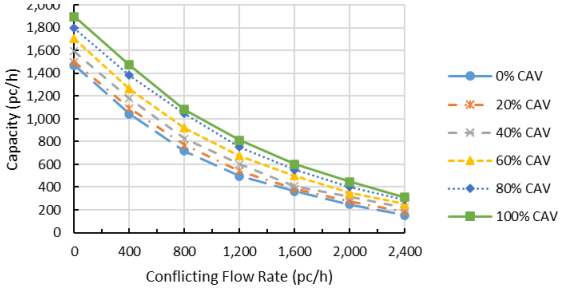

(c) Right Lane of Two-Lane Entry

Figure 7.5: Capacity curves for single-lane and double-lane roundabout entries

The benefit of applying CAVs gradually increases as the conflicting flow rate increases. Specifically, the percent improvement in the entry capacity is more substantial at high conflicting flow rates. This indicates that the CAVs can use gaps created by conflicting traffic more efficiently than human-driven vehicles due to the shorter car-following gaps controlled by the CACC behavior between CAVs. Such benefit is especially significant when the conflicting flow is high.

7.3.2 Effects of CAVs on Critical Headway and Follow-up Headway

In each CAV MPR scenario, follow-up headways and critical headways are measured over the entire range of conflicting flow rates. The variation of the follow-up and the critical headways against the conflicting flow rates under different CAV MPRs are illustrated in Figure 7.6. As shown in Figure 7.6(a), (c), and (e), both the MPR and the conflicting flow impact the follow-up headways. At each conflicting flow rate, the follow-up headway becomes longer with the increase of MPR. Under each MPR condition, the follow-up headway also increases with the increase of the conflicting flow rate, but the percent increase of follow-up headway decreases as CAV MPR increases for each conflicting flow rate. Specifically, as shown in Figure 7.6(a), the rising trend of the follow-up headway against the conflicting flow declines as the MPR increases. Under 0% MPR scenario, the follow-up headway is increased by 17% when the conflicting flow rate rises from 0 to 1200 pc/h, while the follow-up headway under 100% MPR case is increased by only 6%. Similar results can also be found in double-lane roundabout cases from Figure 7.6(c) and (e). From Figure 7.6(b), (d), and (f), we can tell that the critical headways of different entry lane cases are impacted by CAV MPR only and are nearly uninfluenced by the conflicting flow rates.

In the HCM method, both the follow-up headway and the critical headway are treated as constants; i.e., the two headways do not change with the increase of the conflicting flow rate. To derive the capacity formula for each CAV MPR scenario using the HCM method, we take the average values of both the follow-up headway and the critical headway over all conflicting flow rates. The averaged follow-up headways and critical headways for each MPR scenario are listed in Table 7.1. For critical headway, this assumption is consistent with the observed lack of sensitivity of critical headway to conflicting flow. However, for follow-up headway, this assumption may impact the estimation of the capacity, because follow-up headway was observed to vary with conflicting flow. The detailed analysis between the estimated capacity and the actual simulated capacity will be discussed in the next section.

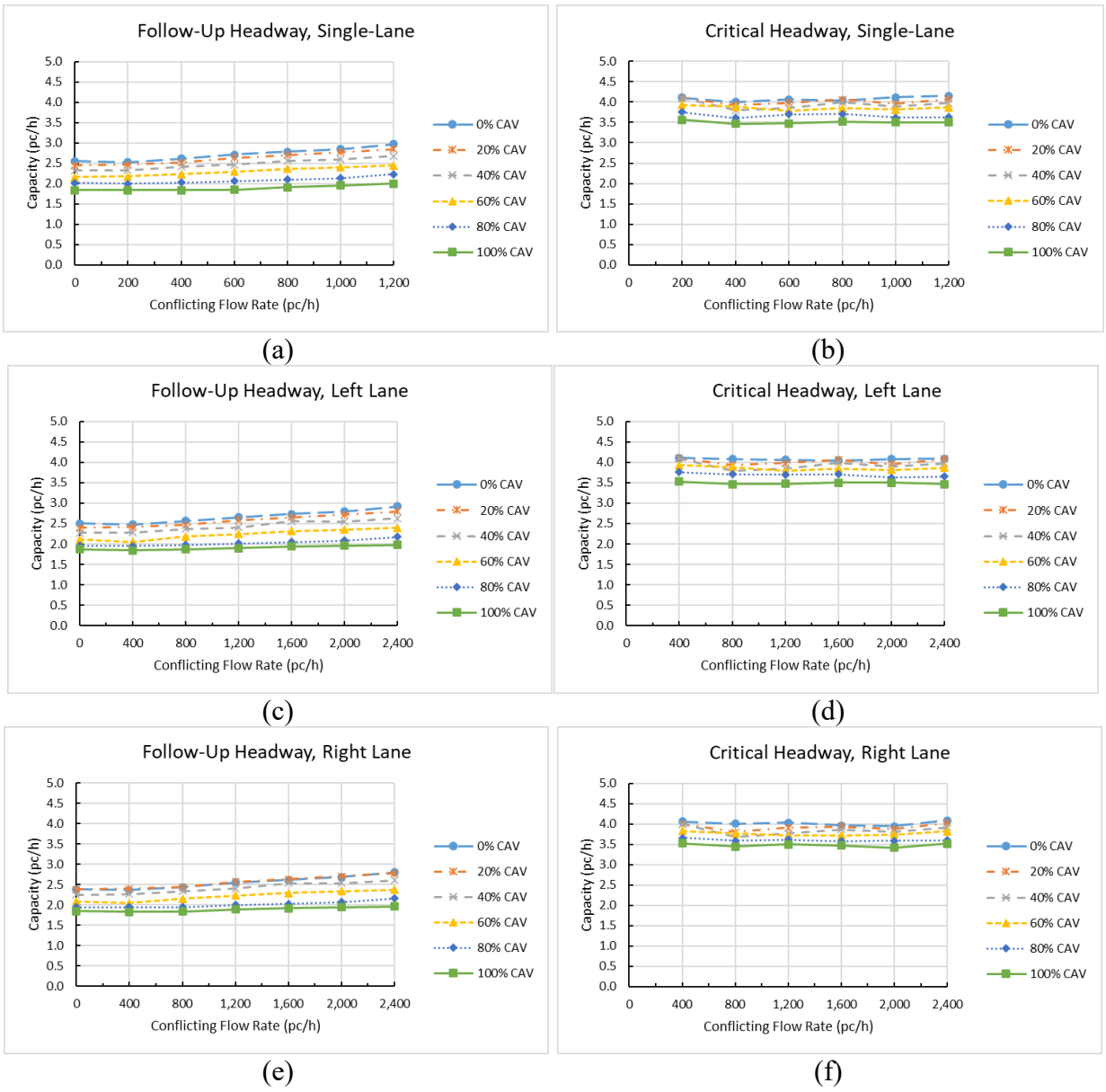

Figure 7.6: Follow-up headway and critical headway curves for single-lane and double-lane roundabouts under different CAV MPRs

Table 7.1: Follow-Up Headways and Critical Headways for Base Models

		CAV Market Penetration Rate (MPR)					
		0%	**20%**	**40%**	**60%**	**80%**	**100%**
Follow-Up headway (sec)	Single-Lane	2.62	2.48	2.34	2.21	2.06	1.93
	Double-Lane, Left	2.60	2.47	2.33	2.19	2.05	1.92
	Double-Lane, Right	2.54	2.46	2.31	2.15	2.01	1.89
Critical headway (sec)	Single-Lane	4.08	3.99	3.86	3.73	3.60	3.48
	Double-Lane, Left	4.02	3.91	3.79	3.67	3.55	3.44
	Double-Lane, Right	3.93	3.83	3.71	3.60	3.49	3.39

As illustrated in Table 7.1, both the follow-up headway and the critical headway decrease as CAV MPR increases. The decrease of the follow-up headway from 0% MPR to 100% MPR for three entry lanes are 26.3%, 26.2%, and 25.6%, whereas the decrease of critical headway from 0% MPR to 100% MPR are 15.3%, 14.4%, and 13.7%, respectively. This indicates that the follow-up headway is more sensitive to the variation of CAV MPR.

The decrease of the follow-up headways over CAV MPRs is largely due to the CACC model that controls the car-following behavior of CAVs in the entering traffic flow. When two or more CAVs from the entering lane accept the same gap created by the conflicting traffic, the CACC function embedded in the CAV's control model allows this group of waiting CAVs to enter the roundabout with a relatively shorter car-following gap than that for human-driven vehicles. Therefore, the average follow-up headway will be significantly reduced with the increase in CAV MPR.

Table 7.1 shows that the critical headways also slightly decrease with an increase of CAV MPR. This is because as the MPR increases, the distribution of the gap lengths in the conflicting flow changes. As described in the methodology part, the critical gaps in this study are calculated by Raff's method using cumulative frequency distribution (CDF) curves of all the rejected gap lengths and the accepted gap lengths and finding the interception point of the two curves. To illustrate how the CDF curves shift with the increase of CAV MPR, we take the single-lane roundabout as an example and plot the CDF curves of different MPRs under the conflicting flow rate of 600 pc/h for illustration.

As shown in Figure 7.7, the x-coordinates of the intersection points between the accepted and the rejected CDFs fall approximately in the interval of gap length between 3 to 4 seconds under six MPR cases; the intersection slightly shifts to the left with the increase of MPR. Specifically, we can tell from Figure 7.7 that, when the MPR increases, the CDFs of the accepted gaps remain consistent in the area where gap lengths are smaller than 4 seconds, whereas the CDFs of the rejected gaps in the interval of gap lengths larger than 3 seconds tends to shift to the left. These two tendencies combine to shift the intersection point to the left, thus leading to a decrease in the critical headway. The shift in the CDFs of the rejected gaps is largely due to the increase of small gaps among all rejected gaps. With an increase in MPR, more vehicles on the conflicting lanes are CAVs and follow the CACC car-following behavior. Because the intra-platoon gaps are 0.7 seconds in this study, which are much smaller than the car-following gaps between human-

driven vehicles, the proportion of small gaps among all rejected gaps increases and thus leads to a shift of the CDF curve.

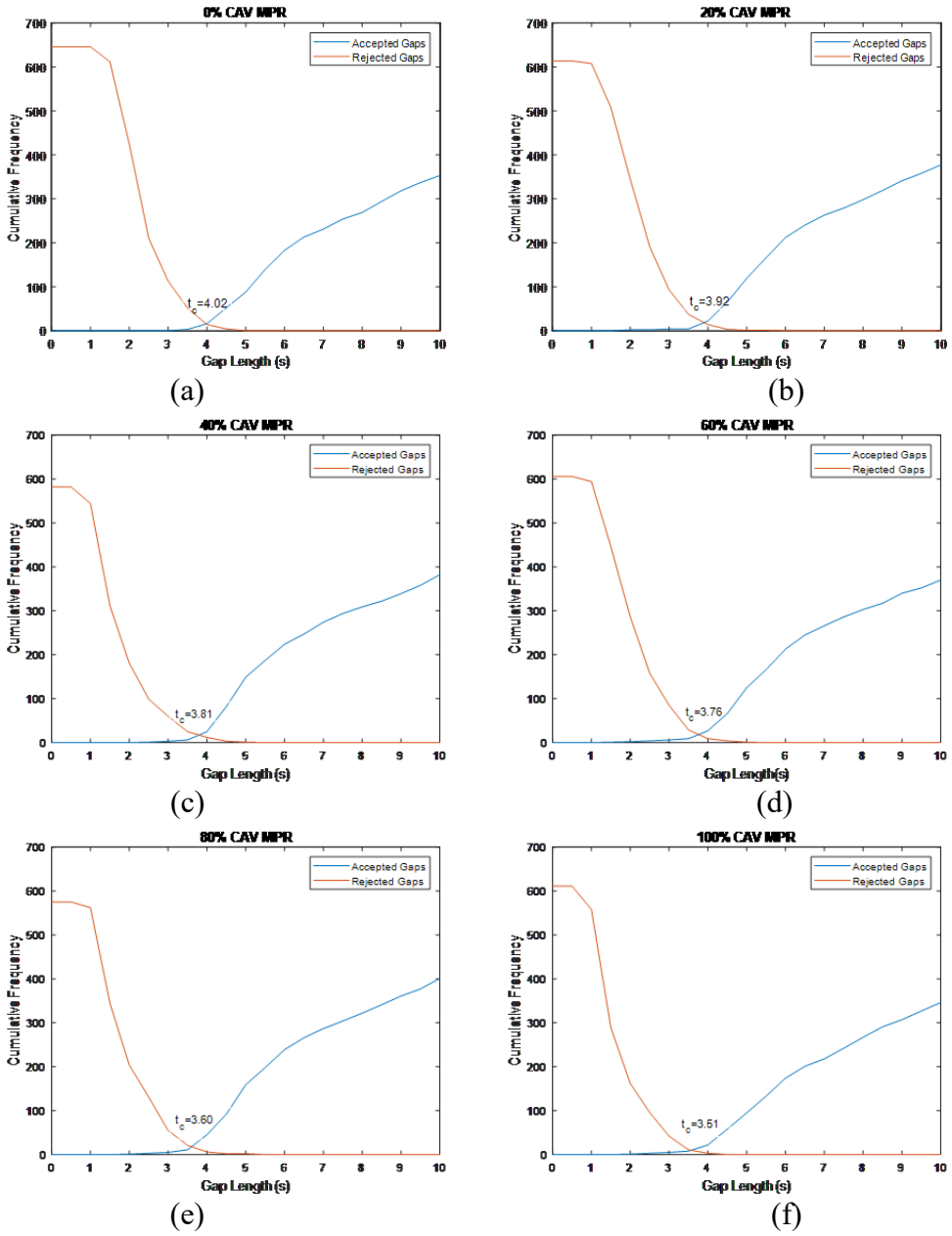

Figure 7.7: Cumulative frequency distribution for accepted and rejected gaps for single-lane roundabout case under the conflicting flow rate of 600 pc/h

7.3.3 Comparison of the HCM Model with Simulation Results

To investigate the goodness of fit of the HCM estimated capacity, the research team compared the HCM results with the VISSIM measured results as shown in Figure 7.8. This figure shows that the goodness of fit of the two results gets better as the CAV MPR increases. Specifically, as the MPR rises, the deviation of the intercepts and the slopes between the two curves decreases.

The root mean squared error (RMSE) of the HCM result is improved from 132 to 64 pc/h with MPR increases from 0% to 100%. The estimation performance of the HCM model in other tested scenarios are presented in Table 7.2. This table indicates that the goodness of fit of the HCM capacity result improved as MPR increased in all tested entry lanes.

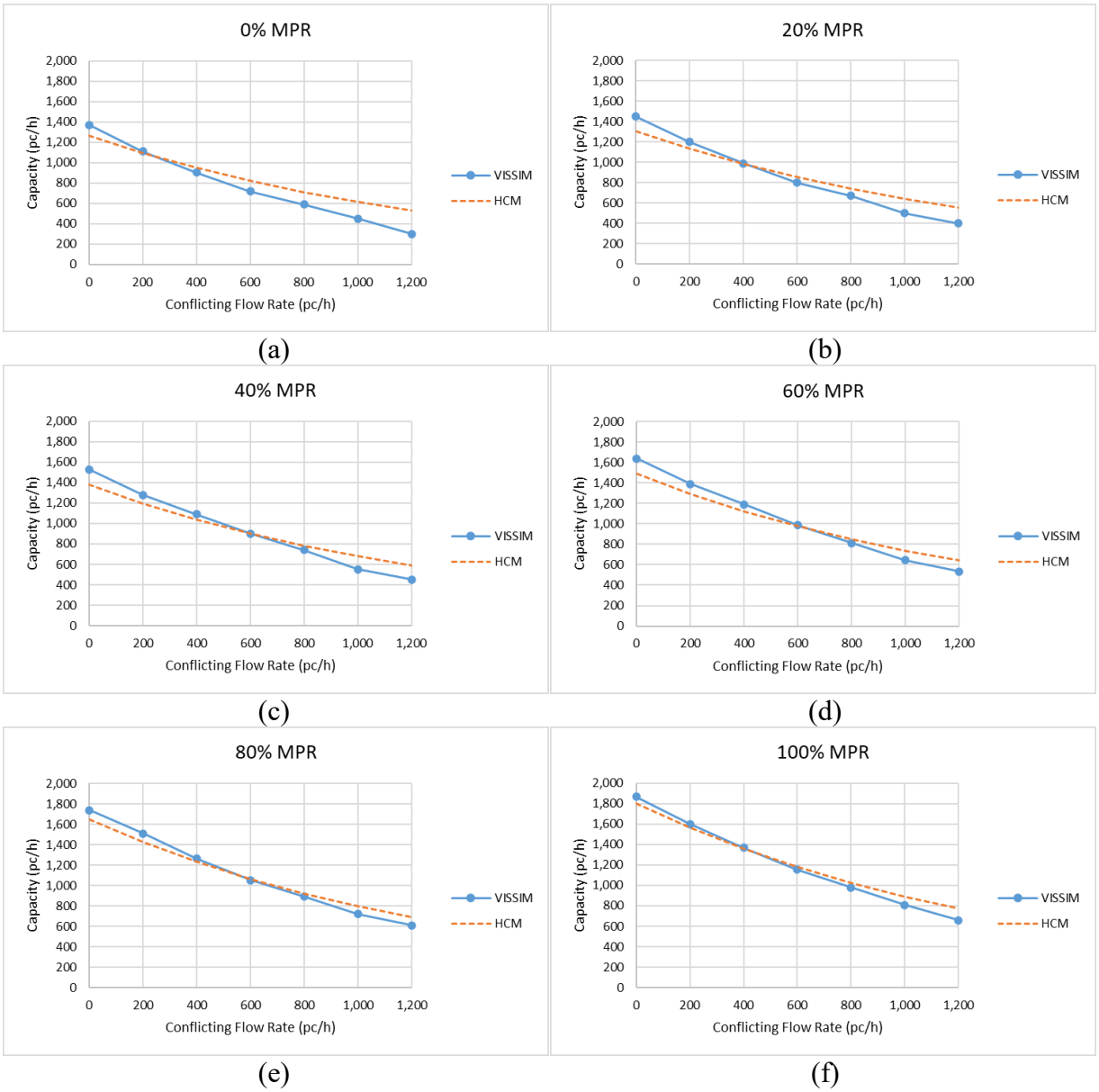

Figure 7.8: Simulation results compared to the HCM

Table 7.2: Root Mean Squared Error (RMSE) Value of HCM Capacity Curves

	Market Penetration Rate (MPR)					
	0%	**20%**	**40%**	**60%**	**80%**	**100%**
Single-Lane	132	106	100	91	67	64
Double-Lane, Left	111	93	83	70	67	48
Double-Lane, Right	105	81	69	65	59	36

The improvement of HCM estimation performance is mainly due to the difference in the trend that the follow-up headway changes against the conflicting flow under different MPRs. As discussed in the previous section, under each CAV MPR scenario, the follow-up headway increases with the increase of the conflicting flow rate, while the critical headway is not impacted by the conflicting flow. Meanwhile, with the increasing MPR, the follow-up headway's rising trend against the conflicting flow is gradually eliminated and the follow-up headway is closer to a constant at each conflicting flow rate. That is to say, when the MPR is low, the error between the averaged follow-up headway and the actual follow-up headway at each conflicting flow rate is large, especially when the conflicting flow rate is too low or too high; as the MPR increases, the error is decreased, and the averaged follow-up headway is closer to the actual follow-up headways at each conflicting flow rate. Because the follow-up headway is the major factor that impacts the intercept and the slope of the capacity curve, and the HCM capacity estimation is calculated using the averaged value for both the follow-up headways and the critical headways, the research team concludes that the goodness of fit between the HCM result and the simulation-measured result increases with increasing MPR.

7.3.4 Effects of CAVs on the Relationship between Exiting Flow and Entry Capacity

In the HCM capacity model, the primary factor influencing the lane capacity of an approach is the conflicting flow because the conflicting flow is the circulating flow that passes directly in front of the subject entry. The effect of exiting vehicles on entry capacity has been explored in previous research but is not accounted for in the HCM 6th Edition. Research that formed the basis for the HCM 2010 roundabout capacity models found that exiting flow did not have enough effect on entry capacity to include in the recommended models (Rodegerdts et al., 2007). Subsequent research supporting the capacity models in the HCM 6th Edition also did not recommend modifying the models to include exiting vehicles (Rodegerdts et al., 2015). As such, the planning-level capacity adjustment factors developed for this project are based solely on circulating flow, for consistency with the current HCM models.

The interaction between CAVs and exiting vehicles may also affect a driver's decision to enter the roundabout. This phenomenon is similar to the effect of the right-turning stream on the major street approaching from the left side of the minor leg of a TWSC intersection. Until these drivers complete their exit maneuver or right turn, there may be some uncertainty in the mind of the driver at the yield or stop line about the intentions of the exiting or turning vehicle.

To investigate how exiting flow may influence the capacity of the subject entry lane, a sensitivity analysis was conducted by adding exiting flow to the circulating flow. In this section, the conflicting flow is still considered as the circulating flow that directly passes in front of the subject entry lane. An additional exiting flow rate is added to the system, set as a percentage of the conflicting flow. This assumption ensures that the exiting flow rate increases proportionally as the conflicting flow rate increases. Three combinations are set for the exiting flow rate: 10%, 30%, and 50% of conflicting flow rate, or 0.1CFR, 0.3CFR, and 0.5CFR, respectively.

For the single-lane roundabout, three exit flow rate scenarios were tested and compared with the scenario of 0% exiting flow rate to investigate the impact of exiting flow on the capacity of the left and right entry lanes. Figure 7.9 compares the capacity reduction after the introduction of the

exiting flow to the single-lane roundabout model. All six CAV MPRs were tested, but only 0% and 100% scenarios are presented here to show the maximum difference. The root mean squared errors (RMSE) were measured to compare the result with or without the exiting flow. The comparison results are presented in Table 7.3.

As shown in Figure 7.9, for 0% CAV MPR, when the exiting flow rate is 10% of conflicting flow rate, the exiting flow causes a negligible reduction in the capacity of the entry in the single-lane roundabout, but the effect increases as the exiting flow rate is increased to 30% and 50% of the circulating flow rate. In addition, the effect of exiting flow on capacity becomes more substantial as the exit flow rate increases.

Two primary insights can be concluded from this result. First, the reduction of the entry capacity caused by the exiting flow appears to be significant, particularly at higher exiting flow rates. Second, under 100% CAV MPR, the influence on the entry capacity of single-lane roundabout caused by exiting flow is relatively small. This demonstrates that the route conflict anticipation function adopted by CAVs can effectively help the entering traffic eliminate the impact of exiting flow on the entry capacity. As such, the current HCM model form that excludes the effect of exiting vehicles appears to be valid for higher MPR cases.

Table 7.3: Root Mean Squared Error (pc/h) of HCM Capacity Curves Under Exiting Flow Scenarios

EFR/CFR	0% MPR	100% MPR
Single-Lane Roundabout		
0.1	25	10
0.3	67	27
0.5	103	34
Double-Lane Roundabout, Left Lane		
0.1	9	3
0.3	23	5
0.5	30	11
Double-Lane Roundabout, Right Lane		
0.1	6	5
0.3	15	6
0.5	26	9

Note: EFR = exit flow rate, CFR = conflicting flow rate.

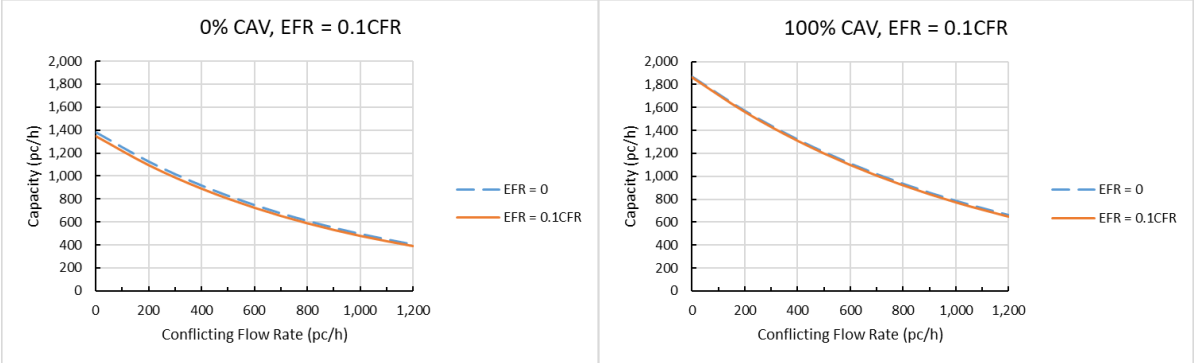

(a) MPR = 0%, EFR = 0.1CFR

(b) MPR = 20%, EFR = 0.1CFR

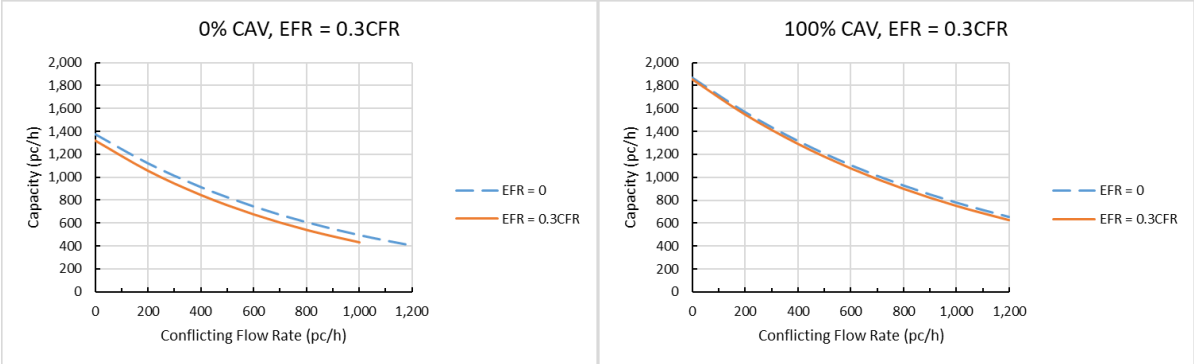

(c) MPR = 40%, EFR = 0.3CFR

(d) MPR = 60%, EFR = 0.3CFR

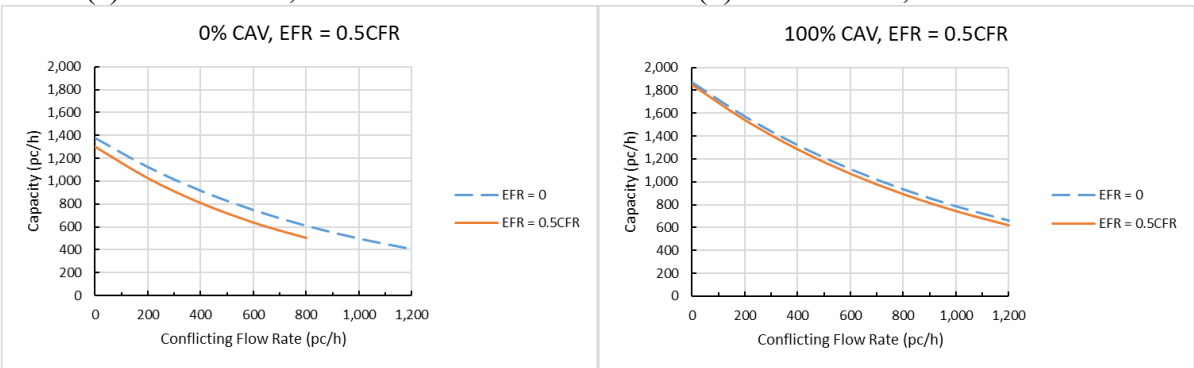

(e) MPR = 80%, EFR = 0.5CFR

(f) MPR = 100%, EFR = 0.5CFR

Figure 7.9: Capacity reduction curves for single-lane roundabout

For the double-lane roundabout, three exit flow rate scenarios (10%, 30%, and 50% of conflicting flow rate, or 0.1CFR, 0.3CFR, and 0.5CFR, respectively) are also tested and compared with the scenario of 0% exiting flow rate to investigate the impact of exiting flow on the capacity of the left and right entry lanes. The root mean squared errors (RMSE) are measured to compare the result with or without the exiting flow.

As shown in Table 7.3, in each EFR scenario, when the MPR increases from 0% to 100%, the RMSEs of double-lane roundabouts are significantly reduced. This is similar to the results in the single-lane roundabout cases. However, when comparing the value of RMSE between the single-lane roundabout cases and the double-lane cases, it is notable that the RMSE in both 0% MPR scenarios and 100% MPR scenarios are much smaller than the results in the single-lane

roundabout. Specifically, the RMSE value of the right lane of the double-lane roundabout is the smallest among the three entry lane models. This indicates that both entries in the double-lane roundabout are less impacted by the exiting flow than the single-lane roundabout, and the influence on the right entry lane is the smallest.

The difference between the impact on the single-lane roundabout and on the double-lane roundabout caused by the exiting flow is believed to be largely due to the different size of the two roundabouts. For the two roundabouts modeled in this study, the distance from the upstream exit to the subject entry lane is 60 ft for the single-lane roundabout and 113 ft for the left lane of the double-lane roundabout. The larger distance from the exit to the entry lane in the double-lane roundabout allows the drivers on the entry lane to be more certain of the upcoming vehicle's path. Specifically, we can assume that the incoming vehicle on the conflicting lane just arrives at the exit and the speed is 15 mph, then the time gap between the incoming vehicle and the subject entry would be 2.6 seconds for the single-lane roundabout and 5 seconds for the left lane of the double-lane roundabout. Because the critical headways measured in this study are between 3.3 to 4.2 seconds, the yielding human-driven vehicle in the single-lane case must wait for the decision of the incoming vehicle before entering the roundabout, while the yielding human-driven vehicle in the double-lane roundabout can more readily accept the gap and neglect the uncertainty of the path decision of the incoming vehicle.

7.3.5 Capacity Adjustment Factors

Table 7.4 provides CAFs for CAVs at roundabouts. To determine the CAV-adjusted capacity, apply the CAFs f_A and f_B to the values for parameters A and B, respectively, used by the HCM's roundabout entry capacity model, as shown in Equation 7-13.

$$C_{adj} = f_A A \cdot e^{-f_B B \cdot v_C} \quad \textbf{(7-13)}$$

Table 7.4: CAFs for CAVs at Roundabouts

	1-Lane Entry				2-Lane Entry					
Proportion of CAVs in	**1 Circulating Lane**		**2 Circulating Lanes[a]**		**1 Circulating Lane, Both Lanes[a]**		**2 Circulating Lanes, Left Lane**		**2 Circulating Lanes, Right Lane**	
Traffic Stream	f_A	f_B	f_A	f_B	f_A	f_B	f_A	f_B	f_A	f_B
0	1.00	1.00	1.00	1.00	1.00	1.00	1.00	1.00	1.00	1.00
20	1.05	0.99	1.03	0.99	1.05	0.99	1.03	0.99	1.05	0.96
40	1.12	0.97	1.08	0.96	1.12	0.97	1.08	0.96	1.12	0.93
60	1.22	0.94	1.18	0.92	1.22	0.94	1.18	0.92	1.20	0.87
80	1.29	0.90	1.28	0.89	1.29	0.90	1.28	0.89	1.27	0.84
100	1.35	0.85	1.38	0.85	1.35	0.85	1.38	0.85	1.34	0.80

Notes: These cases were not specifically analyzed in the research and thus are suggested approximations.

- CAV = connected and automated vehicle, defined here as a vehicle with an operating cooperative adaptive cruise control system.
- Interpolate for other CAV proportions.
- Assumptions: Human-driven vehicles operate with average gaps calibrated to the entry lane capacity given by HCM Chapter 22.

As shown in Table 7.4, f_A increases with increasing MPR for each entry type, indicating that the capacity increases as the MPR increases. The value of f_B decreases as MPR increases, which also indicates that capacity increases as MPR increases. The results in the table illustrate that the adjustment factors are sensitive to the change in MPR in all three entry models. As noted previously, no specific modeling was conducted as part of this project for two other cases in the HCM, for which assumptions are needed to determine appropriate parameters. These two cases are as follows:

- **One entry lane against two circulating lanes.** The factors listed above for the double-lane roundabout, left lane are suggested. The driver behavior for one lane opposed by two circulating lanes is most likely to match that for the left lane of a two-lane entry. This assumption is expected to be reasonable for typical proportions of left-turning and through traffic; if traffic is largely turning right, then it may be more reasonable to use the factors for the right lane of a two-lane entry.

- **Two entry lanes against one circulating lane.** The factors listed above for the single-lane roundabout are suggested for both entry lanes. The capacity of the left lane is anticipated to be very similar to that for the single-lane case. The capacity for the right lane is more dependent on the alignment of the circulating lane and turning movement patterns. For most designs, it is reasonable to assume that traffic in the right lane will yield to the entire circulating flow regardless of the intended turning movement, thus making the suggested assumption valid. If traffic in the right lane is largely turning right with little conflict with circulating traffic, or in some cases going through with little

conflict with circulating traffic due to circulating alignments and turning movement patterns, then the estimated capacity is likely to be conservative.

7.4 FINDINGS

For test cases with the same flow pattern with the basic models, the entry capacities increase with the growth of CAV MPR. The increase in capacity is less substantial at low MPR (20% and 40%) scenarios but very significant at high MPR (60%, 80%, and 100%) scenarios. When CAV MPR increases, the follow-up headway and the critical headway decrease in both single-lane roundabouts and double-lane roundabouts. The follow-up headway decreases significantly with the increasing MPR, while the critical headway decreases only slightly. The entry capacity of each scenario can be estimated with the HCM models by using the measured follow-up headways and critical headways. The goodness of fit of the HCM estimation increases as the MPR rises. These results were integrated to develop capacity adjustment factors in the form of lookup tables which could be used as a quick evaluation measure to assess the effects of CAVs.

Future work is needed in this research. More complicated scenarios with a higher resolution of conflicting flow and exiting flow can be integrated into future studies. Other roundabout models, such as single-entry lane against two conflicting lanes or a double-entry lane against one conflicting lane, can be investigated as well. The initial exploration of the effect of exiting vehicles suggests that further exploration in this area could be valuable. In addition, the combined effect of other CAV functions, or automated operation in the absence of connectivity (i.e., ACC-only operation) may be considered in future studies.

8.0 CONCLUSIONS

Agencies must make decisions today about the future transportation system needs to meet travel demand. Connected and automated vehicles (CAVs) are one application of technology that is expected to impact transportation. The *Highway Capacity Manual* (HCM) is the leading national document for planning-level analysis of the capacity and quality of service of freeways, highways, and urban streets. However, its currently limited in its ability to incorporate the potential impacts of CAVs on capacity and quality of service. The HCM's limitations drive a need to develop capacity adjustment factors (CAFs) for HCM analysis procedures to allow future roadway capacity to be estimated under varying levels of CAV market penetration. This study assessed the potential impact of CAVs on *capacit*y.

The purpose of this study was to develop *capacity adjustment factors* (CAFs) for CAVs at different levels of market penetration (the level of CAVs in the traffic stream). A CAF is an adjustment to base capacity to reflect the effects of severe weather, incidents, and work zones, the presence of CAVs, or other factors. These CAFs are being added to the *Highway Capacity Manual* (HCM) for agencies to use in future scenario planning to analyze CAV applications on freeways and urban streets. This section outlines the key assumptions, findings, and future research needs.

8.1 ASSUMPTIONS

Planning-level estimates can help inform decision-making, but agencies should understand the underlying modeling assumptions. This project tested varying levels of CAVs in the vehicle traffic stream, referred to as the *CAV market penetration rate* in this study. By varying CAV market penetration and traffic volumes, the research team observed how market penetration affected capacity (i.e., maximum pre-breakdown flow rate) under various conditions.

CAVs in this study are defined as vehicles that are equipped with a communication system that can communicate with other CAVs and with roadside infrastructure and are equipped with an automated driving system that enables cooperative vehicle maneuvers. A CAV's cooperative control feature enables safe operation in platoons with shorter headways than possible by either human-driven vehicles or automated vehicles without connectivity, thereby potentially increasing roadway capacity. The CAVs modeled in this study correspond to Society of Automotive Engineers (SAE) Levels 4 and 5: capable of controlling the vehicle for part (e.g., only on freeways, or only within the defined operational design domain) or all of a trip, without requiring human intervention.

We evaluated the impacts of two CAV systems or scenarios: *adaptive cruise control* (ACC) and *cooperative adaptive cruise control* (CACC). ACC is a driver assistance system that automatically adjusts a vehicle's speed to maintain a set following distance from the vehicle in front (USDOT, 2018), relying on data from on-board sensors (e.g., cameras, radar, lidar). ACC systems are conservative and produce time gaps to preceding vehicles similar to, or longer than, those used by human drivers. CACC is an ACC system that also integrates communication from

preceding vehicles, roadside infrastructure, or both to allow faster reactions to changes. This results in safe operation at shorter headways than it would otherwise be possible with either human-driven vehicles or ACC systems relying solely on on-board sensors.

A base assumption for CAV analysis is that all necessary communication elements are in place and working with a high degree of reliability. The impact of CAV aggressiveness was compared by simulating three intra-platoon gap assumptions: *conservative*, *normal*, and *aggressive*.

8.2 FINDINGS

This section summarizes the key findings for freeway segments (basic freeway, merge and diverge, and weave), signalized intersections, two-way stop-controlled intersections, and roundabouts.

8.2.1 Freeway Segments

This research analyzed the impact of ACC- or CACC-equipped CAVs on freeways (basic segments, merge and diverge segments, and weaving segments). Different starting capacities were tested. The capacity benefit of CACC follows a quadratic trend. However, in cases of lower starting capacities, the trend is more linear with higher capacity benefits with increasing penetration rate. This infers that the capacity benefits are not the same across all facility design speeds and operating conditions. We also analyzed the effect of on-ramp demand on merge segment capacity. The results indicated that different roadway capacities are achieved at different ramp demand levels. In addition, CACC coordination can potentially reduce the effect of merging disturbance at on-ramps when the market penetration rate is high. On weaving segments, the results showed that the capacity benefits of CACC decrease as the volume ratio increases. Weaving disturbances drastically reduce the effects of CACC coordination. Even when an advanced merging capability was provided, the effects of weaving intensity were still pronounced.

While this study focuses on CAV effects on capacity due to CACC, we also conducted experiments for freeways on the effects of ACC to show the importance of connectivity in enhancing capacity. For a base capacity of 2,400 pc/h/ln, freeway capacity decreases as the percentage of ACC-equipped vehicles increases. This result is because ACC systems drive more conservatively than HDVs in the traffic. ACC systems are built to prioritize comfort and safety, which generally results in more conservative driving behavior. In the 1,800 pc/h/ln base capacity scenario, capacity increases as the proportion of ACC-equipped vehicles increases. This result occurs because even though ACC systems are designed to drive conservatively, the resulting headways are still lower than those of HDVs under low-capacity base conditions, leading to capacity improvements. This finding suggests that ACC systems can perform better than human-driven vehicles under non-ideal conditions, likely due to the deterministic behavior of ACC systems that stabilizes the traffic flow.

8.2.2 Signalized Intersections

For signalized intersections, this research investigated changes in capacity under increasing CAV market penetration rates (MPRs) for three exclusive movement setups: through movement, single-lane protected left turn, and single-lane permitted left turn.

Results showed that the saturation headway decreases considerably with increasing CAV MPR. For the protected left-turn movement, higher benefits were observed compared to the through movement. With increased CAV MPR, there were no significant changes in start-up and end-lost times, and therefore leading to very marginal effects on effective green time. As a result, only the effects on the saturation headway (or saturation flow rate) were included for the CAF development

For the permitted left-turn scenario, critical gap did not change with increasing CAV MPR compared to the conventional human-driven vehicle traffic. However, by enhancing CAVs with platooning capabilities (CACC), the follow-up headway decreases as the CAV MPR increases. Also, due to the reduced discharge headway of CAVs, queues on the opposing approach dissipated more quickly, thereby providing more unblocked green time for permitted left-turn movement, and subsequently increasing the permitted left-turn capacity.

8.2.3 Two-Way Stop-Controlled Intersections

The two-way stop-controlled intersection (TWSC) model results were inconclusive, as the simulation models were not properly calibrated to HCM capacities. Furthermore, it is unclear what the behavior of CAVs at minor-street approaches of TWSC will be like in the future. For this work, it was assumed that all vehicles would still need to come to a full stop at the stop-bar, which results in little to no capacity improvements due to CAVs or platooning (as platoons are broken up by the stop-sign). As a result, no capacity adjustment factors for CAV effects at TWSC intersections are currently proposed. The report does summarize the modeling activities for TWSC to serve as a foundation for future research efforts.

8.2.4 Roundabouts

This research tested the CAV impacts at a single-lane roundabout and a double-lane roundabout. It was found that the entry capacities increase with the growth of CAV MPR. The increase in capacity is less substantial at low MPR (20% and 40%) scenarios but very significant at high MPR (60%, 80%, and 100%) scenarios. When CAV MPR increases, the follow-up headway and the critical headway decrease in both single-lane roundabouts and double-lane roundabouts. The follow-up headway decreases significantly with the increasing MPR, while the critical headway decreases only slightly. The entry capacity of each scenario can be estimated with the HCM models by using the measured follow-up headways and critical headways. The goodness of fit of the HCM estimation increases as the MPR rises.

8.3 APPLICATION OF CAV CAFs

Capacity adjustment factors are provided in the form of lookup tables that could be used as a quick evaluation tool for planning projects to assess the effects of CAVs, similar to those used in the HCM.

Any evaluation of future conditions requires assumptions about future population growth, mode choice, travel demand, and travel patterns, among other factors. Another uncertainty is how CAVs will operate in real-world applications in the hands of consumers because these vehicles are not yet in production. The CAV CAFs and service volume tables presented in this report should be applied to the evaluation of "*what if*" scenarios, rather than being taken as the final word on what *will* happen once CAVs become widespread.

When applying the CAV CAFs and service volume tables, the analyst should consider:

- What if the minimum headway permitted by technology, regulation, or policy, or the average headway produced by different vehicles' user settings, is longer than the modeling assumed? In this case, the capacity increase would be less than predicted by the CAV CAFs or service volume tables.

- *How reliable will the necessary communications and automation technology be?* To the extent that individual CAV-capable vehicles must be driven by a human at any given time due to equipment malfunction or operational conditions, the proportion of operating CAVs in the traffic stream will be less than the proportion of CAV-capable vehicles. (Alternatively, the demand will be lower, in the situation where only vehicles with functioning systems are allowed on the facility.)

- *How quickly will CAV technology become available and adopted, and how will CAVs affect travel demand?* The assumptions made related to these questions will determine the assumed volume and proportion of CAVs in the traffic stream, along with the assumed CAF.

This report relies on the analyst to determine one or more likely market penetration rates suitable for the analysis horizon year and study area being analyzed, rather than specifying a default market penetration rate applicable to a given year.

8.4 CAV ADOPTION TIMELINE

CAVs will likely increase capacities, but not as soon as agencies might think. Some experts believe it will be decades and not years before a vehicle can drive itself at any speed on any road in any weather (Litman, 2019). AV penetration widespread enough to have a profound impact on the transportation system is likely to be far off (Forsgren et al., 2018). The technology needs perfecting before we will see market saturation of highly automated vehicles. Once technology is perfected it is predicted that it will take another 13 years for 50% of cars and 27 years for 90% of cars to operate at highly automated levels (Straight, 2018). Furthermore, it is unlikely that the technology will be adopted at the same rate throughout the United States. For example, fleet owners may adopt the technology at a faster rate than individuals, and some states may create incentives for CAV ownership (e.g., converting high-occupancy vehicle lanes into CAV-only

lanes) while others do not. Additionally, CAV adoption rates may differ between rural and urban environments or uninterrupted flow and interrupted flow segments.

8.5 FUTURE RESEARCH NEEDS

This section suggests future research needs for interrupted flow facilities (freeways and managed lanes), uninterrupted flow facilities (signalized intersections, two-way stop-controlled intersections, and roundabouts), and other factors that impact capacity.

8.5.1 Freeways and Managed Lanes

More complex freeway scenarios, such as managed lanes, higher weaving ratios, and two-lane on-ramps could be incorporated in future studies. Another area to explore is the effect of trucks (both automated and human-driven) on a traffic stream incorporating CAVs. Finally, future studies could consider the combined effect of other CAV applications that may potentially be implemented in the near future.

8.5.2 Signalized Intersections

While this study evaluated the impacts of CAVs at signalized intersections for exclusive lanes, scenarios of shared lanes with more complex configurations can be a subject of future research. We also considered only CACC and ACC-equipped vehicles and their effect on saturation headway. However, there are other enhancements that can be achieved through communication with the signal controller such as trajectory and signal optimization that are likely to accompany CAV penetration. These hybrid strategies can also be considered and evaluated in future studies.

8.5.3 Roundabouts

More complicated scenarios with a higher resolution of conflicting flow and exiting flow can be integrated into future studies. Other roundabout models, such as single-entry lane against two conflicting lanes or a double-entry lane against one conflicting lane, can be investigated as well. The initial exploration of the effect of exiting vehicles suggests that further exploration in this area could be valuable. In addition, the combined effect of other CAV functions, or automated operation in the absence of connectivity (i.e., ACC-only operation) may be considered in future studies.

8.5.4 Other Factors that Impact Capacity

Capacity is a function of many factor and assumptions. This study addressed some of the most critical factors. Future research is needed to understand how the impacts of CAVs might change given the presence of other factors that impact capacity, such as the presences of heavy vehicles. CAV car following and driver behavior algorithms are different for light vehicles and heavy vehicles. As CAV technology is deployed on trucks, similar studies are needed to understand how the behavior of heavy vehicle CAV platoons could impact capacity on different segment types.

9.0 REFERENCES

Abou-Senna, H., & Radwan, E. (2013). VISSIM/MOVES integration to investigate the effect of major key parameters on CO2 emissions. *Transportation Research Part D: Transport and Environment*, *21*, 39–46. https://doi.org/10.1016/j.trd.2013.02.003

Adebisi, A., Liu, Y., Schroeder, B., Ma, J., Cesme, B., Jia, A., & Morgan, A. (2020). Developing highway capacity manual capacity adjustment factors for connected and automated traffic on freeway segments. *Transportation Research Record: Journal of the Transportation Research Board*, *2674*(10), 401–415. https://doi.org/10.1177/0361198120934797

Ala, M. V., Yang, H., & Rakha, H. (2016). Modeling evaluation of eco–cooperative adaptive cruise control in vicinity of signalized intersections. *Transportation Research Record: Journal of the Transportation Research Board*, *2559*(1), 108–119. https://doi.org/10.3141/2559-13

Alleven, M. (2018). *Qualcomm, Ford and Panasonic mark first U.S. C-V2X deployment in Colorado.* Fierce Wireless. Retrieved from https://www.fiercewireless.com/wireless/qualcomm-ford-and-panasonic-mark-first-u-s-deployment-c-v2x

Almutairi, F., Yang, H., & Rakha, H. (2017). Eco-cooperative adaptive cruise control at multiple signalized intersections: Network-wide evaluation and sensitivity analysis. *2017 5th IEEE International Conference on Models and Technologies for Intelligent Transportation Systems (MT-ITS)*. https://doi.org/10.1109/mtits.2017.8005727

Abuelsamid, S. (2018). Every Cadillac to soon get hands-off super cruise automated driving system for highways. *Forbes*. Retrieved from https://www.forbes.com

Aria, E., Olstam, J., & Schwietering, C. (2016). Investigation of automated vehicle effects on driver's behavior and traffic performance. *Transportation Research Procedia*, *15*, 761–770. https://doi.org/10.1016/j.trpro.2016.06.063

Behrisch, M., Bieker-Walz, L., Erdmann, J., & Krajzewicz, D. (2011). SUMO – Simulation of urban mobility: An overview. *Proceedings from, Third International Conference on Advances in System Simulation*, *Barcelona,* 55–60. http://www.thinkmind.org/index.php?view=instance&instance=SIMUL+2011

Bhuiyan, J. (2016). The complete timeline to self-driving cars. *Voxmedia.* Retrieved from https://www.vox.com/2016/5/16/11635628/self-driving-autonomous-cars-timeline

Brooks, R. (2017). The big problem with self-driving cars is people. *IEEE Spectrum*. Retrieved from https://spectrum.ieee.org/the-big-problem-with-selfdriving-cars-is-people

Bujanovic, P., & Lochrane, T. (2018). Capacity predictions and capacity passenger car equivalents of platooning vehicles on basic segments. *Journal of Transportation Engineering, Part A: Systems*, *144*(10), 04018063. https://doi.org/10.1061/jtepbs.0000188

Bureau of Transportation Statistics (BTS). (1969–2020). *Average age of automobiles and trucks in operation in the United States* [Dataset]. Retrieved from https://www.bts.gov/content/average-age-automobiles-and-trucks-operation-united-states

Calvert, S. C., Schakel, W. J., & van Lint, J. W. C. (2017). Will automated vehicles negatively impact traffic flow? *Journal of Advanced Transportation*, *2017*, 1–17. https://doi.org/10.1155/2017/3082781

Chai, L., Cai, B., ShangGuan, W., Wang, J., & Wang, H. (2018). Connected and autonomous vehicles coordinating approach at intersection based on space–time slot. *Transportmetrica A: Transport Science*, *14*(10), 929–951. https://doi.org/10.1080/23249935.2018.1452308

Davis, S. C., & Boundy, R. G. (2019). *Transportation energy data book* (ORNL/TM-2018/987). Oak Ridge National Laboratory. Retrieved from https://tedb.ornl.gov/wp-content/uploads/2020/02/Edition37_Full_Doc.pdf

European Commission. (2020). CoEXist: "AV-Ready" transport models and road infrastructure for the coexistence of automated and conventional vehicles. Retrieved from https://company.ptvgroup.com/en/about/research/research-projects/coexist

Forsgren, K., Shah, D., & Lum, D. (2018). *The road ahead for autonomous vehicles* (S401972C). Standard & Poor's Financial Services LLC. Retrieved from https://www.ibtta.org/sites/default/files/documents/SP%20Global%20Ratings%20-%20Road%20Ahead%20For%20Autonomous%20Vehicles-Enhanced%20May-14-2018.pdf

Ghiasi, A., Hussain, O., Qian, Z. S., & Li, X. (2017). A mixed traffic capacity analysis and lane management model for connected automated vehicles: A Markov chain method. *Transportation Research Part B: Methodological*, *106*, 266–292. https://doi.org/10.1016/j.trb.2017.09.022

Goñi-Ros, B., Schakel, W. J., Papacharalampous, A. E., Wang, M., Knoop, V. L., Sakata, I., . . . Hoogendoorn, S. P. (2019). Using advanced adaptive cruise control systems to reduce congestion at sags: An evaluation based on microscopic traffic simulation. *Transportation Research Part C: Emerging Technologies*, *102*, 411–426. https://doi.org/10.1016/j.trc.2019.02.021

Gouy, M., Wiedemann, K., Stevens, A., Brunett, G., & Reed, N. (2014). Driving next to automated vehicle platoons: How do short time headways influence non-platoon drivers' longitudinal control? *Transportation Research Part F: Traffic Psychology and Behaviour*, *27*, 264–273. https://doi.org/10.1016/j.trf.2014.03.003

Guo, R. J., Wang, X. J., & Wang, W. X. (2014). Estimation of critical gap based on raff's definition. *Computational Intelligence and Neuroscience*, *2014*, 1–7. https://doi.org/10.1155/2014/236072

Guo, Y., & Ma, J. (2020). Leveraging existing high-occupancy vehicle lanes for mixed-autonomy traffic management with emerging connected automated vehicle applications. *Transportmetrica A: Transport Science*, *16*(3), 1375–1399. https://doi.org/10.1080/23249935.2020.1720863

Guo, Y., & Ma, J. (2021). SCoPTO: Signalized corridor management with vehicle platooning and trajectory control under connected and automated traffic environment. *Transportmetrica B: Transport Dynamics*, *9*(1), 673–692. https://doi.org/10.1080/21680566.2021.1938282

Hartmann, M., Motamedidehkordi, N., Krause, S., Hoffmann, S., Vortisch, P., & Busch, F. (2017). Impact of automated vehicles on capacity of the German freeway network. *Proceedings from ITS World Congress 2017*. Retrieved from https://www.researchgate.net/publication/320868890_Impact_of_Automated_Vehicles_on_Capacity_of_the_German_Freeway_Network

Jiang, H., Hu, J., An, S., Wang, M., & Park, B. B. (2017). Eco approaching at an isolated signalized intersection under partially connected and automated vehicles environment. *Transportation Research Part C: Emerging Technologies*, *79*, 290–307. https://doi.org/10.1016/j.trc.2017.04.001

Jones, S. (2013). *Cooperative adaptive cruise control: Human factors analysis* (FHWA-HRT-13-045). Office of Safety Research and Development Federal Highway Administration. Retrieved from https://www.fhwa.dot.gov/publications/research/safety/13045/13045.pdf

Karakikes, I., Spangler, M., & Margreiter, M. (2017). Designing a Vissim-Model for a motorway network with systematic calibration on the basis of travel time measurements. *Transportation Research Procedia*, *24*, 171–179. https://doi.org/10.1016/j.trpro.2017.05.086

Keeney, T. (2017). *Mobility as a service: Why self driving cars could change everything*. ARK Investment Management LLC. Retrieved from https://www.parking-mobility.org/2020/07/01/mrc-mobility-as-a-service-why-self-driving-cars-could-change-everything/

Kesting, A., Treiber, M., & Helbing, D. (2010). Enhanced intelligent driver model to access the impact of driving strategies on traffic capacity. *Philosophical Transactions of the Royal Society A: Mathematical, Physical and Engineering Sciences*, *368*(1928), 4585–4605. https://doi.org/10.1098/rsta.2010.0084

Kiefer, R. J., Cassar, M. T., Flannagan, C. A., LeBlanc, D. J., Palmer, M. D., Deering, R. K., & Shulman, M. A. (2003). *Forward collision warning requirements project: Refining the CAMP crash alert timing approach by examining "Last-Second" braking and lane change maneuvers under various kinematic conditions* (DOT HS 809 574). National

Highway Traffic Safety Administration U.S. Dept of Transportation. Retrieved from https://www.nhtsa.gov/DOT/NHTSA/NRD/Multimedia/PDFs/Crash%20Avoidance/2003/HS809574Report.pdf

Krajzewicz, D., Erdmann, J., Behrisch, M., & Bieker, L. (2012). Recent development and applications of SUMO – Simulation of Urban MObility. *International Journal on Advances in Systems and Measurements, 5*(3 & 4), 128–138. http://www.iariajournals.org/systems_and_measurements/sysmea_v5_n34_2012_paged.pdf

Krajzewicz, D., Hertkorn, G., Wagner, P., & Rossel, C. (2002). An example of microscopic car models validation using the open source traffic simulation SUMO. In *Simulation in industry: 14th european simulation symposium*. Dresden, Germany: Society for Modeling and Simulation International.

Krechmer, D., Blizzard, K., Cheung, M. G., Campbell, R., Alexiadis, V., Hyde, J., . . . Bitner, J. (2016). *Connected vehicle impacts on transportation planning—Primer and final report* (FHWA-JPO-16-420). Intelligent Transportation System Joint Program Office, U.S. Department of Transportation. Retrieved from https://rosap.ntl.bts.gov/view/dot/31397/dot_31397_DS1.pdf

Kyte, M., Tian, Z., Mir, Z., Hameedmansoor, Z., Kittelson, W., Vandehey, M., . . . Troutbeck, R. (1996). *Capacity and level of service at unsignalized intersections: Volume 1—Two-way stop-controlled intersections* (03–46). Washington, DC: The National Academies Press. https://doi.org/10.17226/6340

Lazar, C., Tiganasu, A., & Caruntu, C. (2018). Arterial intersection improvement by using vehicle platooning and coordinated start. *IFAC-PapersOnLine*, *51*(9), 136–141. https://doi.org/10.1016/j.ifacol.2018.07.023

le Vine, S., Zolfaghari, A., & Polak, J. (2015). Autonomous cars: The tension between occupant experience and intersection capacity. *Transportation Research Part C: Emerging Technologies*, *52*, 1–14. https://doi.org/10.1016/j.trc.2015.01.002

Leisch, J. (1974). *Capacity analysis techniques for design and operation of freeway facilities* (FHWA-RD-74-24). Washington, D.C.: Federal Highway Administration Department of Transportation. Retrieved from http://libraryarchives.metro.net/dpgtl/usdot/1974-capacity-analysis-techniques-for-design-and-operation-of-freeway-facilities-february.pdf

Letter, C., & Elefteriadou, L. (2017). Efficient control of fully automated connected vehicles at freeway merge segments. *Transportation Research Part C: Emerging Technologies*, *80*, 190–205. https://doi.org/10.1016/j.trc.2017.04.015

Li, Z., DeAmico, M., Chitturi, M., Bill, A., & Noyce, D. (2013). Calibration of VISSIM roundabout model: A critical gap and follow-up headway approach. In *Transportation Research Board 92nd Annual meeting: January 13-17, 2013: Washington, D.C.* Washington, DC: Transportation Research Board. Retrieved from

https://www.researchgate.net/publication/277558085_Calibration_of_VISSIM_Roundabout_Model_A_Critical_Gap_and_Follow-up_Headway_Approach

Li, Z., Elefteriadou, L., & Ranka, S. (2014). Signal control optimization for automated vehicles at isolated signalized intersections. *Transportation Research Part C: Emerging Technologies*, *49*, 1–18. https://doi.org/10.1016/j.trc.2014.10.001

Litman, T. (2019). *Autonomous vehicle implementation predictions: Implications for transport planning*. Victoria, BC: Victoria Transport Policy Institute. Retrieved from https://www.vtpi.org/avip.pdf

Liu, H., Kan, X. D., Shladover, S. E., Lu, X. Y., & Ferlis, R. E. (2018a). Impact of cooperative adaptive cruise control on multilane freeway merge capacity. *Journal of Intelligent Transportation Systems*, *22*(3), 263–275. https://doi.org/10.1080/15472450.2018.1438275

Liu, H., Kan, X. D., Shladover, S. E., Lu, X. Y., & Ferlis, R. E. (2018b). Modeling impacts of cooperative adaptive cruise control on mixed traffic flow in multi-lane freeway facilities. *Transportation Research Part C: Emerging Technologies*, *95*, 261–279. https://doi.org/10.1016/j.trc.2018.07.027

Lu, X., Kan, X., Shladover, S., Wei, D., & Ferlis, R. (2017). An enhanced microscopic traffic simulation model for application to connected automated vehicles. In *Transportation Research Board 96th Annual Meeting*. Retrieved from https://www.researchgate.net/publication/322017533_An_Enhanced_Microscopic_Traffic_Simulation_Model_for_Application_to_Connected_Automated_Vehicles

Ma, J., Leslie, E., Ghiasi, A., Sethi, S., Hale, D., Shladover, S., . . . Huang, Z. (2021). *Applying bundled speed-harmonization, cooperative adaptive cruise control, and cooperative-merge applications to managed-lane facilities* (FHWA-HRT-21-008). Washington, D.C.: U.S. Department of Transportation Federal Highway Administration. Retrieved from https://www.fhwa.dot.gov/publications/research/operations/21008/21008.pdf

Ma, J., Li, X., Zhou, F., Hu, J., & Park, B. B. (2017). Parsimonious shooting heuristic for trajectory design of connected automated traffic part II: Computational issues and optimization. *Transportation Research Part B: Methodological*, *95*, 421–441. https://doi.org/10.1016/j.trb.2016.06.010

Mahmassani, H. S., Elfar, A., Shladover, S. E., & Huang, Z. (2018). *Development of an analysis/modeling/simulation (AMS) framework for V2I and connected/automated vehicle environment* (FHWA-JPO-18-725). McLean, VA: Federal Highway Administration Turner-Fairbank Highway Research Center. Retrieved from https://rosap.ntl.bts.gov/view/dot/39965/dot_39965_DS1.pdf

Mahmood, B., & Kianfar, J. (2019). Driver behavior models for heavy vehicles and passenger cars at a work zone. *Sustainability*, *11*(21), 6007. https://doi.org/10.3390/su11216007

Makridis, M., Mattas, K., Ciuffo, B., Raposo, M., Toledo, T., & Thiel, C. (2018). Connected and automated vehicles on a freeway scenario. Effect on traffic congestion and network capacity. *7th Transport Research Arena, Vienna, Austria*. doi:10.5281/zenodo.1483132

McGowen, P., & Stanley, L. (2012). Alternative methodology for determining gap acceptance for two-way stop-controlled intersections. *Journal of Transportation Engineering*, *138*(5), 495–501. https://doi.org/10.1061/(asce)te.1943-5436.0000358

Milanés, V., & Shladover, S. E. (2014). Modeling cooperative and autonomous adaptive cruise control dynamic responses using experimental data. *Transportation Research Part C: Emerging Technologies*, *48*, 285–300. https://doi.org/10.1016/j.trc.2014.09.001

Miloslavov, A., & Veeraraghavan, M. (2012a). An integrated vehicular-wireless evaluation of WAVE/DSRC connected vehicle probe data service. *2012 Computing, Communications and Applications Conference*. https://doi.org/10.1109/comcomap.2012.6154865

Miloslavov, A., & Veeraraghavan, M. (2012b). Sensor data fusion algorithms for vehicular cyber-physical systems. *IEEE Transactions on Parallel and Distributed Systems*, *23*(9), 1762–1774. https://doi.org/10.1109/tpds.2012.107

Nowakowski, C., O'Connell, J., Shladover, S., & Cody, D. (2010). Cooperative adaptive cruise control: Driver acceptance of following gap settings less than one second. *Human Factors and Ergonomics Society Annual Meeting, San Francisco, CA*. doi:https://doi.org/10.1177%2F154193121005402403

Ntousakis, I. A., Nikolos, I. K., & Papageorgiou, M. (2015). On microscopic modelling of adaptive cruise control systems. *Transportation Research Procedia*, *6*, 111–127. https://doi.org/10.1016/j.trpro.2015.03.010

Nyame-Baafi, E., Adams, C. A., & Osei, K. K. (2018). Volume warrants for major and minor roads left-turning traffic lanes at unsignalized t-intersections: A case study using VISSIM modelling. *Journal of Traffic and Transportation Engineering (English Edition)*, *5*(5), 417–428. https://doi.org/10.1016/j.jtte.2018.01.005

Park, S., Kim, J., Lee, S., & Hwang, K. (2017). Experimental analysis on control constraints for connected vehicles using Vissim. *Transportation Research Procedia*, *21*, 269–280. https://doi.org/10.1016/j.trpro.2017.03.097

Perraki, G., Roncoli, C., Papamichail, I., & Papageorgiou, M. (2018). Evaluation of a model predictive control framework for motorway traffic involving conventional and automated vehicles. *Transportation Research Part C: Emerging Technologies*, *92*, 456–471. https://doi.org/10.1016/j.trc.2018.05.002

Porfyri, K., Mintsis, E., & Mitsakis, E. (n.d.). Assessment of ACC and CACC systems using SUMO. In *SUMO 2018 – Simulating Autonomous and Intermodal Transport Systems, Berlin.* Retrieved from https://easychair.org/publications/open/HvLp

PTV Group. (2018). *PTV Vissim version 11 user manual*. PTV, Karlsruhe, Germany. Retrieved from https://www.scribd.com/document/418753937/Vissim-11-Manual

Raff, M. S. (1950). *A volume warrant for urban stop Signs.* Saugatuck, CT: Eno Foundation for Urban Traffic Control. Retrieved from https://rosap.ntl.bts.gov/view/dot/16265/dot_16265_DS1.pdf

Rakha, H. A., Ahn, K., & Moran, K. (2012). Integration framework for modeling eco-routing strategies: Logic and preliminary results. *International Journal of Transportation Science and Technology*, *1*(3), 259–274. https://doi.org/10.1260/2046-0430.1.3.259

Rakha, H., & Ahn, K. (2004). Integration modeling framework for estimating mobile source emissions. *Journal of Transportation Engineering*, *130*(2), 183–193. https://doi.org/10.1061/(asce)0733-947x(2004)130:2(183)

Reilly, W., Harwood, D., Schoen, J., & Holling, M. (1990). *Capacity and LOS procedures for rural and urban multilane highways* (NCHRP Project 03-33). Yagoona, Australia: JHK & Associates.

Ren, L., Qu, X., Guan, H., Easa, S., & Oh, E. (2016). Evaluation of roundabout capacity models: An empirical case study. *Journal of Transportation Engineering*, *142*(12), 04016066. https://doi.org/10.1061/(asce)te.1943-5436.0000878

Rodegerdts, L., Blogg, M., Wemple, E., Myers, E., Kyte, M., Dixon, M., . . . Carter, D. (2007). *Roundabouts in the United States* (NCHRP Report 572). Washington, DC: The National Academies Press. https://doi.org/10.17226/23216

Rodegerdts, L. A., Malinge, A., Marnell, P. S., Beaird, S. G., Kittelson, M. J., & Mereszczak, Y. S. (2015). *Accelerating roundabout implementation in the United States, volume II of VII: Assessment of roundabout capacity models for the highway capacity manual* (Report No. FHWA-SA-15-070). Washington, D.C.: Federal Highway Administration United States Department of Transportation. Retrieved from https://safety.fhwa.dot.gov/intersection/roundabouts/fhwasa15070.pdf

Roess, R. P., & Ulerio, J. M. (1993). *Capacity of ramp–freeway junctions* (NCHRP Project 03-37). Polytechnic University.

Rouphail, N., Aghdashi, S., Ko, K., Hadi, M., & Khazraeian, S. (2015). Flow allocation at congested freeway ramp merges. In *Transportation Research Board 94th Annual Meeting, Washington, D.C.* Retrieved from https://www.researchgate.net/publication/317054447_Flow_Allocation_at_Congested_Freeway_Ramp_Merges

SAE International. (2018). *Taxonomy and definitions for terms related to driving automation systems for on-road motor vehicles* (Standard No. SAE J 3016-2018).Retrieved from https://www.sae.org/standards/content/j3016_201806/

Schoen, J. A., May, A., Reilly, W., & Urbanik, T. (1995). *Speed–flow relationships for basic freeway sections* (Report no. NCHRP Project 3-45). JHK & Associates. Retrieved from https://www.hcmvolume4.org/system/datas/163/original/NCHRP%2003-45%20final%20report%20searchable.pdf

Schroeder, B. (2012). Calibrating roundabout simulation models to deterministic capacity relationships. *Roundabouts Now Online Journal*, http://roundaboutsnow.com.

Schwartz, H. (2018). America's aging vehicles delay rate of fleet turnover. Retrieved from http://energyfuse.org/americas-aging-vehicles-delay-rate-fleet-turnover/

Shaaban, K., & Kim, I. (2015). Comparison of SimTraffic and VISSIM microscopic traffic simulation tools in modeling roundabouts. *Procedia Computer Science*, *52*, 43–50. https://doi.org/10.1016/j.procs.2015.05.016

Sharon, G., Levin, M. W., Hanna, J. P., Rambha, T., Boyles, S. D., & Stone, P. (2017). Network-wide adaptive tolling for connected and automated vehicles. *Transportation Research Part C: Emerging Technologies*, *84*, 142–157. https://doi.org/10.1016/j.trc.2017.08.019

Shi, L., & Preveduros, P. (2016). Autonomous and connected cars: HCM estimates for freeways with various market penetration rates. In *ISEHP 2016 International Symposium on Enhancing Highway Performance*. München: Elsevier. https://doi.org/10.1016/j.trpro.2016.06.033

Shladover, S. E., Su, D., & Lu, X. Y. (2012). Impacts of cooperative adaptive cruise control on freeway traffic flow. *Transportation Research Record: Journal of the Transportation Research Board*, *2324*(1), 63–70. https://doi.org/10.3141/2324-08

Siddharth, S., & Ramadurai, G. (2013). Calibration of VISSIM for Indian heterogeneous traffic conditions. *Procedia - Social and Behavioral Sciences*, *104*, 380–389. https://doi.org/10.1016/j.sbspro.2013.11.131

Siegloch, W. (1973). Die leistungsermittlung an knotenpunkten ohne lichtsignalsteuerung (Capacity calculations for unsignalized intersections). *Schriftenreihe Strassenbau und Strassenverkehrstechnik, 154*.

Song, J., Wu, Y., Xu, Z., & Lin, X. (2014). Research on car-following model based on SUMO. In *2014 IEEE 7th International Conference on Advanced Infocomm Technology (ICAIT 2014) Fuzhou, China, 14 - 16 November 2014*. Piscataway, NJ: IEEE. doi:10.1109/ICAIT.2014.7019528

Stevanovic, J., Stevanovic, A., Martin, P. T., & Bauer, T. (2008). Stochastic optimization of traffic control and transit priority settings in VISSIM. *Transportation Research Part C: Emerging Technologies*, *16*(3), 332–349. https://doi.org/10.1016/j.trc.2008.01.002

Straight, B. (2018). Autonomous vehicle timeline: Perhaps your kids will ride in one. Retrieved from https://www.freightwaves.com/news/autonomous-vehicle-timeline

Tass International. (2020). PreScan: Simulation of ADAS and active safety. Retrieved from https://tass.plm.automation.siemens.com/prescan

Tideman, M., & Noort, M. (2013). A simulation tool suite for developing connected vehicle systems. In *2013 IEEE intelligent vehicles symposium (IV)*. Gold Coast, Australia: IEEE. doi:10.1109/IVS.2013.6629551

Tomar, R., Prateek, M. & Sastry, H. G. (2018). Simulation of information dissemination using flooding in VANET. *Journal of Communications Technology, Electronics and Computer Science*, *19*, 1–4. http://dx.doi.org/10.22385/jctecs.v19i0.271

Transportation Research Board (TRB). (2016). *Highway capacity manual: A guide for multimodal mobility analysis* (6th ed.). Washington, D.C.: National Academies Press. Retrieved from https://www.mytrb.org/MyTRB/Store/Product.aspx?ID=8313

Troutbeck, R. J. (1992). *Estimating the critical acceptance gap from traffic movements*. Amsterdam, Netherlands: Amsterdam University Press.

Troutbeck, R. J. (2016). Revised Raff's method for estimating critical gaps. *Transportation Research Record: Journal of the Transportation Research Board*, *2553*(1), 1–9. https://doi.org/10.3141/2553-01

U.S. Department of Transportation (USDOT). (2018). *Preparing for the future of transportation: Automated vehicles 3.0.* Retrieved from https://www.transportation.gov/sites/dot.gov/files/docs/policy-initiatives/automated-vehicles/320711/preparing-future-transportation-automated-vehicle-30.pdf

U.S. Department of Transportation (USDOT). (2020a). *Explore ITS CodeHub*. Office of the Assistant Secretary for Research and Technology (OST-R). https://its.dot.gov/code/

U.S. Department of Transportation (USDOT). (2020b). *ITS - research - automation*. Office of the Assistant Secretary for Research and Technology (OST-R). https://www.its.dot.gov/research_areas/automation.htm

U.S. Department of Transportation (USDOT). (2020c). *What are the benefits of connected vehicles?* Office of the Assistant Secretary for Research and Technology (OST-R). https://www.its.dot.gov/cv_basics/cv_basics_benefits.htm

U.S. Energy Information Administration (USEIA). (2018). *U.S. households are holding on to their vehicles longer*. Today in Energy - U.S. Energy Information Administration (EIA). https://www.eia.gov/todayinenergy/detail.php?id=36914

Vander Werf, J., Shladover, S. E., Miller, M. A., & Kourjanskaia, N. (2002). Effects of adaptive cruise control systems on highway traffic flow capacity. *Transportation Research Record: Journal of the Transportation Research Board*, *1800*(1), 78–84. https://doi.org/10.3141/1800-10

Vent, R. (2015). *Real traffic flow modelling with SUMO* (student paper). Estonia: University of Tartu,. Retrieved from https://pdfs.semanticscholar.org/870c/9dd6c1421bf2dfc023d06b06faa79c9d6aea.pdf

Wang, Y., Liu, X., Rouphail, N., Schroeder, B., Yin, Y., & Bloomberg, L. (2012). *Analysis of managed lanes on freeway facilities*. Washington, D.C.: National Cooperative Highway Research Program, Transportation Research Board of the National Academies. https://doi.org/10.17226/22677

Washburn, S. S., Al-Kaisy, A., Luttinen, T., Dowling, R., Watson, D., Jafari, A., . . . Elias, A. (2018). *Improved analysis of two-lane highway capacity and operational performance*. Washington, D.C.: National Cooperative Highway Research Program, Transportation Research Board of the National Academies. https://doi.org/10.17226/25179

Wei, T., Shah, H., & Ambadipudi, R. (2012). VISSIM calibration for modeling single lane roundabouts: Capacity-based strategies. In *TRB 91st annual meeting: January 22-26, 2012, Washington, D.C.* Washington, D.C.: Transportation Research Board.

Yeo, H., Skabardonis, A., Halkias, J., Colyar, J., & Alexiadis, V. (2008). Oversaturated freeway flow algorithm for use in next generation simulation. *Transportation Research Record: Journal of the Transportation Research Board*, *2088*(1), 68–79. https://doi.org/10.3141/2088-08

Zhandong, Z., Shaohui, C., Yanquan, Y., Aixiu, H., & Xinyi, Z. (2016). VISSIM simulation based expressway exit control modes research. *Procedia Engineering*, *137*, 738–746. https://doi.org/10.1016/j.proeng.2016.01.311

Zhao, L., Malikopoulos, A., & Rios-Torres, J. (2018). Optimal control of connected and automated vehicles at roundabouts: An investigation in a Mixed-Traffic environment. *IFAC-PapersOnLine*, *51*(9), 73–78. https://doi.org/10.1016/j.ifacol.2018.07.013

Zhao, L., & Sun, J. (2013). Simulation framework for vehicle platooning and car-following behaviors under connected-vehicle environment. *Procedia - Social and Behavioral Sciences*, *96*, 914–924. https://doi.org/10.1016/j.sbspro.2013.08.105

Zheng, Y., Jin, L., Gao, L., Li, K., Wang, Y., & Wang, F. (2016). Development of a distributed cooperative vehicles control algorithm based on V2V communication. *Procedia Engineering*, *137*, 649–658. https://doi.org/10.1016/j.proeng.2016.01.302